SECURITY CLASSIFICATION OF THIS PAGE

REPORT DOCUMENTATION PAGE

Form Approved
OMB No 0704-0188

1a REPORT SECURITY CLASSIFICATION	1b RESTRICTIVE MARKINGS: N/A
2a SECURITY CLASSIFICATION AUTHORITY	3 DISTRIBUTION/AVAILABILITY OF REPORT: Distribution Unlimited
2b DECLASSIFICATION/DOWNGRADING SCHEDULE	
4 PERFORMING ORGANIZATION REPORT NUMBER(S)	5 MONITORING ORGANIZATION REPORT NUMBER(S): N/A
6a NAME OF PERFORMING ORGANIZATION: University of Alabama at Birmingham	6b OFFICE SYMBOL (If applicable): N/A
7a NAME OF MONITORING ORGANIZATION: Office of Naval Research	
6c ADDRESS (City, State, and ZIP Code): Laboratory or Molecular Biophysics, P.O. Box 300, UAB Station, Birmingham, AL 35294	7b ADDRESS (City, State, and ZIP Code): 800 N. Quincy Street, Arlington, VA 22217-5000
8a NAME OF FUNDING/SPONSORING ORGANIZATION: Office of Naval Research	8b OFFICE SYMBOL (If applicable): ONR
9 PROCUREMENT INSTRUMENT IDENTIFICATION NUMBER: N00014-86-K-0402	
8c ADDRESS (City, State, and ZIP Code): 800 N. Quincy Street, Arlington, VA 22217-5000	10 SOURCE OF FUNDING NUMBERS: PROGRAM ELEMENT NO 61153N; PROJECT NO RR04106; TASK NO; WORK UNIT ACCESSION NO

11 TITLE (Include Security Classification)
Development of Elastomeric Polypeptide Biomaterials

12 PERSONAL AUTHOR(S)
Urry, Dan W.; Prasad, K. U., and Morrow, Casey

13a TYPE OF REPORT	13b TIME COVERED	14 DATE OF REPORT (Year, Month, Day)	15 PAGE COUNT
Annual	FROM 6/1/88 TO 5/31/89	1989, July 1	

16 SUPPLEMENTARY NOTATION

17 COSATI CODES		
FIELD	GROUP	SUB-GROUP
06	03	

18 SUBJECT TERMS (Continue on reverse if necessary and identify by block number)
sequential polypeptides, inverse temperature transition, chemomechanical and electromechanical transduction, sensors and transducers, gene cassette methodology.

19 ABSTRACT (Continue on reverse if necessary and identify by block number)

In the past year, there have been 10 papers published or in press which resulted in part from N00014-86-K-0402. These involve the synthesis, physical characterization and computations of poly(VPGVG) and of Glu and Ile containing analogs. The physical characterizations and molecular dynamics computations further characterize an entropic elastomeric force arising from a regular, non-random structure in which there is a damping of internal chain dynamics on extension. The studies also further characterize a new mechanism of chemomechanical transduction described phenomenologically as chemical modulation of an inverse temperature transition, more mechanistically as chemical modulation of the hydrophobic effect or at the molecular level as an hydration mediated apolar-polar interaction free energy. The mechanochemical coupling appears to be more efficient than the charge-charge repulsion mechanism when considering the carboxyl/carboxylate couple and the quantity $(\delta\mu/\delta f)_n$, appears to have the opposite sign, being positive for the charge-charge repulsion mechanism and negative for chemical modulation of the hydrophobic effect. Future work involves formal determination of the efficiency by means of

20 DISTRIBUTION/AVAILABILITY OF ABSTRACT: ☒ UNCLASSIFIED/UNLIMITED ☐ SAME AS RPT ☐ DTIC USERS	21 ABSTRACT SECURITY CLASSIFICATION: (U)
22a NAME OF RESPONSIBLE INDIVIDUAL: Mike Marron	22b TELEPHONE (Include Area Code): (202) 696-4760 / 22c OFFICE SYMBOL: ONR

DD Form 1473, JUN 86 — Previous editions are obsolete — SECURITY CLASSIFICATION OF THIS PAGE

S/N 0102-LF-014-6603

AD-A210 295

19. Abstract (continued)
experimentally determined work cycles and microbial preparation of sequential polypeptides.

Accesion For	
NTIS CRA&I	☑
DTIC TAB	☐
Unannounced	☐
Justification	
By	
Distribution /	
Availability Codes	
Dist	Avail and / or Special
A-1	

ANNUAL REPORT

Contract Title: Development of Elastomeric Polypeptide Biomaterials

Contract Number: N00014-86-0402

I. BRIEF SUMMARY OF PROJECT GOALS: (Same as Previously)

To design, prepare and characterize novel elastomeric polymers comprised of repeating peptide sequences, primarily the elastin pentamer and analogs of it alone and combined with repeating related hexapeptides and/or tetrapeptides. The purpose is to develop polymers with different elastic moduli and increased extension limits, polymers with different temperature ranges for their inverse temperature transitions over which elastomeric force dramatically changes, polymers in which different heat changes effect the large changes in elastomeric force, polymers with different intensities and frequencies of their dielectric relaxations and polymers with wider temperature ranges over which they function as nearly ideal elastomers. In the elastomer design, the dominant repeat units will be pentamers and tetramers. Hexamers and alanine-rich, lysine-containing cross-linking sequences will be used to fine-tune properties.

II. SUMMARY OF ACCOMPLISHMENTS IN THE THIRD YEAR

Since the last report six papers have been published, three are at the galley stage and an additional one is in press giving a total of ten papers published or in press. In what follows, the list of the publications is given each with the abstract. These, as Part A, constitute a report of the chemical synthesis and the physical and computational characterizations. This is foliowed by Part B which is a report on the progress toward microbial biosynthesis of the polypentapeptide of elastin.

A. Publications

1. Urry, Dan W., "An Hydration Mediated Free Energy Driving Force for Protein Folding and Assembly," *American Assoc. for the Advancement of Science* Publications (in press).

Abstract: The hydrophobic effect and electrostatic interactions are two prominent considerations for protein folding and assembly in an aqueous medium. With the known crystal structures of globular proteins in an aqueous mother liquor, it is appreciated that hydrophobic side chains of residues such as Phe, Ile, Leu, Val, etc. are generally buried within the interior of the protein. Additionally, there are examples where the change in a single charge can cause dramatic changes in the assembly of protein subunits. Such dramatic effects are cited as indicating the exquisite importance of electrostatic interactions in protein structure. In the present review, it is argued with experimental data that the existence of an interactive hydrophobic-electrostatic repulsive free energy in an aqueous environment is responsible for this exquisite modulation of protein structure. This has been called an aqueous mediated apolar-polar repulsion free energy. It is demonstrated here in terms of 1) the effect of changes in hydrophobicity on the pK_a of a weak acid, 2) the effect of added charge on the endothermic heat of an inverse temperature transition, and 3) the interconversion of mechanical and chemical work in elastic polypeptides which are capable of folding due to an inverse temperature transition (thermomechanical transduction) and which may also be designed to exhibit chemomechanical transduction by application of the apolar-polar free energy of interaction.

2. Chang, D.K. and Urry, Dan W., "Polypentapeptide of Elastin: Damping of Internal Chain Dynamics on Extension." J. of Computational Chemistry (in press).

Abstract: Molecular dynamics simulations out to 100 ps have been carried out at 300 K in vacuo on the repeating pentapeptide, (VPGVG), of the elastin fiber. The structure employed in the simulation is a β-spiral (helical structure) with 2.7 pentamers per turn and with a 9.45 Å rise per turn and 21.6 Å rise per turn in the relaxed and extended states, respectively. Large amplitude backbone torsion angle fluctuations are observed in the relaxed state, and significant damping is observed upon extension, particularly in the suspended segments of the β-spiral structure. Accordingly the entropy change on extension was computed and found to be a substantial -1.1 entropy units per residue. The various energy components are compared for relaxed and extended states and the relevance of the results to the molecular mechanism of entropic elasticity is discussed.

3. Chang, D.K. and Urry, Dan W. "The Molecular Dynamics of the β-spiral of the Polypentapeptide of Elastin in "State III" with 2.9 Pentamers/Turn," Theochem, Special Issue in Honor of Prof. Per Olov Löwdin. (in press).

Abstract: In vacuo molecular dynamics simulation using the CHARMm program was carried out on a putative structure ("state III") of the repeating pentapeptide, (VPGVG), of elastin at two different extensions. "State III" is the proposed structure for the experimental state III which develops after prolonged heating at temperatures greater than 60°C. "State III" is a helix, called a β-spiral, with 2.9 pentamer units per turn in which the type II β-turns fan outward in propeller fashion and the Val^4 side chains turn inward displacing the former intra-spiral water and increasing the intramolecular hydrophobic interactions. The fluctuations in backbone dihedrald angles for this "state III" are found to be smaller for the structure on extension. These results are compared with previous calculations on the proposed structure for the physiological state, state II, in which the β-turns function as spacers between turns of the dynamic β-spiral and in which there is much water within the β-spiral. The magnitude of dihedral angle damping

upon elongation of "state III" is, however, much smaller than that calculated from the β-spiral structure for state II. The computational result is consistent with the experimental observations of shrinking and expulsion of water loss of elastic modulus on heating above 60°C. The implications of this modelling of state III and state II on the damping of internal chain dynamics on extension are discussed with regard to the source of entropic elasticity.

4. Chang, D.K., Venkatachalam, C. M., Prasad, K.U., and Urry, D.W. "Nuclear Overhauser Effect and Computational Characterization of the β-Spiral of the Polypentapeptide of Elastin" J. of Biomolecular Structure & Dynamics, 6, (5), 851-858 (1989).

Abstract: The structure of the elastin polypentapeptide, poly(VPGVG), was studied by nuclear Overhauser effect experiments using perdeuterated Val^1 and Val^4 samples under the condition where intermolecular interactions are absent. More extensive interaction was found between the Val^1 $\gamma C\underline{H}$ and Pro^2 $\beta C\underline{H}$ protons than between the Val^4 $\gamma C\underline{H}$ and Pro^2 $\beta C\underline{H}$ protons. The Val^1 $\gamma C\underline{H}_3$-Pro^2 $\beta C\underline{H}$ interaction does not occur within the same pentamer as previously shown experimentally and as expected from steric considerations. The results are incompatible with the presence of a random chain network in poly(VPGVG) at room temperature but are readily explicable in terms of interturn interactions in a β-spiral structure. More specifically, the results indicate that the β-spiral conformation with 2.9 pentamers/turn is more prevalent than that with 2.7 pentamers/turn. Using conformations developed by molecular mechanics calculations, molecular dynamics simulations were carried out to compare the relative energies of these two variants of this class of β-spiral structures. It was found in vacuo that the structure with 2.9 pentamers/turn is indeed more stable than that of 2.7 pentamers/turn by ~1kcal/mole-pentamer.

5. Zhang, H., Prasad, K.U., and Urry, D.W. "Synthesis of 4% Glu-Containing Val^1 and Ile^1- Polypentapeptides: Model Protein Systems for Demonstrating Mechanochemical Coupling," J. of Protein Chemistry, 8(2), 173-182, 1989.

Abstract: The synthesis of 4% Glu-polypentapeptide (PPP) (i.e., 4 Glu residues per 100 amino acid residues) and 4% Glu-Ile^1-PPP, in which Val^1 is substituted by a more hydrophobic Ile residue, is carried out by copolymerizing the p-nitrophenyl-active esters of GE(OMe)GVP and GE(OMe)GIP with their parent pentamers GVGVP and GVGIP in 1:4 ratios, respectively. After removal of the methyl ester on the side chain of Glu, these polymers exhibited a remarkable pH dependence of the temperature for their inverse temperature transitions, which are followed as turbidity development at 300 nm. On γ-irradiation crosslinking, the elastomeric bands obtained exhibited a pH-mediated contraction and relaxation. Thus, for the first time, mechanochemical coupling is demonstrated in a synthetic polypeptide system. That the basic mechanism involves the hydrophobic effect (chemical modulation of an inverse temperature transition) and not ion-ion electrostatic repulsion is also discussed.

6. Urry, D. W., Chang, D.K., Krishna, R., Trapane, T.L. and Prasad, K.U., "Two Dimensional Proton Nuclear Magnetic Resonance Studies on Poly(VPGVG) and its Cyclic Conformational Correlate, $Cyclo(VPGVG)_3$." Biopolymers, 28, 819-833 (1989).

Abstract: Two-dimensional nuclear overhauser enhancement (2D NOESY) data are reported for the polypentapeptide of elastin, poly(VPGVG), and the cyclopentadecapeptide, $cyclo(VPGVG)_3$. In both, the repeating type II Pro^2-Gly^3 β-turn can be derived from the NOE data, providing confirmation of many previous studies. In addition, other through-space connectivities are detailed that also compare favorably with previously determined crystal and solution structures for $cyclo(VPGVG)_3$. Also, near identical data for the cyclpentadecapeptide and the polypentapeptide demonstrate the cyclic conformation-linear (helical) conformational correlate relationship between the two molecules. The 2D NOESY experiment is seen to be an effective means of establishing

the presence or absence of a conformational relationship between a cyclic repeating sequence and its higher molecular weight linear counterpart. This is an approach of substantial practical value when developing the conformation of sequential polypeptides and when attempting to identify the presence of the conformati9on of a repeating peptide sequence within a more complex primary structure.

Having established the basic conformational relationship between a cyclic conformation and its linear helical counterpart, cross peaks present in the linear helical structure that are not present in the cyclic conformational correlate can provide information on the interactions between adjacent turns of the helix. In this connection. a Val$\gamma C\underline{H}_3 \leftrightarrow$ Pro/$\beta C\underline{H}_2$ interaction is reported that can be the basis for determining the number of pentamers per turn of helix once it is determined whether it is dominantly the Val^1 or $Val^4\gamma C\underline{H}_3$ that is interacting with the $Pro^2\beta C\underline{H}_2$.

7. Urry, Dan W., Chang, Ding-Kwo, Zhang, Hong, and Prasad, Kari U. pK Shift of Functional Group in Mechanochemical Coupling Due to Hydrophobic Effect: Evidence for an Apolar-Polar Repulsion Free Energy in Water." Biochem. and Biophys. Res. Comm. 153 (2), 832-839 (1988).

Abstract: In the sequential polypeptide $(L\text{-}Val^1\text{-}L\text{-}Pro^2\text{-}Gly^3\text{-}L\text{-}Val^4\text{-}Gly^5)_n$, abbreviated as PPP, and its more hydrophobic analog $(L\text{-}Ile^1\text{-}L\text{-}Pro^2\text{-}Gly^3\text{-}L\text{-}Val^4\text{-}Gly^5)_n$, referred to as Ile^1-PPP when there are introduced into the sequence 4 Glu residues/100 residues of polypeptide in place of the Val at position four and when the material is γ-irradiation cross-linked to form an elastomeric matrix, mechanochemical coupling occurs on changing the pH, that is, motion and mechanical work are achieved by a change in proton chemical potential. The pH dependence of contraction or relaxation for each elastomer and the temperature dependence of aggregation at different pH values in phosphate buffered saline define pK values which demonstrate the pK to be shifted approximately one pH unit higher for the more hydrophobic sequential polypeptide. Data are reviewed and 2D-NMR data are presented which argue that the pK shift is not due to

different conformations of the polypentapeptides. The data are taken to indicate that the pK shift of a functional group can be due to a generalized hydrophobic effect and specific mechanisms are considered whereby differences in water structure within the matrix as the result of the hydrophobic effect could result in different pK values.

8. Chang, D.K. and Urry, D.W. "Molecular Dynamics on Relaxed and Extended States of the Polypentapeptide of Elastin." Chem. Phys. Ltrs., 147 (4), 395-400 (1988).

Abstract: Reported are the first molecular dynamics calculations on the elastomeric calculations on the elastomeric polypentapeptide of elastin as $(VPGVG)_7$. The salient points are that (1) there is little change in internal energy on extension; (2) a trajectory of 50 ps is insufficient to refelct the primary structural periodicity in rms displacements of torsion angles, but does show librational processes and their damping on extension; and (3) the recurring β-turn structure is retained.

9. Urry, Dan W. "Free Energy (Chemomechanical) Transduction in Elastomeric Polypeptides by Chemical Potential Modulation of an Inverse Temperature Transition," Internatl J. of Quantum Chem.: Quantum Biology Symp., 15, 235-245 (1988).

Abstract: Data and analyses are presented on the first synthetic polypeptide system to exhibit mechanochemical coupling; the mechanochemical coupling can also be demonstrated to be both polymer-based and solvent-based with respect to where the result of the change in the chemical potential is focused. Both polymer-based and solvent-based processes are the result of chemomechanical transduction in which the change in chemical potential results in a change in the temperature at which an inverse temperature transition occurs. In the polymer-based process, the contraction/relaxation occurs due to a change in the chemical nature of the polypeptide; in the solvent-based process there is no change in the chemical nature of the polypeptide

on contraction or relaxation, but rather the change in chemical potential changes the state of hydration of the polypeptide.

The new mechanochemical system provides an experimental system with which to clarify and to quantitate what may be called aqueous mediated apolar-polar interaction energies in polypeptides and proteins with hydrophobic groups that may be variously exposed to the aqueous solution or buried within the folded polypeptide or protein. Furthermore, it is noted that any conformational change exhibited by a polypeptide or protein that is the result of a binding of a chemical moiety, the change in chemical nature of a bound moiety or the change in chemical potential of the medium can be viewed in terms of mechanochemical coupling or chemomechanical transduction.

10. Urry, D.W., Haynes, B., Zhang, H., Harris, R.D., and Prasad, K.U.m "Mechanochemical Coupling in Synthetic Polypeptides by Modulation of an Inverse Temperature Transition," Proc. Natl. Acad. Sci. USA, 3407-3411.

Abstract: For the polypentapeptide of elastin, $(L\text{-}Val^{1}\text{-}L\text{-}Pro^{2}\text{-}Gly^{3}\text{-}L\text{-}Val^{4}\text{-}Gly^{5})_{n>120}$ and appropriate analogs when suitably cross-linked, it has been previously demonstrated that development of elastomeric force at fixed length and length changes at fixed load occur as the result of an inverse temperature transition with the temperature of the transition being inversely dependent on the hydrophobicity of the polypeptide. This suggests that at fixed temperature a chemical means of reversibly changing the hydrophobicity could be used for mechanochemical coupling. Evidence for this new mechanism of mechanochemical coupling is given here with a 4%-Glu-polypentapeptide in which the valine in position four is replaced in one out of five pentamers by a glutamic acid residue. Before cross-linking, the temperature for aggregation of 4%-Glu-polypentapeptide is remarkably sensitive to pH shifting from 25°C at pH 2 to 70°C at pH 7.4 in phosphate buffered saline (PBS). At 37°C, the cross-linked 4%-Glu polypentapeptide matrix in PBS undergoes a pH modulated contraction and relaxation with a change from pH 4.3 to 3.3 and back. The mean distance between carboxylates at

pH 4.3 in the elastomeric matrix is 70Å, more than twice the mean distance between negatively charged species in phosphate buffered saline. Accordingly, charge-charge repulsion is expected to make little or no contribution to the coupling. Mechanochemical coupling is demonstrated at fixed load by monitoring pH dependence of length and at constant length by monitoring pH dependence of force. To our knowledge, this is the first demonstration of mechanochemical coupling in a synthetic polypeptide and the first system to provide a test of the recent proposal that chemical modulation of an inverse temperature transition can be a mechanism for mechanochemical coupling. It is suggested that phosphorylation and dephosphorylation may modulate structure and forces in proteins by locally shifting the temperatures of inverse temperature transitions.

B. Progress Toward Microbial Biosynthesis of Polypentapeptides of Elastin

Recent advances in oligonucleotide synthesis and molecular cloning technologies provide new opportunities for the design and high level expression of a variety of novel gene products. The initial approaches, proposed in order to investigate the possibility of expressing elastin repeating sequences in microbial cells, were: 1) To synthesize synthetic genes that encode the basic polypentapeptide repeat unit; 2) to insert these synthetic genes into the bacterial expression plasmid pUC118; 3) to express the elastin sequences as a fusion polypeptide with the alpha-subunit of ß-galactosidase and 4) to investigate procedures for purification of the fusion protein. Significant progress has been made toward achieving these goals during the current funding period, but results obtained in the interim have necessitated some modification to these approaches.

1. Synthesis of polypentapeptide-encoding genes: In order to generate a double stranded DNA fragment of 150bp capable of coding for a decameric repeat of the basic (Val-Pro-Gly-Val-Gly) pentamer,overlapping oligonucleotides were synthesized that after

hybridization and enzymatic extension yielded the 150bp synthetic gene. In addition to the 2 oligonucleotides described in the initial proposal (JG1 and JG2, shown below) which were designed to yield the lowest redundancy based on codon redundancy, also synthesized were 2 additional overlapping oligonucleotides in which the sequence was optimized for prokaryotic codon usage. The respective oligonucleotides are shown below.

JG1-82mer
5'-GTTCCTGGTGTTGGTGTCCCCGGCGTCGGCGTACCAGGAGTAGGAGTGCCGGGGGTGGGGGTTCCCGGAGTGGGTGTCCCAGGGG-
3'

JG2-85mer
5-TCCGACACCGGGTACCCCTACGCCAGGGACACCAAACGCCTGGCACACCGACTCCCGGTACGCCTACCCCTGGGACACCCACTCCG-
3'

JG3-85mer
5'-GTTCCGGGTGTTGGTGTACCGGGTGTTGGTGTGCCGGGTGTTGGTGTTCCGGGCGTAGGCGTACCGGGCGTAGGCGTGCCGGGCG-
3'

JG4-86mer
5'-ACCTACACCCGGAACGCCCACACCCGGCACGCCCACGCCCGGTTACGCCCACGCCCGGAACGCCTACGCCCGGCACGCCTACGCCC-
3'

All four oligonucleotides were synthesized in the UAB oligonucleotide core facility on an Applied Biosystems oligonucleotide synthesizer. The high GC content of these oligonucleotides significantly lowered the efficiency of coupling and thus the overall yield of the product. The overall yield of full length oligonucleotide calculated after end labeling with gamma-labeled ATP and electrophoresis on a 6% polyacrylamide gel was approximately 5.0% (versus >50% seen with shorter, less GC rich oligonucleotides). Each oligonucleotide was purified from a preparative polyacrylamide gel and the actual yield in µg calculated from the O.D. 260 of the solution.

Approximately 300ng of oligonucleotides JG1 and JG2 or JG3 and JG4 were annealed and the 3' ends extended with either the Klenow fragment of E. coli DNA polymerase I or with AMV reverse transcriptase, to generate double stranded DNA fragments of approximately 150bp. The efficiency of double strand synthesis was significantly better when reverse transcriptase was used for this reaction; probably reflecting its ability to melt out G-C rich hairpins. The products of the reaction, which contained trace levels of ^{32}P-dATP were

separated on preparative 4% polyacrylamide gels, together with appropriate size markers, the region containing the 150bp band excised and the fragment eluted. Approximately 0.6µg of double-stranded product was obtained in each case.

2. Cloning into the expression vector: The initial vector of choice for these studies was the pUC118 of Messing and Viera (20). This cloning/expression vector contains a polylinker cloning site in the ß-galactosidase coding region; expression being under control of the lacZ operator and promoter. Cloning of the 150bp synthetic gene into the unique SmaI site in this vector results in an in-frame gene fusion and a hybrid polypeptide that consists of a decameric repeat of the elastin pentamer and the first 80 amino acids of ß-galactosidase (α-subunit). Since this fusion protein retains the ability to complement bacterial strains with a defective ß-galactosidase α-subunit, bacteria carrying the recombinant pUC118 yield blue colonies in the presence of X-gal and the inducer IPTG.

In initial experiments we attempted to clone directly into the SmaI cut pUC118 plasmid, and following transformation to screen colonies by colony hybridization using ^{32}P-labelled oligonucleotides. The high G+C content of the oligonucleotides however resulted in very high background and an inability to identify positive colonies. We have therefore first cloned into the SmaI site of the single stranded phage M13mp18. The cloning of tandem arrays of the insert was avoided by leaving the double stranded 150 base pair insert non-kinased (i.e., without 5'-phosphate) Those phage containing the insert in the correct orientation for expression could be identified by using only JG1 and JG3 oligonucleotides to probe nitrocellulose lifts of the ensuing phage plaques.

Approximately 20 plaques for each of the JG1/JG2 and JG3/JG4 series were picked and both double stranded RF form DNA and single stranded phage DNA was prepared. The insert in each was sized by cutting the RF DNA with EcoRI and PstI (unique enzyme sites that flank the insert) and by sequencing using the M13 universal primer. Many of the inserts which yielded blue plaques (i.e., in-frame fusions) nevertheless represented incomplete copies of

the synthetic gene. For each of the 2 synthetic genes, one clone, containing a full length in-frame copy of the gene, was chosen, and the 190 base pair EcoRI/PstI fragment transferred to pUC118. The presence of the fragment was confirmed by restriction enzyme analysis and the insert sequenced by the Maxam-Gilbert chemical cleavage method. In this way, we have confirmed the sequence and in-frame fusion for both the JG1/JG2 (Clone 14) and JG3/JG4 (Clone 16) genes. The sequencing studies did reveal 2 nucleotide changes in the JG1/JG2 gene (one A to C and one C to A) but neither affected the amino acid encoded by the codon.

3. Expression of the polypentapeptide sequences. Since bacteria containing the pUC118 plasmids with either full length insert yielded blue colonies in the presence of IPTG and X-gal, it is clear that both fusion proteins can be synthesized in this prokaryotic system. Furthermore the inserts, despite their redundancy of sequence, appear to be maintained in a stable fashion in their bacterial hosts in the absence of induction. The expected size of the fusion product is in the order of 13-14kD and we initiated experiments to identify and characterize the product synthesized in induced cells. In these preliminary experiments we grew cells overnight in minimal medium containing glucose, diluted 1:100 in B-broth and grown to an OD 600 of 0.6 prior to inducing the lac-fusion gene expression with IPTG. To investigate the size and abundance of the fusion protein (which would be predicted to be 13-14kd), cells were grown overnight in minimal medium containing glucose, diluted 1:100 in B-broth and grown to an OD of 0.6 prior to induction with 1PTG. These initial experiments yielded faint, poorly reproducible bands of the expected molecular weight although in some experiments diffuse bands at a M.W. of approximately 40kd were seen in cell extracts of bacteria carrying the JG3/JG4 insert. Given the unusually high proline content of the polypentapeptide sequence (20%) abnormal migration on SDS-polyacrylamide gels is highly likely. These experiments clearly demonstrate that the highly reiterated polypentapeptide sequence can be propagated in a stable fashion in bacterial plasmids and the products, consistent with those expected from a polypentapeptide-ß-gal fusion, could be observed. However, despite these promising results, it became clear that the pUC expression system

would not be appropriate for the long term goals of this project. First: the levels of fusion protein seen after induction were insufficient for scale-up; second, the construction yielded a fusion protein too small for easy detection and characterization.

In an attempt to overcome these problems we have attempted to develop expression of the polypentapeptide sequence using two additional expression vector systems. In addition, in order to produce biological products that approach the sizes of those obtained by synthetic approaches we have constructed dimer and trimer inserts of the n = 10 polypentapeptide sequences. The ability to synthesize in bacteria proteins of 50, 100, and 150 amino acids should facilitate biophysical studies on the microbial-derived product. In order to generate these multimeric inserts the overlapping oligonucleotides were hybridized and extended as before, sized on a polyacrylamide gel, phosphorylated and then ligated at moderate concentrations. The preligated inserts were then blunt-end ligated into the SmaI site of pUC118. Plasmids containing suitably sized inserts were selected and the inserts subjected to sequence analysis either by the Maxam-Gilbert chemical degradation method or by the Sanger dideoxy-method. Initial sequencing results indicated that monomer, dimer and trimer sequences capable to encoding polypentapeptide molecules of 50, 100 and 150 amino acids had been obtained and that these could be stably propagated in E. coli. In collaboration with Dr. Casey Morrow, Department of Microbiology, the monomer, dimer and trimer inserts were removed from the pUC plasmid by EcoRI/Pst I digests and inserted into the pATH3 vector of Koorner, et al. This vector utilized the highly efficient inducible tryptophan operator-promoter system for expression of foreign genes. Thus bacteria can be grown to high density then depleted of tryptophan and induced to express by addition of the tryptophan competitor indole acrylic acid (1AA). The pATH vectors have the advantage that the inserted gene is preceded by trpE coding sequences that encode a 34kd protein, and followed immediately by a termination codon. Thus the presence of foreign coding sequences can be assayed by a mobility shift of the trpE-polypentapeptide fusion protein. In addition to providing a method for assessing the size of the translated protein sequences, the large size of the product makes

identification by gel electrophoresis and immunological blotting procedures much more straightforward. The vector also has the advantage that, once expression has been confirmed, the bulk of the trpE coding sequencing can be removed by cutting the plasmid with unique restriction enzymes. The synthetic gene insert can then be expressed with just a minimal leader sequence.

Through the use of a trpE expression vector, trpE fusion proteins have been produced containing both n=10 and n=20 elastin sequences. The level of fusion protein synthesis in the recA$^-$ bacterial host (DH-1) is approximately 5-10 fold lower that in recA$^+$ (C600) but in the latter a ladder of products are observed consistent with deletion of coding sequences through homologous recombination..

It is clear that we are only at the beginning of exploiting microbial synthesis of the sequential polypeptides, but it is also clear that development of this technology will be essential in order to explore fully the potential of synthetic protein comprised of repeating sequences.

AN HYDRATION MEDIATED FREE ENERGY DRIVING FORCE FOR PROTEIN FOLDING AND ASSEMBLY

Dan W. Urry
Laboratory of Molecular Biophysics
University of Alabama at Birmingham
Birmingham, Alabama

Send Correspondence and Proofs to:

Dan W. Urry, Ph.D., Director
Laboratory of Molecular Biophysics
University of Alabama at Birmingham
UAB Station, P.O. Box 300
Birmingham, AL 35294

I. INTRODUCTION

The hydrophobic effect and electrostatic interactions are two prominent considerations for protein folding and assembly in an aqueous medium. With the known crystal structures of globular proteins in an aqueous mother liquor, it is appreciated that hydrophobic side chains of residues such as Phe, Ile, Leu, Val, etc. are generally buried within the interior of the protein. Additionally, there are examples where the change in a single charge can cause dramatic changes in the assembly of protein subunits. Such dramatic effects are cited as indicating the exquisite importance of electrostatic interactions in protein structure. In the present review, it is argued with experimental data that the existence of an interactive hydrophobic-electrostatic repulsive free energy in an aqueous environment is responsible for this exquisite modulation of protein structure. This has been called an aqueous mediated apolar-polar repulsion free energy. It is demonstrated here in terms of 1) the effect of changes in hydrophobicity on the pK_a of a weak acid, 2) the effect of added charge on the endothermic heat of an inverse temperature transition, and 3) the interconversion of mechanical and chemical work in elastic polypeptides which are capable of folding due to an inverse temperature transition (thermomechanical transduction) and which may also be designed to exhibit chemomechanical transduction by application of the apolar-polar free energy of interaction (1).

II. ASSAY SYSTEM FOR EVALUATING APOLAR-POLAR INTERACTION FREE ENERGIES

A. Sequential Polypeptides in Helical Array

The aqueous polypeptide systems wherein the apolar-polar interaction free energies have been observed utilize elastomeric sequential polypeptides with repeating sequences which can become arranged in a dynamic, regular, helical array as the result of an inverse temperature transition , i.e., as the result of an increase in order within

the polypeptide as the temperature is raised over the transition temperature range (2). The parent molecular system is poly(VPGVG) or $(L\text{-}Val^1\text{-}L\text{-}Pro^2\text{-}Gly^3\text{-}L\text{-}Val^4\text{-}Gly^5)_n$. On raising the temperature of this sequential polypeptide in water, it orders into a helical array of pentamers in which there occur $Val^1C\text{-}O \cdots HN\text{-}Val^4$ hydrogen bonds in the formation of Type II β-turns (as seen in Figure 1A)(3). This helical array of β-turns is called a β-spiral, and there are approximately three pentamers per turn of spiral (helix)(4). The β-turns function as hydrophobic spacers between turns of the spiral with the Pro β $C\underline{H}_2$ hydrogens of one turn of the spiral in hydrophobic contact with the $Val^1\gamma\ C\underline{H}_3$ hydrogens of the adjacent turn. The interturn interactions are apparent in Figure 1B which is a space filling model of the structure in Figure 1A. Furthermore, these β-spirals associate by hydrophobic intermolecular interactions to form twisted filaments that may be seen by transmission electron microscopy using negative staining techniques (5).

B. Elastic Matrices

Thermomechanical Transduction: When the aggregated state, which forms on raising the temperature above that of the inverse temperature transition, is γ-irradiation cross-linked, the result is an elastomeric matrix without detectable change in carbon-13 and nitrogen-15 NMR spectra (2). At temperatures below that of the inverse temperature transition, the elastomeric matrix swells and the polypeptide chains would become dispersed over the entire solution if it were not for the cross-linking. With 20 Mrad cross-linking, the increase in length due to swelling is about a factor of 2.2. On raising the temperature above that of the inverse temperature transition, the elastomeric matrix contracts and is capable of picking up weights that are several thousand times the dry weight of the matrix. The temperature at which this thermomechanical transduction occurs depends on the hydrophobicity of the polypentapeptide. For poly(IPGVG) where I = Ile, the contraction and, of course, the

responsible inverse temperature transition occurs at a lower temperature, near 10°C, rather than at 30°C as occurs for poly(VPGVG) (2). For poly(VPGAG) where A = Ala, the inverse temperature transition occurs near 70°C. (T. Parker, K. U. Prasad and D. W. Urry, unpublished data).

Chemomechanical Transduction: When poly[4(VPGVG),(VPGEG)] where E = Glu is prepared and cross-linked, the temperature for the inverse temperature transition and for the contraction depends on the pH. In phosphate buffered saline (0.15 N NaCl, 0.01 M phosphate) at pH 2, the contraction occurs near 25°C whereas at pH 7, the contraction occurs near 70°C (1). Thus, it is possible to remain at 37°C and by changing the pH, to bring about contraction and relaxation. This is chemomechanical transduction (mechanochemical coupling); it is a chemically induced folding and unfolding of the β-spiral. Determination of the chemical work, of lowering the pH (increasing proton concentration) required both to achieve the mechanical work and to drive the inverse temperature transition, provides a measure of the free energy changes involved. This is one means of demonstrating the presence of an interaction free energy, but there are more direct demonstrations of what is occurring at the molecular level as is also discussed below.

III. MEANS OF DIRECTLY DETERMINING THE INTERACTION FREE ENERGY

A. Hydrophobicity- Induced pK Shifts

One of the advantages of a repeating sequence in a regular helical array is that an interaction free energy is amplified or multiplied by the number of repeats. This is particularly apparent when comparing the two sequential polypeptides: poly[4(VPGVG),(VPGEG)] and poly[4(IPGVG),(IPGEG)]. The conformations of these two molecular systems have been shown to be the same at low pH and to change to the same new conformation at high pH as has been shown by 2D NMR, particularly 2DNOESY

studies (6). This had also been shown by circular dichroism for poly(VPGVG) and poly(IPGVG) at temperatures below and then above their respective temperature ranges for their inverse temperature transitions (7). If, however, the polymers are titrated by acid or base to determine the pK_a of the carboxyl moiety in the Glu side chain, it is found that the pK_a is one pH unit higher for the more hydrophobic sequential polypeptide as shown in Figure 2. This pK_a shift is also apparent in the pH dependence of the temperatures of the inverse temperature transition and in the plots of the pH dependence of length at similar loads for the cross-linked elastomeric matrices (6). Thus, the addition of one CH_2 moiety per pentamer in a polypentapeptide that contains only four carboxyl functions in 100 residues is sufficient to make the occurrence of the COO^- moiety energetically less favorable.

An estimate of this repulsive free energy of interaction can be achieved from the change in chemical potential required to achieve 50% ionization, i.e., $\Delta\mu = -2.3RT\Delta pK_a$. Since the ΔpK_a (= 4.4 – 5.4) is approximately minus one at 37°C, then $\Delta\mu$ is 1400 cal/mole. Interestingly, this is the difference in the hydrophobicities of Val and Ile on the Nozaki and Tanford (8) hydrophobicity scale as listed by Bull and Breese (9).

B. Stretch-Induced pK Shifts and Comparison of Contractile Mechanisms

As noted above, the contraction aspect of the thermomechanical transduction is the result of the polypeptide folding into a dynamic, regular, helical array of β-turns with formation of intramolecular as well as intermolecular hydrophobic contacts. Thus, on stretching of the elastomer by the application of a force, Δf, as shown in Figure 1C, hydrophobic side chains become exposed to the water and clathrate-like water forms. Now it becomes of interest to know the direction of pK_a shift, if any, on increasing the force by stretching. On stretching, the pKa of the carboxyl moiety is increased, i.e., $\Delta\mu$ is negative. Thus, the $(\partial\mu/\partial f)_n < 0$. This is exactly the opposite of what is found for the polyelectrolyte mechanochemical system: polymethacrylic acid, [-(COOH)C(CH_3)-CH_2-

]$_n$ (10). In this mechanochemical system, contraction also occurs on lowering the pH. But in this case, it is the relieving of electrostatic repulsion that causes the collapse of extended chains on lowering the degree of ionization from 50% or more to 0 or 10%. In this case, the $(\partial\mu/\partial f) > 0$ which means that the pK_a is lowered on stretching (11,12). Thus for the same moiety, we have a clear distinction between the long appreciated electrostatic interaction mechanism, actually charge-charge repulsion, and the new mechanism, referred to above, as an aqueous mediated apolar-polar repulsion free energy. Since both the cross-linked polymethacrylic acid and poly[4(VPGVG),(VPGEG)] systems contract to about one-half their extended length and since both can pick up weights that are several thousand times their dry weight, it is interesting to compare the amount of chemical work that is required to achieve the similar amount of mechanical work. For polymethacrylic acid it takes the conversion of some 50 carboxylates to carboxyls to do the work, whereas for poly[4(VPGVG),(VPGEG)], it takes only the conversion of some four carboxylates to carboxyls in a matrix with more than an order of magnitude lower density of carboxyl moieties. Thus, it would seem that the new mechanism is more efficient than electrostatic interactions by an order of magnitude. As will be shown below, a chemically elicited conformational change in a protein can be viewed as chemomechanical transduction. With the above-considered efficiency, it is natural to expect that the mechanism of preference for the chemically elicited protein structural changes, which occur in the process of function in living organisms, would be that of an aqueous mediated apolar-polar interaction free energy because much less food (chemical energy) would be required for the organism to function.

C. Effect of Charge on the Endothermic Heat of the Inverse Temperature Transition

The above shift in pK_a resulting from a change in hydrophobicity provides one means of evaluating the interaction free energy of charge hydration when proximal to

hydrophobic hydration. As was seen from the increase in pK_a with increase in hydrophobicity, this is a repulsive interaction free energy, that is, on replacing Val by Ile the increase in free energy of the carboxylate moiety is 1400 cal/mole. Thus an interpretation of this data is that there exists an antagonism between the structure of water required for polar hydration and that required for apolar hydration when these disparate hydration processes are sufficiently proximal. This is the source of the proposed hydration mediated apolar-polar repulsive free energy of interaction. What is now desired is a means of observing the effect from the opposite perspective, i.e., to determine whether the addition of charge does indeed result in the destructuring of clathrate-like water surrounding hydrophobic groups.

At this stage it is useful to recall 1) that the solubility of a solute in water depends on the change in Gibb's free energy of dissolution $\Delta G = \Delta H - T\Delta S$ where ΔH and ΔS are the change of heat content or enthalpy and the change in entropy, respectively, on hydration, 2) that a negative ΔG is favorable for dissolution, 3) that the dissolution of hydrophobic solutes in water is exothermic (i.e., ΔH is negative) (13,14), but 5) that solubility of hydrophobic solutes is low due to a substantially negative ΔS such that the quantity $(-T\Delta S)$ is positive. Accordingly for hydrophobic solutes in water, ΔH and $(-T\Delta S)$ are of similar magnitude but of opposite sign. The positive ΔS is considered to arise from an increase in the order of the water that is at the surface of the hydrophobic moiety (13-15). This more-ordered water abutting hydrophobic moieties has been referred to as clathrate water, and pentagonal dodecahedral water structure has been found surrounding methane gas molecules in crystals of gas hydrates (16) and in Monte Carlo studies on the structure of a dilute aqueous solution of methane (17).

Returning to our polypentapeptide of interest, poly[4(VPGVG),(VPGEG)], the dissolution in water below 25°C is considered to be an exothermic reaction dominated by the hydration of the Val and Pro side chains and resulting in the formation of clathrate-like water. On raising the temperature through the range of the inverse temperature

transition, the more-ordered clathrate-like water is expected by an endothermic reaction to become less-ordered bulk water as the polypentapeptide folds into the β-spiral conformation. By means of differential scanning calorimetry, this inverse temperature transition is indeed seen to be an endothermic transition (18) which is, therefore, reasonably interpreted to be due to the destructuring of the clathrate-like water, that is, to be simply the inverse of the exothermic reaction of hydration of the hydrophobic side chains. The endothermic heat of the transition at pH 2.5, where essentially all of the Glu side chains are COOH, is 0.97 kcal/mole (18). Now it is of interest to see the effect of converting carboxyls to carboxylate anions. At pH 4 one of the four carboxyl moieties per 100 residues has been converted to a carboxylate anion, and significantly the endothermic heat of the transition has been remarkably reduced to 0.27 kcal/mole (18). Since the endothermic heat of the inverse temperature transition is taken to cause the destructuring of the clathrate-like water, then the effect of converting one carboxyl moiety to a carboxylate anion per every 100 residues is to have destructured three-quarters of the clathrate-like water. Thus, hydration mediated apolar-polar repulsion free energy has been seen from both perspectives. From one perspective, when an increase in hydrophobicity is forced on the molecular system by replacing the Val residue with the more hydrophobic Ile residue, then the pK_a of the carboxyl moiety is increased indicating the energetically less favorable situation for the carboxylate anion (6). From the other perspective, if the carboxylate anion is forced on the molecular system by a change in pH, then the system responds by a destructuring the clathrate-like water surrounding hydrophobic groups (18). It is this aspect of the capacity of a polar species to destructure clathrate-like water that is considered below as a primary means of modulating protein folding and assembly.

IV. RELEVANCE OF APOLAR-POLAR INTERACTION FREE ENERGIES TO PROTEIN FOLDING AND ASSEMBLY

Protein Folding: Analogy to a Clam-Shaped Globular Protein

By way of illustration, the effect of aqueous mediated apolar-polar interaction free energy can be demonstrated by consideration of a clam-shaped protein which is capable of existing in two conformations, open and closed (see Figure 3). Above the temperature of the inverse temperature transition for folding to form the closed state, the hydrophobic residues are buried within the fold. To the extent allowed by the Gibb's free energy difference, there can be an occasional opening, in which case the formerly buried hydrophobic side chains become exposed to water with the formation of clathrate-like water at the contact surface. It is the formation of so much clathrate-like water that is unfavorable at the considered temperature. If, however, the polar phosphate species is added at the edge of the folding cleft, then this very polar species would destructure the clathrate-like water in its vicinity as shown in Figure 3. Just as the formation of one carboxylate anion per 100 residues destructures three-fourths of the thermodynamically-evidenced clathrate-like water in poly[4(VPGVG),(VPGEG)], phosphorylation is considered to remove a critical part of the thermodynamic driving force for closure and the equilibrium is shifted toward the open state as indicated.

If it were possible to string together a series of clam-shaped globular proteins by means of fine wires attached near the mouth and connecting adjacent globular proteins, as shown in Figure 4, it would be possible to measure the driving force for closure. While it is not possible to measure the driving force in this way for the conformational change of the clam-shaped globular protein, it is possible to do the equivalent with the polypentapeptide because of its β-spiral conformation. The continuous polypeptide backbone of the polypentapeptide β-spiral replaces the need for the wire, and the interturn hydrophobic interactions (apparent when comparing Figures

1B and C) become equivalent to the hydrophobic interactions that occur on closure of the clam-shaped globular protein. It becomes possible, therefore, to measure the driving forces for the conformational change giving rise to contraction, and, by chemical modulation, (e.g., protonation or deprotonation) to demonstrate the existence of the apolar-polar interaction free energy. The simplicity of an experiment, wherein contraction and relaxation and the picking up and setting down of a weight occur, leaves little to the imagination as to whether or not work has been done and as to whether or not driving forces are turned on and off.

Protein Assembly: Modulation of filament formation

By way of illustration for protein assembly, consider a filament comprised of globular proteins as shown in Figure 5. The contact surfaces are hydrophobic such that at one end where the hydrophobic side chains are exposed to the aqueous milieu, there is a layer of clathrate-like water. At a temperature above that of the inverse temperature transition for association, the equilibrium favors filament formation. If, however, phosphorylation occurs near the contact surface, as shown, then the polar phosphate moiety will cause the destructuring of the clathrate-water in its vicinity that would have otherwise formed. This shifts the equilibrium toward dissociation.

Acknowledgments: We would like to express appreciation to Larry Hayes for carrying out the titrations of Figure 2, and to D. K. Chang for generating the molecular structure of Figure 1. We would also like to acknowledge NIH grants GM26898, HL29785 and Department of the Navy Office of Naval Research contract N00014-86-K-0402.

References

1. Urry, D. W., Haynes, B., Zhang, H., Harris, R.D., and Prasad, K.U., "Mechanochemical Coupling in Synthetic Polypeptides by Modulation of an Inverse Temperature Transition," Proc. Natl. Acad. Sci. USA, 85, 3407-3411, 1988.

2. Urry, D. W., "Entropic Elastic Processes in protein Mechanisms. I. Elastic Structure Due to an Inverse Temperature Transition and Elasticity Due to Internal Chain Dynamics," J. Protein Chem., 7, 1-34, 1988.

3. Chang, D.K., and Urry, D. W., in preparation

4. Chang, D.K., Venkatachalam, C. M., Prasad, K.U. and Urry, D.W., "Nuclear Overhauser Effect and Computational Characterization of the β-Spiral of the Polypentapeptide of Elastin," J. of Biomolecular Structure & Dynamics (in press).

5. Urry, D.W., "Characterization of Soluble Peptides of Elastin by Physical Techniques," In Methods in Enzymology (L.W.Cunningham and D.W. Frederiksen, Eds.) Academic Press, Inc., New York, NY, 82, 673-716, 1982.

6. Urry, D.W., Chang, D.K., Zhang, H., and Prasad, K.U. "pK Shift of Functional Group in Mechanochemical Coupling Due to Hydrophobic Effect," Biochem. Biophys. Res. Commun., 153, 832-839, 1988.

7. Urry, D.W., Long, M.M., Harris, R.D., and Prasad, K.U., "Temperature Correlated Force and Structure Development in Elastomeric Polypeptides: The Ile^1 Analog of the Polypentapeptide of Elastin," Biopolymers, 25, 1939-1953, 1986.

8. Nozaki, Y. and Tanford, C. J., "The Solubility of Amino Acids and Two Glycine Peptides in Aqueous Ethanol and Dioxane Solutions," Biol. Chem. 246, 2211-2217, 1971.

9. Bull, H. B., & Breese, K., "Surface Tension of Amino Acid Solution: A Hydrophobicity Scale of the Amino Acid Residues." Arch. Biochem. Biophys. 161, 665-670, 1974.

10. Kuhn, W., Hargitay, B., Katchalsky, A., and Eisenberg, H., "Reversible Dilation and Contraction by Changing the State of Ionization of High-Polymer Acid Networks," Nature, 165, 514-516, 1950.

11. Katchalsky, A., Lifson, S., Michaeli, I., and Zwick, "Elementary Mechanochemical Processes," Size & Shape of Contractile Polymers: Conversion of Chemical into Mechanical Energy, A. Wasserman, Ed. (Pergamon, New York) 1-40, 1960.

12. Kuhn, W., Ramel, A., and Walters, D. H., "Conversion of Chemical into Mechanical Energy by Homogenous and Cross-striated Polymeric Systems" in

Size & Shape of Contractile Polymers: Conversion of Chemical Into Mechanical Energy. A. Wasserman, Ed. (Pergamon, New York) 1-40, 1960.

13. Franks, H. S., Evans, M.W., "Entropy of Vaporization in Liquids and the Pictorial Theory of the Liquid States," J. Chem. Phys. 13 493-507, 1945.

14. Kauzmann, W., "Some Factors in the Interpretation of Protein Denaturation," Adv. Protein Chem. 14 1,1959.

15. Edsall, J. T., and McKenzie, H. A., "Water and Proteins. II The Location and Dynamics of Water in Protein Systems and Its Relation to Their Stability and Properties" Adv. Biophys. 16 53-183, 1983.

16. Stackel, M. V. and Muller, H. R., "Zur Struktur der Gashydrate," Naturwissenschaften, 38, 456, 1951.

17. Swaminathan, S., Harrison, S.W., and Beveridge, D., "Montecarlo Studies on the Structure of a Dilute Aqueous Solution of Methane," J. Amer. Chem. Soc. 5705-5711, 1978.

18. Urry, D.W., Luan, C. H., Harris, R.D., and Prasad, K.U., "Chemical Modulation of the Hydrophobic Effect, A Driving Force in Protein Folding and Assembly." (in preparation).

Figure Legends

Figure 1 A. Stereo pair of the relaxed state of the poly(VPGVG) β-spiral with 2.9 pentamers/turn.

B. Space filling model of the relaxed state of the poly(VPGVG) β-spiral with 2.9 pentamers/turn. The interturn hydrophobic contacts are apparent.

C. Space filling model of the 130% extended state of the poly(VPGVG) β-spiral. Extension demonstrates the removal of the interturn hydrophobic contacts.

Figure 2 Plots of percent ionization derived from the acid → base titrations of a. poly[4(VPGVG),(VPGEG)] and of b. poly[4(IPGVG),(IPGEG)]. The presence of one added CH_2 moiety in each pentamer achieved by replacing Val^1 by Ile^1 causes the pK_a of the Glu residues to be raised by one pH unit. This represents an increase in free energy of interaction for the carboxylate anion of 1400 cal/mole in the Ile^1 polypentapeptide.

Figure 3 Model of a clam-shaped globular protein capable of existing in two states, closed and open.

A. Above the temperature of the inverse temperature transition, the equilibrium favors the closed state with hydrophobic side chains in intramolecular interaction. On opening, the hydrophobic surfaces become covered with a layer of clathrate-like water which at this temperature is not thermodynamically favored.

B. On phosphorylation near the cleft, the effect of the added negatively charged phosphate is to destroy or to destructure, from the

thermodynamically measurable point of view, the clathrate-like water in its vicinity such that now the open state is favored. This is chemomechanical transduction which with the proper cross-linking could be used to demonstrate mechanochemical coupling.

Figure 4 Schematic drawing showing analogy between an aligned series of attached (cross-linked) clam-shaped globular proteins with about one-half opened and one-half closed and a partially extended β-spiral in which there are some interturn hydrophobic interactions and some turns of the β-spiral are too far apart to make hydrophobic contact. This demonstrates that a protein conformational change as occurs in the opening and closing of a globular protein can develop a mechanical force and that such forces can actually be measured in the polypentapeptide β-spiral system once interchain cross-linking has occurred to form the macroscopic elastomeric matrix.

Figure 5 Chemical modulation of filament assembly by means of hydration mediated apolar-polar interaction free energies. Demonstrated is a filament comprised of a globular protein subunit with two hydrophobic surfaces. Above the temperature of the inverse temperature transition for intermolecular hydrophobic association of subunits, on dissociation a thermodynamically unfavorable coat of clathrate-like water forms on the hydrophobic surfaces shifting the equilibrium toward association. Once phosphorylated on dissociation there is less thermodynamically measurable clathrate-like water formation and the equilibrium is shifted toward dissociation.

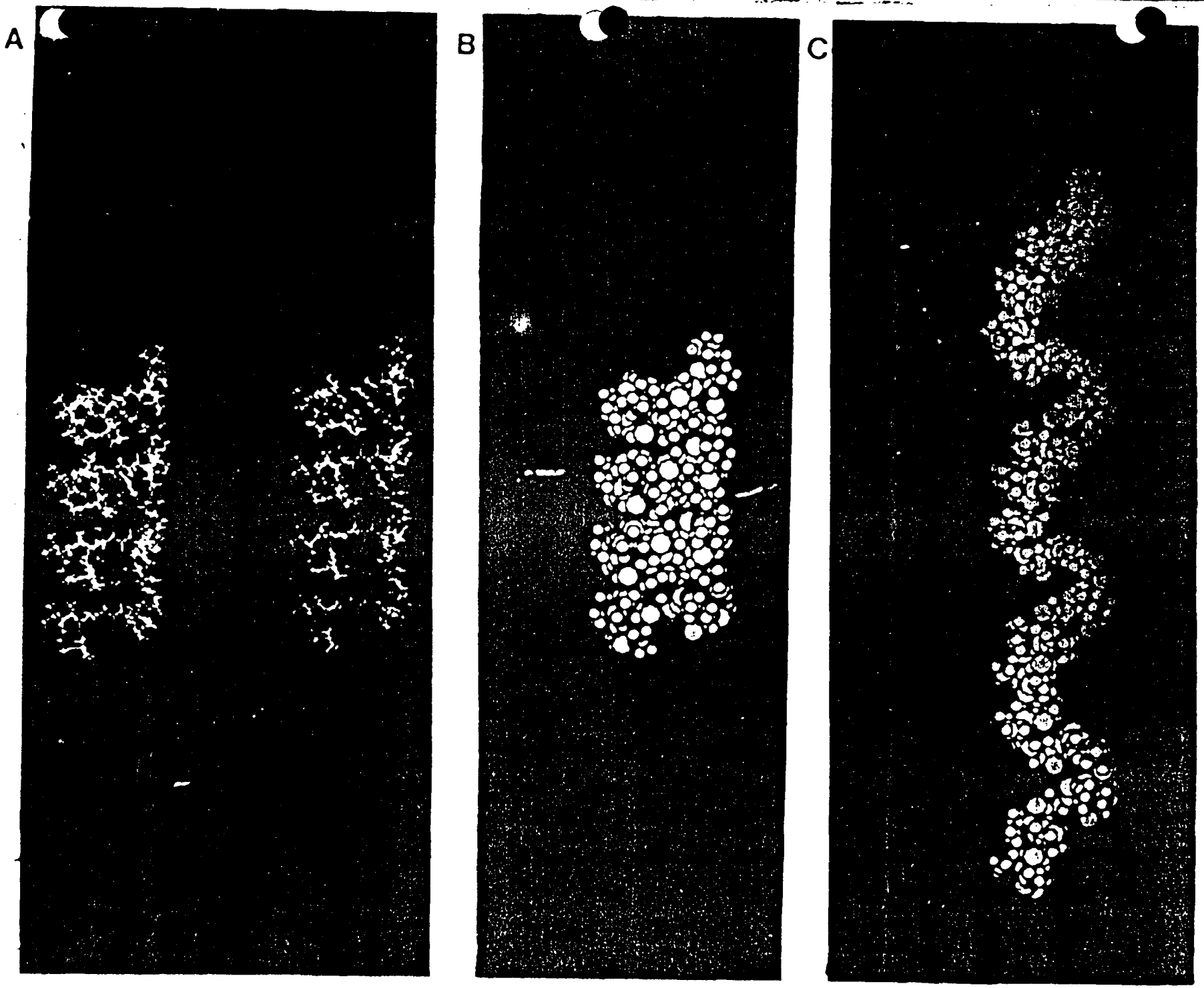

FIGURE 1

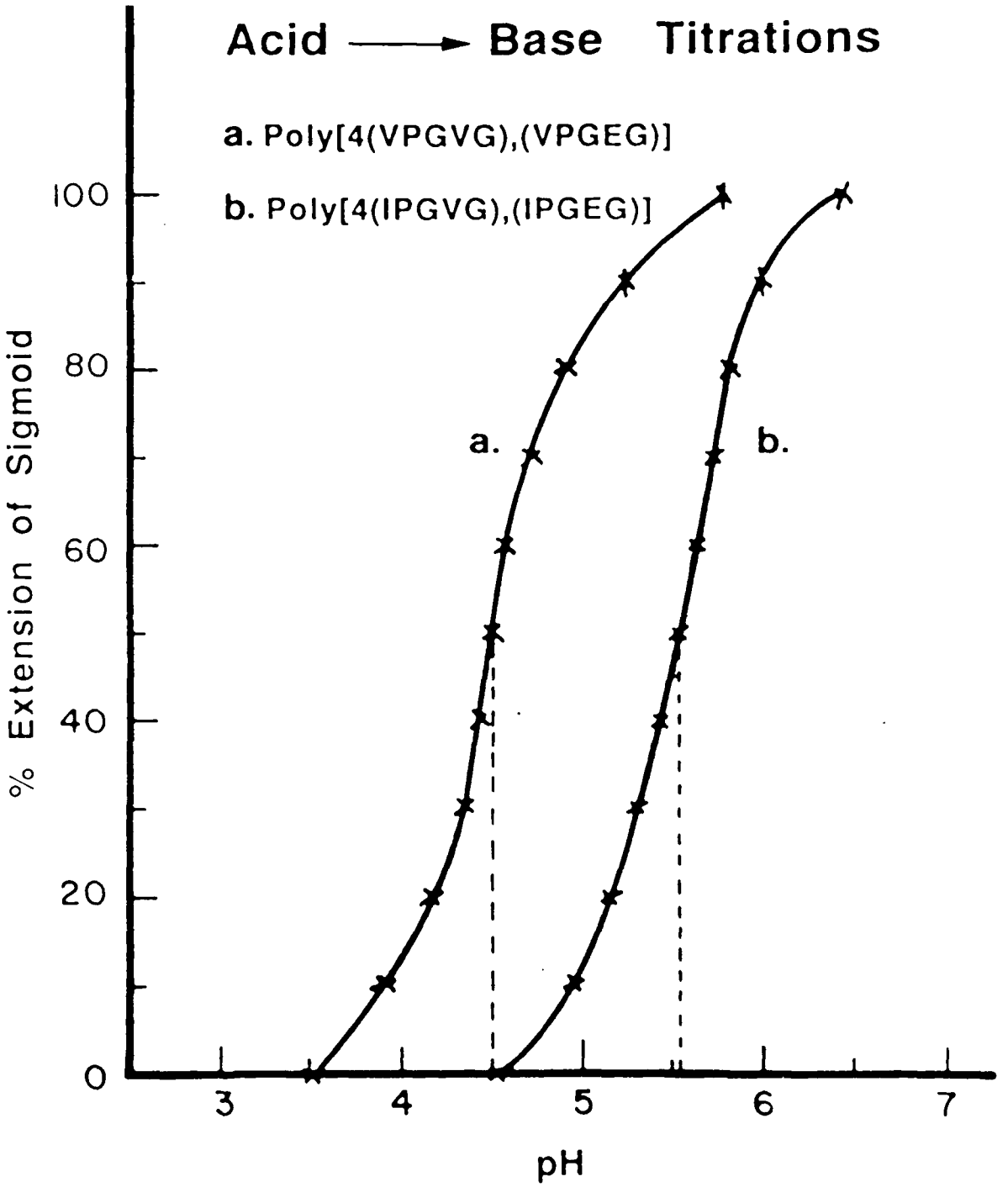
Acid ⟶ Base Titrations
a. Poly[4(VPGVG),(VPGEG)]
b. Poly[4(IPGVG),(IPGEG)]
% Extension of Sigmoid
100
80
60
40
20
0
a.
b.
3
4
5
6
7
pH

FIGURE 2

Clam-shaped Globular Protein

On opening, above the temperature of inverse temperature transition, there forms a thermodynamically unfavorable clathrate-like shell of water surrounding exposed hydrophobic moieties.

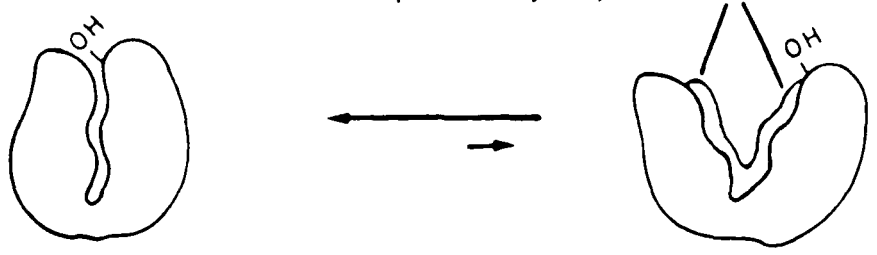

closed
(Intramolecular hydrophobic interactions)

open

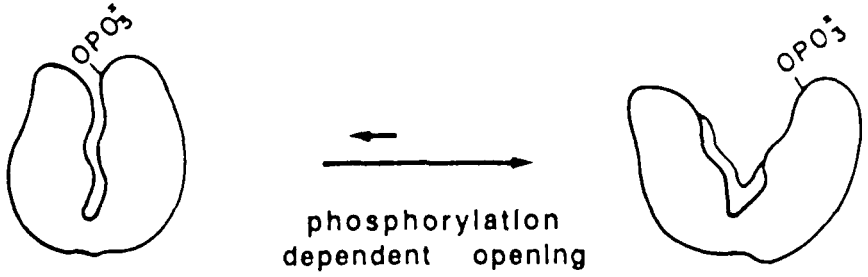

phosphorylation dependent opening

On phosphorylation, there forms less thermodynamically measurable clathrate-like water on opening. Transition termperature is raised due to decrease in magnitude of ΔH and ΔS with $\delta\Delta H < \delta\Delta S$.

FIGURE 3

Analogy between Conformational Change in Globular Proteins and Contraction in Elastomeric Filaments

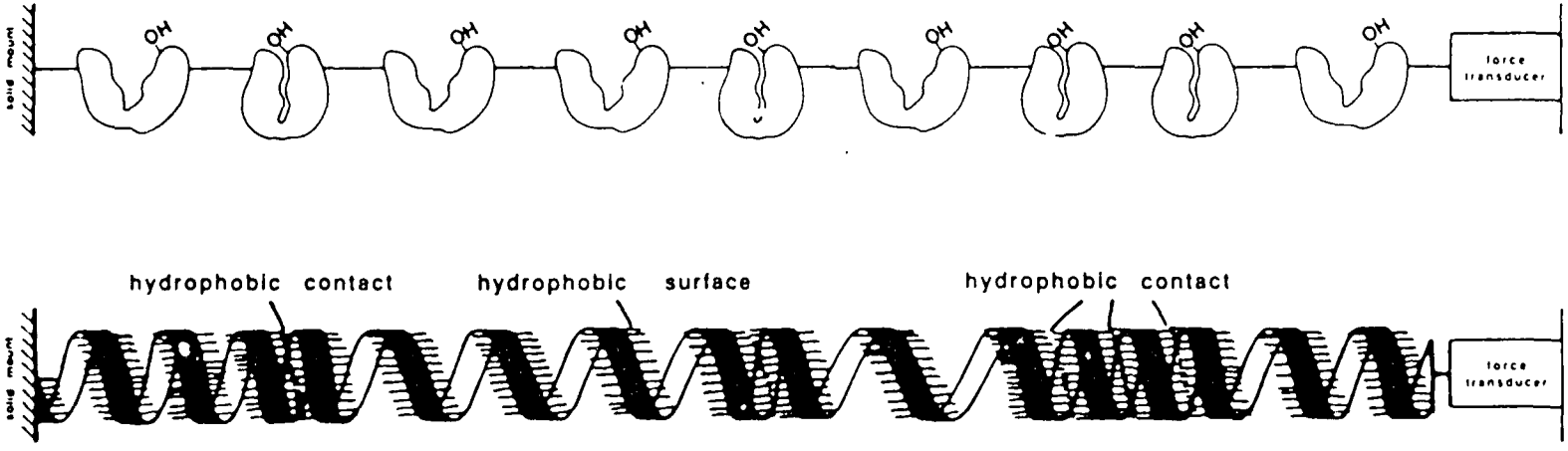

FIGURE 4

MODULATION OF FILAMENT ASSEMBLY

filament of globular proteins

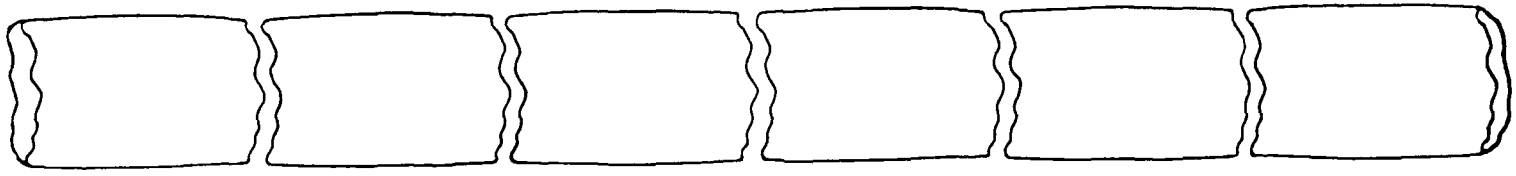

modulation of association at filament growth end

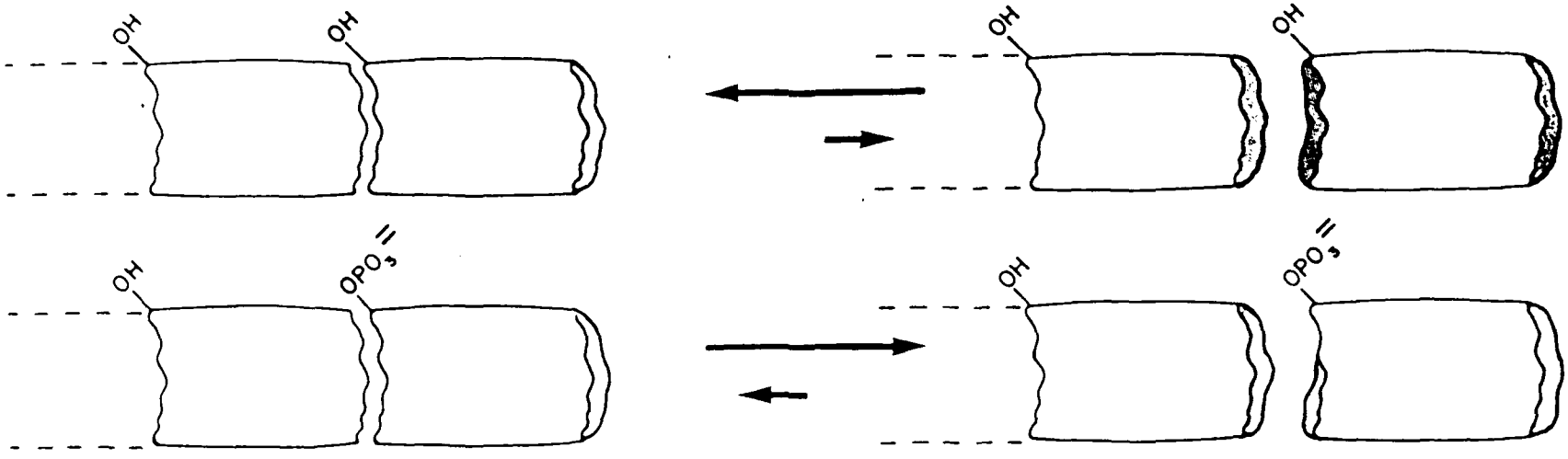

(shaded areas represent a shell of clathrate water)

FIGURE 5

m. 6/2/89
CH

Polypentapeptide of Elastin: Damping of Internal Chain Dynamics on Extension

D. K. Chang and D. W. Urry

The Laboratory of Molecular Biophysics, University of Alabama at Birmingham, P.O. Box 300/UAB Station, Birmingham, AL 35294

Received 12 October 1988; accepted 8 March 1989

Molecular dynamics simulations out to 100 ps have been carried out at 300 K in vacuo on the repeating pentapeptide, (VPGVG), of the elastin fiber. The structure employed in the simulation is a β-spiral (helical structure) with 2.7 pentamers per turn and with a 9.45 Å rise per turn and 21.6 Å rise per turn in the relaxed and extended states, respectively. Large amplitude backbone torsion angle fluctuations are observed in the relaxed state, and significant damping is observed upon extension, particularly in the suspended segments of the β-spiral structure. Accordingly the entropy change an extension was computed and found to be a substantial −1.1 entropy units per residue. The various energy components are compared for relaxed and extended states and the relevance of the results to the molecular mechanism of entropic elasticity is discussed.

INTRODUCTION

The thermodynamics of the elasticity of elastin is reasonably well understood. By extending the approach for classical rubber elasticity, Flory and co-workers[1,2] satisfactorily attributed the elasticity of elastin to entropic change upon deformation. This has been confirmed by other authors.[3,4] However, the molecular origin of the entropy change requires continued consideration. The proposition that the solvent molecules provide the dominant source of entropic change[5] has its drawbacks. This is because the characteristic relaxation time for elastin backbone atoms is on the order of 10 ns, which is several orders of magnitude longer than the characteristic time for water and because the half life for loss of elasticity of elastin fibers at 80°C is about three days, which is difficult to interpret in terms of change in the solvent structure particularly at this high temperature.[6] On the other hand, it is natural to regard the peptide polymer as the agent for the entropy change. Applying the random chain network theory to elastin fibers, Flory and co-workers[2] asserted that the elastin system is a particular case of a general, classical rubber-like network theory. Accordingly, all the results derivable from the rubber random chain network model were considered applicable to the case of the elastin protein.

In other studies, the ultrastructural characterization of elastin fibers has been carried out in several laboratories.[6-9] It has been reported that the elastin fibers are filamentous and anisotropic rather than random and isotropic. In particular, in thermoelasticity studies, the development of force at fixed length correlated well with the increase in order as the temperature of aqueous elastin solutions is raised from 20° to 40°C. The development of more ordered structures of elastin polypeptides is accompanied by the extrusion of solvent molecules from the concentrated elastin solution. This can be readily interpreted as the loss of clathrate-like water molecules associated with the elastin peptides resulting in an increase in entropy for the solvent.[9] The study of the synthetic polypentapeptide (PPP), (L-Val[1]-L-Pro[2]-Gly[3]-L-Val[4]-Gly[5])$_n$, which is the most prominent repeating sequence in the elastin protein of cow and pig,[10,11] shows that it is similar to elastin fibers in terms of physical properties.[6] Based on molecular mechanics calculations on (VPGVG)$_3$ and other related peptides,[12] Urry and co-workers proposed a damping of librational motion of peptide backbone moieties as a mechanism

for entropy decrease on extension. A β-spiral structure derived from experimental and computational results[13,14] was used in the study. Specifically, β-turns formed by Val_i^1-Pro_i^2- Gly_i^3-Val_i^4 function as a spacers between turns of helix and Val_i^4-Gly_i^5-Val_{i+1}^1 acts as a suspended segment. The stereo pair plots of the β-spiral poly (*VPGVG*) for seven pentamers are given in Figure 1. An axis view is shown in Figure 1(a)[15] whereas the side view is shown in Figure 1(b).[13] The relaxed and extended states for the pentadecapeptide, $(VPGVG)_3$, β-spiral are given in Figure 1(c) and 1(d), respectively. Damping on extension is observed by molecular mechanics calculations to occur primarily in the suspended segment region.[4] It is depicted in a $Val_i^1\alpha C$ to $Val_{i+1}^1\alpha C$ central pentamer unit of Figure 1(c) and 1(d) with a 2 Kcal/mole residue cut-off energy.[12]

As the mechanism of librational damping of internal chains is dynamic in nature, it would seem that the methods of molecular dynamics in which atoms are assigned kinetic energy would be appopriate. Furthermore, the characteristic correlation times of poly(VPGVG) backbone motion in the coacervate and elastic states, as estimated from

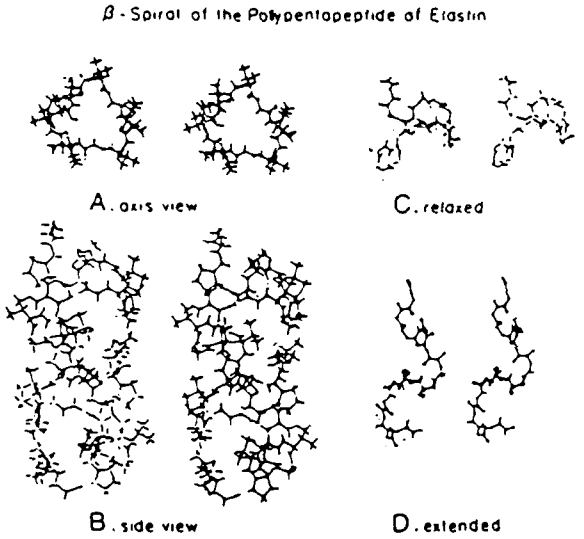

Figure 1. β-spiral structure of the polypentapeptide of elastin, $(VPGVG)_n$, with $n = 7$ in a and b and $n = 3$ for c in the relaxed and for d at 130% extension. The librational damping on extension is shown for the central pentamer unit in c and d as obtained from a molecular mechanics computation with a 2Kcal/mole residue cut-off energy. a and b are reproduced with the [illegible] respectively and c

^{13}C NMR and as determined from dielectric permittivity experiments are on the order of 10 ns.[16,17] Although such long trajectories cannot as yet be reached by molecular dynamics simulation, interesting questions can be asked, such as: Is the β-turn of PPP retained after the dynamics simulation? Is there a damping of internal chain dynamics on extension? Is the internal energy unchanged with stretching? How do various components of energy change with deformation? What is the calculated entropy change for a given extension? In contrast to the random chain network theory, which requires consideration of the distribution of an ensemble of crosslinked chains, only a single chain is needed in the internal chain dynamics approach. In a preliminary attempt, a peptide with seven repeating VPGVG pentamers was employed to carry out 50 ps of molecular dynamics simulation.[18] For such a chain length, end effects are observed probably arising from the need to consider as representatives a central turn of β-spiral wherein turns on each side would provide steric constraints. Consequently only the dihedral angle fluctuations of a limiting central seven residues, i.e., residues 15 to 21, of the chain molecule could be considered as being representative of the effect of elongation. As $n = 11$ in bovine and porcine elastins,[10,11] in the present communication, the results of 11 repeating pentamers are presented that now include 27 representative residues (from 15 to 41) where the primary end effects are absent. The differences between the relaxed and extended states in total internal energy and in van der Waals energy, which is an important element in energetics of protein conformation are noted and their significance is discussed. The in vacuo calculations reported here demonstrate the effects of stretching on polypeptide chain dynamics to be the damping of torsion angle fluctuations on extension.

METHODS

The helical structure was obtained by the procedure of Go and Scheraga[19] as modified by Go and Okuyama[20] for generating helical structures and as described by Venkatachalam and Urry.[21] The structure was then sub-

unfavorable van der Waals contacts first by steepest descents and then by conjugate gradient algorithms. The CHARMm (version 20.3) software package, developed by Karplus and coworkers[22] and adapted by Polygen, Inc., was used in the calculation. All of the hydrogen atoms are explicitly used in all of the energy computations as the interturn interactions involving prolyl ring protons and valyl side chain protons are important. The potential energy functions are as described by Brooks et al.[22] Total potential energy (E_p) is expressed as $E_p = E_b + E_\Theta + E_\phi + E_\omega + E_{vdW} + E_{el}$ where E_b, E_Θ, E_ϕ, E_ω, E_{vdW}, and E_{el} are the potential energies for bond length, bond angle, dihedral angle, improper torsion, van der Waals interaction and electrostatic interactions, respectively. The harmonic approximation was used in E_b, E_Θ, and E_ω. $E_\phi = k_\phi(1 - \cos n\phi)$ where k_ϕ is the force constant for dihedral angle deformation and $n = 1, 2, 3, 4, 6$. E_{el} is represented according to Coulomb's law. The Lennard–Jones 6–12 potential was utilized in evaluation of E_{vdW}.

NH_2-$(VPGVG)_{11}$-OH was used as a model molecule as it is the repeating pentamer sequence in aortic tropoelastin from pig and cow.[10,11,23] A helical structure of 2.7 pentamer units per turn was used in both relaxed and extended states.[12,13] The axial rise was 9.45 Å per turn in the relaxed state and 21.6 Å per turn in the extended state, corresponding to a 130% extension. As in the previous study, the amide nitrogen atom of residue one and carbonyl carbon of residue 55 were fixed in space consistent with the presence of cross-links on both sides of this sequence in the protein.[10,11] In the simulation, chemical bonds to protons were fixed in length such that, with the SHAKE algorithm,[22] a step size of 10^{-15} s could be used The minimized structures for both relaxed and extended states were thermalized to 300 K with 2.5°C rise per 50 steps and the molecules were then equilibrated to distribute more uniformly the kinetic energy and to stabilize the structures after thermalization. During equilibration, since the kinetic energy of the atoms is proportional to the temperature, the kinetic energy was scaled down or up when the temperature of the system became higher or lower than 10°C from the preset temperature of 300 K. It was found that the kinetic energy fluctuated in the process of equilibration, but stabilized to an acceptable value after 45 ps.[18] The importance of a sufficiently long equilibration period in molecular dynamics simulations has been pointed out by Karplus and McCammon.[24] The equilibration period was followed by 100 ps of production stage. The algorithm used for integrating the classical equation of motion adopted in CHARMm was that of Verlet.[25] The root-mean-square (RMS) fluctuations of backbone dihedral angle as well as internal energy (the sum of kinetic and potential energies) were noted during the production period. One set of coordinates for every 50 molecular dynamics steps was stored in the data files.

RESULTS AND DISCUSSION

Table I shows the averages of total internal energy and various potential energy terms for 100 ps of molecular dynamics production time for both relaxed and extended states of $(VPGVG)_{11}$. It is evident that the electrostatic energy is the largest in magnitude among all the energy components. Interestingly, the total energy is lower by 37 Kcal/mole for the relaxed state than for the extended state. Significantly, from Table I, however, it is clear that the van der Waals (vdW) terms account for most of the difference, as had been observed in the shorter trajectory for $(VPGVG)_7$. In the extended state, the vdW interactions between the side chains of residues in adjacent helical turns are absent or much weaker than those in the relaxed state. It is noteworthy in this connection that the hydrophobic interaction between the exposed hydrophobic groups and the solvent upon elongation, an exothermal reaction not taken into account in the present in vacuo calculation, would overcome the loss in vdW interactions. Qualitatively this can explain the small energy contribution, allowing the dominant entropic contribution, to the elastomeric force exhibited by cross-linked poly(VPGVG) when immersed in water.

The RMS fluctuations of backbone dihedral angles for $(VPGVG)_{11}$ are shown in Table II. With a 100 ps trajectory, there is yet a lack of strict pentapeptide periodicity in the RMS fluctuations for the dihedral an-

Table I. Internal energy components of $(VPGVG)_{11}$ in relaxed and extended states resulting from 100 ps molecular dynamics simulation.[a,b]

	Relaxed	Extended	Δ(Extended-relaxed)
Total energy	551	587	36
Total potential energy	51	94	43
van der Waals	−97	−58	39
Bond length	107	105	−2
Bond angle	329	325	−4
Dihedral angle	144	136	−8
Improper torsional angle	36	34	−2
Electrostatic terms	−470	−449	21
Entropy change[c] on 130% extension = −1.1 cal/mol-deg			

[a]Values are rounded off to the nearest Kcal/mole

[b]The potential energy listed are relative to the minimum value of the potential functions with respect to the given internal coordinates. Total energy is defined as the sum of total potential energy and kinetic energy, with 0°K used as the reference for zero atomic kinetic energy.

[c]Only the dihedral angles of the internal residues, i.e., from ψ_{14} to ϕ_{44}, are taken into account in the computation of entropy change. The entropy change is defined as

$$\Delta S = R \ln \frac{\prod (\text{RMS fluctuation in backbone dihedral angles in extended state})_i}{\prod (\text{RMS fluctuation in backbone dihedral angles in relaxed state})_i}$$

gles in the same position of each peptide, i.e., $\Delta\phi_i^2 \neq \Delta\phi_{i+5}^2$ or $\Delta\psi_i^2 \neq \Delta\psi_{i+5}^2$. This is true for internal segments as well as end segments in both relaxed and extended states. It is likely due to the short time trajectory as compared to the experimentally determined characteristic backbone correlation times of around 10 ns. Nonetheless, it is en-

Table II. Root mean square (RMS) fluctuation of torsion angles (ϕ and ψ) of $(VPGVG)_{11}$ (45 ps of equilibration time and 80 ps of molecular dynamics simulation.)

	angle	relaxed	extended	angle	relaxed	extended	angle	relaxed	extended
β-turns	ψ_{16}	10.87	14.17	ψ_{26}	27.33	07.64	ψ_{36}	20.19	14.84
	ϕ_{17}	09.86	15.18	ϕ_{27}	11.71	08.33	ϕ_{37}	08.99	10.47
	ψ_{17}	47.59	46.68	ψ_{27}	11.70	13.51	ψ_{37}	21.53	32.96
	ϕ_{18}	61.70	47.41	ϕ_{28}	08.61	10.36	ϕ_{38}	11.15	10.66
	ψ_{18}	09.37	16.05	ψ_{28}	09.33	08.16	ψ_{38}	11.09	27.29
	ϕ_{19}	14.25	08.67	ϕ_{29}	09.70	07.31	ϕ_{39}	12.70	10.24
suspended segments	ψ_{19}	44.09	10.99	ψ_{29}	47.32	10.48	ψ_{39}	52.00	12.50
	ϕ_{20}	41.94	09.29	ϕ_{30}	48.57	11.39	ϕ_{40}	55.88	08.37
	ψ_{20}	14.50	11.15	ψ_{30}	42.56	10.62	ψ_{40}	40.67	11.08
	ϕ_{21}	27.13	24.17	ϕ_{31}	11.43	11.38	ϕ_{41}	36.44	19.06
β-turns	ψ_{21}	09.39	22.73	ψ_{31}	12.17	09.21	ψ_{41}	12.97	14.80
	ϕ_{22}	09.94	08.00	ϕ_{32}	09.90	08.93	ϕ_{42}	11.59	07.33
	ψ_{22}	11.58	16.13	ψ_{32}	15.30	10.80	ψ_{42}	11.34	13.17
	ϕ_{23}	16.37	09.33	ϕ_{33}	09.60	07.62	ϕ_{43}	09.23	09.76
	ψ_{23}	14.33	14.25	ψ_{33}	09.88	09.43	ψ_{43}	10.60	12.53
	ϕ_{24}	11.39	29.20	ϕ_{34}	11.86	09.71	ϕ_{44}	11.06	12.82
suspended segments	ψ_{24}	19.53	37.87	ψ_{34}	63.80	08.36	ψ_{44}	41.89	35.22
	ϕ_{25}	25.02	23.06	ϕ_{35}	91.70	10.20	ϕ_{45}	48.98	31.31
	ψ_{25}	49.32	32.10	ψ_{35}	15.03	11.51	ψ_{45}	42.05	56.89
	ϕ_{26}	31.43	27.24	ϕ_{36}	21.49	18.66	ϕ_{46}	21.55	30.33

tirely evident from Table II that the largest RMS fluctuations occur in the relaxed state and that they are localized primarily in the suspended segments that are the sites where the greatest damping is observed upon extension. Therefore, the previous conclusions using the molecular mechanics approach are substantiated in the present molecular dynamics study.

With both ends fixed in space duing the molecular dynamics calculation, the overall structure of both relaxed and extended peptide chain does not change significantly after thermalization from 0 K to 300 K, after 45 ps of equilibration and after 100 ps of production. In particular, the β-turns are essentially retained as measured from C_i-N_{i+3} distance. Thus, the average C_i-N_{i+3} distances for the relaxed state are 4.05 ± 0.1 Å and 4.37 ± 0.25 Å before and after molecular dynamics simulation, respectively. The average C_i-N_{i+3} distances for 130% extended states are 4.20 ± 0.90 Å and 4.86 ± 0.90 Å before and after molecular dynamics simulation respectively. The retention of the β-turn even in vacuo implies both for the relaxed and extended states that it is meaningful to regard the β-spiral as a structural feature for polypentapeptide of elastin at room temperature.

Since the present calculation is based on Newtonian mechanics in the absence of external forces, the total energy is conserved during the simulation, i.e., the authors' system is microcanonical. Therefore, the entropy change can be represented by the ratio of volumes in configurational space for both relaxed and extended states, i.e.,

$$\Delta S = R \ln \frac{\prod (\text{RMS fluctuation in backbone dihedral angles in extended state})_i}{\prod (\text{RMS fluctuation in backbone dihedral angles in relaxed state})_i}$$

The torsion angle changes involving valyl side chains are not taken into account since the entropy change due to changes in these side chain torsional fluctuations is not considered to contribute significantly to elasticity. The entropy contribution due to the cross terms between various internal coordinates is also neglected in the present consideration.[25] Since only 100 ps of molecular dynamics production is used, the entropy due to motions characterized by longer correlation times also are not directly taken into consideration. The last two approximations may not be as serious as they might first appear since we compute the difference in entropy between two different states of the same molecule. The approximations involved would tend to cancel when taking the ratio. The entropy decrease on 130% extension according to Table II (using residues 14 through 44) is 34 cal/mole-deg. or 1.1 cal/mole-deg per residue. The decrease in entropy for β-turn regions is small and the effect is by and large cancelled out. The primary source of entropy decrease clearly arises from the suspended segments. This is in agreement with the conclusion drawn from the early molecular mechanics study on $(VPGVG)_3$ where ends of a central pentamer were fixed in space.[12] It should be noted that this entropy change is not considered in the classical random chain network theory. Accordingly what has been demonstrated here is the contribution of internal chain dynamics to the elastic retractive force. While the concepts of classical rubberlike network theory and internal chain dynamics are entirely different, they are not mutually exclusive. For example, damping of internal chain dynamics could occur on extension of elastic random chain networks. Furthermore, the role played by the solvent in the elasticity of polypeptide networks is not adequately understood on the molecular level and is not explicitly taken into account in either theory.

Since the authors compare the difference of energies, RMS fluctuations of dihedral angles, etc. between two different states of the same molecule, the approximation caused by employing Newtonian mechanics and harmonic energy function may not be as great as when considering the direct results. Similarly, the effect of insufficient trajectory time (being two orders of magnitudes

smaller than the time scale determined by NMR and dielectric relaxation experiments) on the entropy calculation may not be as great as that of the absolute RMS fluctuation values of each of the two states.

This work was supported in part by National Institutes of Health Grant HL 29578 and the Department of Navy, Office of Naval Research Contract N00014-86-K-0402.

References

1. C. A. J. Hoeve and P. J. Flory, *J. Amer. Chem. Soc.*, 80, 6523 (1958).
2. C. A. J. Hoeve and P. J. Flory, *Biopolymers*, 13, 677 (1974).
3. K. L. Dorrington and N. H. McCrum, *Biopolymers*, 16, 120 (1977).
4. D. W. Urry, C. M. Venkatachalam, S. A. Wood and K. U. Prasad, in *Structure and Motion: Membranes, Nucleic Acids and Protein*, E. Clementi, G. Corongiu, M. H. Sarma, and R. H. Sarma, Eds., Academic Press, Guilderland, New York, 185 (1985).
5. T. Weis-Fogh and S. O. Anderson, *Nature*, 227, 718 (1970).
6. D. W. Urry, *J. Prot. Chem.*, 7 1 and 81, (1988).
7. L. Gotte, D. Volpin, R. W. Horne and M. Mammi, *Micron.*, 7, 95, (1976).
8. E. G. Cleary and W. J. Cliff, *Exp. Mol. Pathol.*, 28, 227, (1978).
9. D. W. Urry, Int. J. Quantum Chem.: *Quantum Biol. Symp.*, 14, 261 (1987).
10. H. Yeh, N. Ornstein-Goldstein, Z. Indik, P. Sheppard, N. Anderson, J. C. Rosenbloom, G. Cicila, K. Yoon, and J. Rosenbloom, *Collagen and Related Res.*, 7, 235, (1987).
11. L. B. Sandberg, J. G. Leslie, C. T. Leach, V. L. Torres, A. R. Smith, and D. W. Smith, *Pathol. Biol.*, 33, 266, (1985).
12. D. W. Urry and C. M. Venkatachalam, *Int. J. Quantum Chem: Quantum Biol. Symp.*, 10, 81 (1983).
13. C. M. Venkatachalam and D. W. Urry, *Macromolecules*, 14, 1225, (1981).
14. D. W. Urry, T. L. Trapane, H. Sugano, and K. U. Prasad, *J. Am. Chem. Soc.*, 103, 2080, (1981).
15. D. W. Urry, *Ultrastruct. Pathol.*, 4, 227, (1983).
16. D. W. Urry, T. L. Trapane, M. Iqbal, C. M. Venkatachalam, and K. U. Prasad, *Biochemistry*, 24, 5182 (1985).
17. D. W. Urry, R. Henze, R. D. Harris, and K. U. Prasad, *Biochem. Biophys. Res. Comm.*, 125, 1082 (1984).
18. D. K. Chang and D. W. Urry, *Chem. Phys. Lett.*, 147, 395 (1988).
19. N. Go and H. A. Scheraga, *Macromolecules*, 6, 273 (1973).
20. N. Go and K. Okuyama, *Macromolecules*, 9, 867 (1976).
21. C. M. Venkatachalam and D. W. Urry, *J. Comp. Chem.*, 5, 64 (1984).
22. B. R. Brooks, R. E. Bruccoleri, B. O. Olafson, D. J. States, S. Swaminathan and M. Karplus, *J. Comp. Chem.*, 4, 187 (1984).
23. L. B. Sandberg, N. T. Soskel and J. B. Leslie, *N. Engl. J. Med.*, 304, 566 (1981).
24. M. Karplus and J. A. McCammon; *Ann. Rev. Biochem.*, 53, 263 (1983).
25. L. Verlet, *Phys. Rev.*, 159, 98 (1967).
26. M. Karplus and J. N. Kushick, *Macromolecules*, 14, 325 (1981).

ELSET

DATE: 28 APR. 1989

Elsevier Science Publishers
Amsterdam, The Netherlands
P.O. Box:
Postcode:

In all correspondence concerning this paper please refer to:

LSET07 THEOCH1817

AUTHOR

PLEASE CHECK CAREFULLY

Please return corrected proof by AIR MAIL within 1 week of receipt

Journal of Molecular Structure (Theochem),
Elsevier Science Publishers B.V., Amsterdam — Printed in The Netherlands

THE MOLECULAR DYNAMICS OF THE β-SPIRAL OF THE POLYPENTAPEPTIDE OF ELASTIN IN "STATE III" WITH 2.9 PENTAMERS PER TURN*

D.K. CHANG and DAN W. URRY

University of Alabama at Birmingham, Laboratory of Molecular Biophysics, UAB Station, P.O. Box 300, Birmingham, AL 35294 (U.S.A.)

(Received 9 February 1989)

ABSTRACT

In vacuo molecular dynamics simulation using the CHARMm program was carried out on a putative structure ("state III") of the repeating pentapeptide, (VPGVG), of elastin at two different extensions. "State III" is the proposed structure for the experimental state III which developes after prolonged heating at temperatures greater than 60 °C. "State III" is a helix, called a β-spiral, with 2.9 pentamer units per turn in which the type II β-turns fan outward in propeller fashion and the Val[4] side chains turn inward displacing the former intra-spiral water and increasing the intramolecular hydrophobic interactions. The fluctuations in backbone dihedral angles for this "state III" are found to be smaller for the structure on extension. These results are compared with previous calculations on the proposed structure for the physiological state, state II, in which the β-turns function as spacers between turns of the dynamic β-spiral and in which there is much water within the β-spiral. The magnitude of dihedral angle damping upon elongation of "state III" is, however, much smaller than that calculated from the β-spiral structure for state II. The computational result is consistent with the experimental observations of shrinking and expulsion of water and of loss of elastic modulus on heating above 60 °C. The implications of this modelling of state III and state II on the damping of internal chain dynamics on extension are discussed with regard to the source of entropic elasticity.

INTRODUCTION

Poly(VPGVG), i.e. $(Val^1\text{-}Pro^2\text{-}Gly^3\text{-}Val^4\text{-}Gly^5)_n$, is the primary repeating sequence in bovine, and porcine elastins [1–3]. The structure and physical properties of synthetic poly(VPGVG) and designed analogs have been studied both as models of elastin fiber and recently as bioelastic materials under development in such diverse fields as prevention of adhesion, synthetic arteries and ligaments, desalination, and chemomechanical transduction [4–6]. It was found that poly(VPGVG) (MW > 50 000 D) begins to aggregate above 25 °C. More significantly, the crystal-diffraction pattern becomes characteristic of a

*Dedicated to Professor Per-Olov Löwdin, whose decades of encouragement, support and stimulus of research in the basic physics and chemistry of biomolecules has enormously contributed to progress in this area.

0166-1280/89/$03.50

more ordered structure and numerous other physical methods demonstrate increased order as the temperature is raised above 25°C [7,8]. This transition is termed an inverse temperature transition to signify the increase in order of the polypentapeptide molecules on raising the temperature. A contractile development of force of cross-linked poly(VPGVG) coincides with the inverse temperature transition in thermoelasticity studies [8]. This indicates that the cross-linked polypeptide system exhibits behavior not common to random-chain networks. Light-microscopic investigations show the polypentapeptide to self assemble into fibers and transmission electron microscopy studies show twisted filaments with a diameter of ca. 50 Å [9]. A more detailed conformation has been characterized by nuclear magnetic resonance [10,11] and Raman spectroscopies [12]. It was deduced from these experiments that there is a type-II β turn which is formed by Val^1–Pro^2–Gly^3–Val^4. The β-turn structure is partially stabilized by a Val^1 C=O···Val^4NH hydrogen bond [13,14]. The peptide segments between two β turns are called suspended segments because of the manner in which they connect β-turn moieties, once the β turns become arranged into a helical array called a β spiral. This is called state II with the structure occurring at temperatures below that of the inverse temperature transition being called state I.

[13,14]

Interestingly, the CD pattern for the poly(VPGVG) sample after prolonged heating at 80°C (ca. 14 days) is distinct from that before heating [8]. For the cross-linked matrix, this is accompanied by a contraction of the sample and the extrusion of water. The Young's modulus of γ-irradiation cross-linked poly(VPGVG) is dramatically lower after the heat treatment [8]. This process is irreversible so that the physical properties are different when the heated sample is cooled back to room temperature. This is referred to as state III. Since water molecules are extruded in the process [15], it is considered that, in the helical structure of poly(VPGVG), the Val^4 side chains are folded inside the helix [16], displacing water from the interior of the helix. The structure is demonstrated for a cyclopentadecapeptide analogue in Fig. 1 [16]. The linear counterpart of the structure in Fig. 1B is referred to as the working model for state III of poly(VPGVG) as opposed to state II which is the structure that occurs at 37°C before 80°C treatment. The thermoelasticity studies suggest that the reduced elastomeric force exhibited by state III continues to be dominantly entropic. Moreover, it has been proposed that the primary mechanism of elasticity for elastin is the damping of the peptide backbone dihedral angle dynamics upon elongation [17,18]. This has been called the librational entropy mechanism of elasticity. Thus, it is of interest to examine by molecular-dynamics simulation the mechanism whereby loss of elastic modulus and contraction occurs at 80°C using the β spiral of the PPP with 2.7 pentamer units per turn [19].

Young's

Fig 1B

2.9

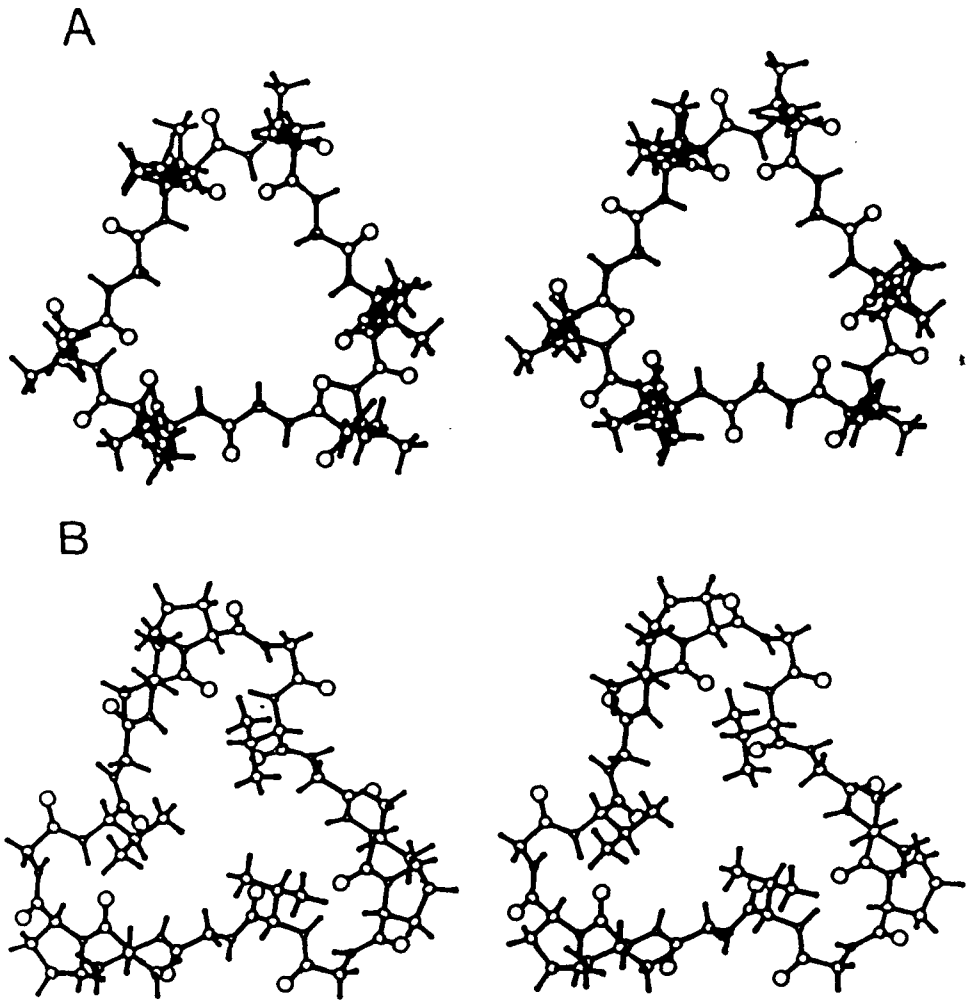

Fig. 1. ORTEP stereoviews down the three-fold axis of two of the six minimum-energy conformations of cyclo-$(VPGVG)_3$. (A) The cyclic analog of state II; (B) the cyclic analog of "state III." Reprinted with permission from ref. 16.

III''

METHODS

The working model for the helical structure for state III of the polypentapeptide, poly(VPGVG), was obtained by a modification of the Go–Scheraga procedure [20]. The dihedral angles that give rise to a cyclic pentadecapeptide were first generated as described by Venkatchalam and Urry [21]. The major differences between the β spirals of state II and the working model of state III are that the side chains of the Val^4 residues are directed inward in the latter

displacing intraspiral water of the β spiral of state II and the β turns, which function as spacers between turns of the β spiral of state II, are turned outward causing a collapsing of the β spiral, as occurs in state III to a shorter pitch. For simplicity, in the following, the working model of state III will be referred to as "state III".

After the cyclic structure was generated, the dihedral angles were varied, primarily in ϕ and ψ of Gly^5 in order to attain the desired helical structure of 2.9 pentamer units per turn and the end-to-end distance for NH_2-$(VPGVG)_{11}$-OH used in the present study. The generated structure was then subjected to minimization by the conjugated gradient and adapted-basis Newton-Raphson algorithms. The CHARM (version 20.3) software package, developed by Karplus and co-workers [22] and adapted by Polygen, Inc., was used in the molecular-dynamics simulation. In the computation, the potential energy is taken to be the sum of bond-length energy (E_b), energy for bond angle (E_θ), energy for dihedral angle (E_ϕ), improper torsional energy (E_w), van der Waals energy (E_{vdw}) and electrostatic energy (E_e). The hydrogen atoms are explicitly considered in the energy computation as the inter-turn interactions involving prolyl and valyl side-chain protons are of major concern here. The harmonic approximation was employed for E_b, E_θ, E_w, and $E_\phi = K_\phi(-\cos n\phi)$, where K_ϕ is the force constant for dihedral angle deformation and n = 1, 2, 3, 4 or 6. E_{el} is represented according to Coulomb's law. The Lennard-Jones 6-12 potential was used for E_{vdw}.

In the computation, the end-to-end distance between the Val^1 amide nitrogen and Gly^{55} carbonyl carbon were held fixed in space at 42 Å and 81.5 Å, respectively, for states at two different extensions, representing an approxi-

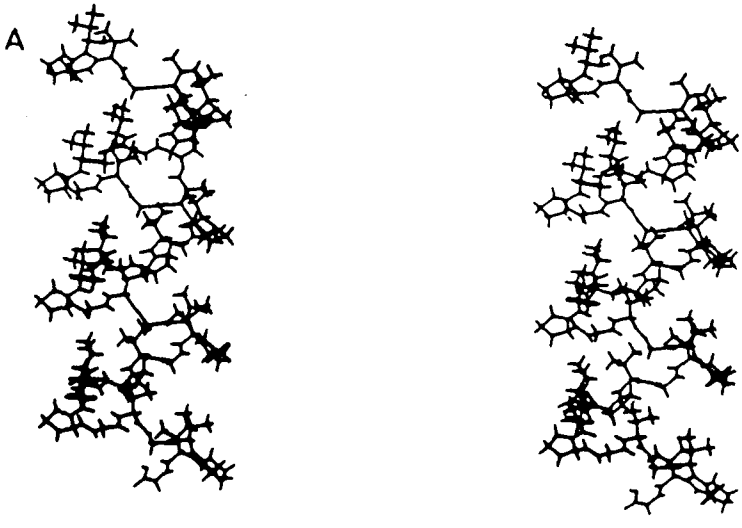

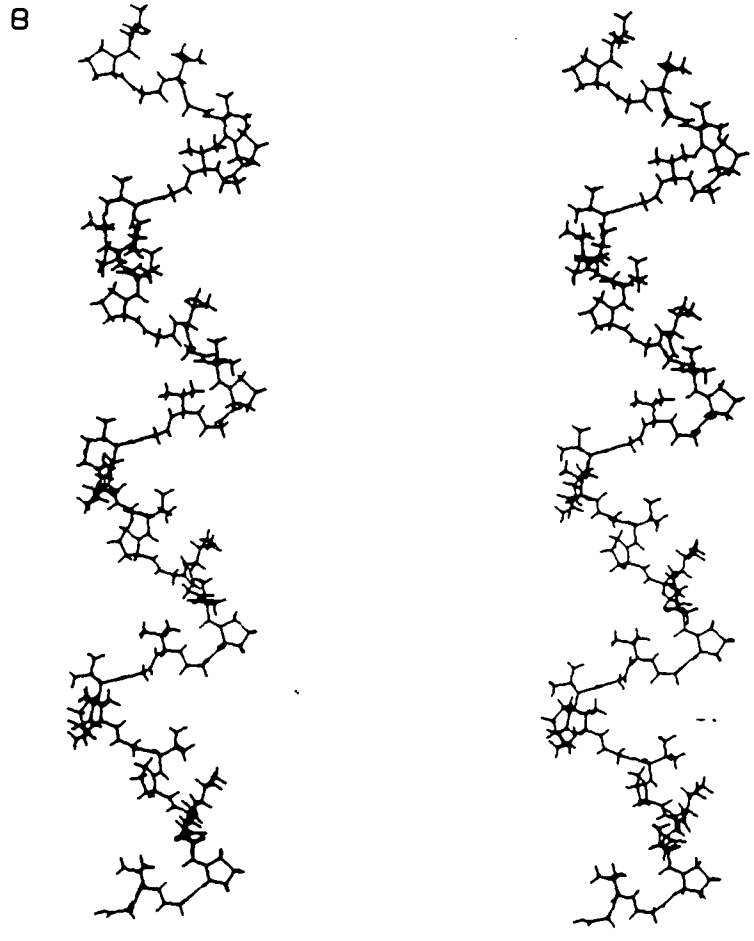

Fig. 2. Sideview of the stereo diagrams of "state III" poly(VPGVG): (A) at 35% extension (42 Å end-to-end distance); (B) at 165% extension (81.5 Å end-to-end distance).

mately 100% change in extension. In addition, chemical bonds to protons were fixed in length in the SHAKE algorithm [22], allowing the step size of 1×10^{-15} s in the molecular dynamics simulation. The minimized structures for both states were then subjected to thermalization to 300 K with a rise of 2.5°C achieved in 50 steps. The thermalized molecules were equilibrated to stabilize the structure during the heating process. It was found that the total energy of the system decreases initially and fluctuated after about 20 ps into the equilibration stage. The fluctuation was reduced to an accepted level after 50 ps. The final step of simulation is the production stage in which the molecules are allowed to undergo random thermal motion at constant total energy. The structures are given in

rise of 2.5°C

Fig. 2. Other details of molecular-dynamics calculations for state II ar reported elsewhere [23].

Due to the immensity of data, only one set of coordinates for every 50 steps was stored in the data file. The internal energy as well as components of the potential energy were noted. In addition, the root-mean-square (rms) fluctuation of backbone dihedral angles was used to calculate the entropy change due to extension, for the present microcanonical system [24].

$$\Delta S = R \ln \frac{\prod_i (\text{rms fluctuation in backbone dihedral angles in more extended state})}{\prod_i (\text{rms fluctuation in backbone dihedral angels in more relaxed state})}$$

To ensure the more stable structure for rms fluctuation values, the 50 ps of molecular dynamics trajectory was taken from 32 ps to 82 ps of the production period.

RESULTS AND DISCUSSION

Table 1 shows the average of a 50-ps molecular-dynamics simulation for

TABLE 1

Internal-energy components of NH_2-9VPGVG)$_{11}$-OH in "state III" in two different extensions for a 50-ps molecular-dynamics simulation[a]

Energy	End-to-end distance (Å)		Difference
	42[b]	81.5	
Total	524	579	55
Total potential	41	83	42
Van der Waals	−87	−60	27
Bond length	104	106	2
Bond angle	321	326	5
Dihedral angle	141	138	−3
Improper torsional angle	36	34	−2
Electrostatic terms	−476	−463	13
Entropy change[c] on 100% extension = 0.1 cal °C^{-1} (mol residue)$^{-1}$			

[a]Values are rounded to the nearest kcal mol^{-1} °C^{-1}. The values of the potential-energy components are relative to the minimum of the potential function for the given internal coordinates. The total energy is defined as the sum of the total potential energy and kinetic energy, with 0 K used as the reference for the zero atomic kinetic energy.

[b]End-to-end distance refers to the distance between Val^1 NH and Gly^{55}C=O.

[c]The calculation of entropy change is based on the dihedral angles of residues 14 to 40 for 50 ps of molecular dynamics simulation from 32 ps to 82 ps.

TABLE 2

Root mean square (rms) fluctuation of the torsion angles (ϕ and ψ) of ($VPGVG)_{11}$ (50 ps of equilibration time and 50 ps of molecular dynamics simulation)

Angle	Extension (%)		Angle	Extension (%)		Angle	Extension (%)	
	35	135		35	135		35	135
Suspended segments								
			ψ24	19.39	30.54	ψ34	20.97	27.87
ϕ15	85.34	15.85	ϕ25	10.02	35.94	ϕ35	19.7	33.05
ψ15	16.14	33.88	ψ25	10.93	18.88	ψ35	13.27	32.40
ϕ16	25.08	31.78	ϕ26	12.40	31.94	ϕ36	34.38	27.34
β turns								
ψ16	13.54	7.93	ψ26	14.51	11.87	ψ36	9.51	8.21
ϕ17	10.77	8.75	ϕ27	9.76	11.35	ϕ37	9.98	8.56
ψ17	36.50	11.74	ψ27	18.13	17.50	ψ37	14.61	12.46
ϕ18	34.95	9.21	ϕ28	8.09	9.53	ϕ38	8.33	8.80
ψ18	9.18	8.90	ψ28	10.60	10.48	ψ38	8.41	9.74
ϕ19	10.60	8.98	ϕ29	8.90	11.12	ϕ39	7.77	7.66
Suspended segments								
ψ19	24.82	10.66	ψ29	14.90	10.75	ψ39	15.18	8.91
ϕ20	23.96	29.14	ϕ30	14.90	18.26	ϕ40	22.93	20.56
ψ20	12.74	41.54	ψ30	12.88	10.56	ψ40	12.62	13.24
ϕ21	24.19	47.95	ϕ31	25.97	11.32			
β turns								
ψ21	21.80	34.29	ψ31	9.04	14.41			
ϕ22	9.58	6.54	ϕ32	9.23	8.60			
ψ22	22.55	10.06	ψ32	12.22	30.86			
ϕ23	27.41	8.32	ϕ33	8.35	9.11			
ψ23	13.59	9.66	ψ33	10.23	12.43			
ϕ24	25.14	12.66	ϕ34	9.25	10.94			

energy

various components of the two different extensions (i.e. the end-to-end distances of 42 Å and 81.5 Å) for the "state III" conformation at 300 K. As demonstrated previously [23], the total potential-energy difference can be largely attributed to the difference in energy arising from differences in van der Waals interaction. This difference would be largely removed in the presence of water molecules as discussed previously [23]. Qualitative agreement in the energy difference has been demonstrated consistent with the entropic elasticity mechanism of damping of internal-chain dynamics on extension.

300 °K

Table 2 summarizes the rms fluctuation of backbone dihedral angles of the internal segment where the end effects can be largely neglected. With a 50-ps

trajectory, the lack of regularity in the rms fluctuation for the dihedral angle in the same position of each pentapeptide, i.e. $\Delta\phi_i^2 \neq \Delta\phi_{i+5}^2$ or $\Delta\psi_i^2 \neq \Delta\psi_{i+5}^2$, suggests that the time trajectory probably short as compared with the experimentally determined backbone correlation time of about 10 ns [8]. The computation of entropy change on elongation, as discussed previously, involves approximations. Therefore, while the results using rms fluctuations are not strictly quantitative, they are both qualitative and instructive. The entropy change on a 100% extension using the data in Table 2 is 2.6 cal mol^{-1} °C^{-1} for the internal segment from residue 14 to 40. The entropy change per amino acid residue is thus 0.1 cal mol^{-1} °C^{-1}. The previous entropy change per residue for a 130% extension of pPP in state II with 2.7 pentamer units per turn was found to be 1.1 cal mol^{-1} °C^{-1}. The present "state III" simulation, therefore, yields an entropy change of about one-tenth that of the previous value for state II. Qualitatively, therefore, the theoretical result compares favorably with

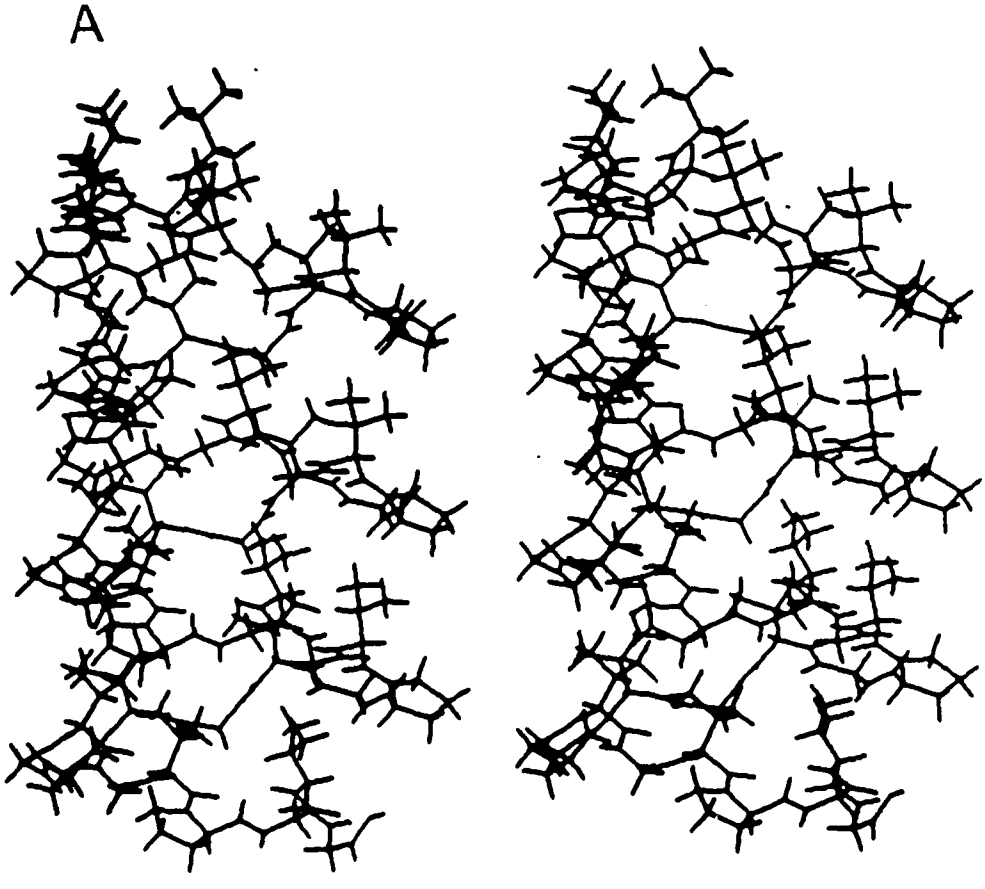

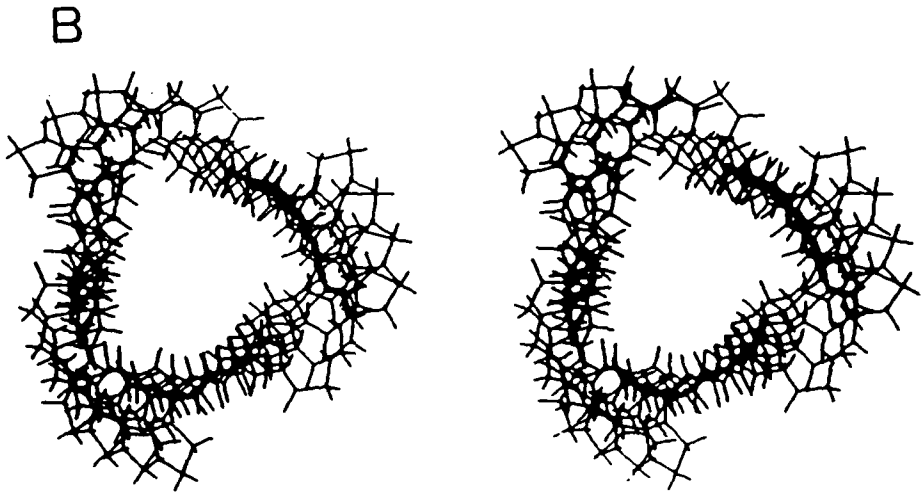

Fig. 3. (A) Sideview of a *stereo* diagram of the relaxed "state III" poly(VPGVG) at 31 Å end-to-end distance. While this is a shortened state, it is probably not the final shortened state due to 80°C heating. (B) Axial view of a stereo diagram of the relaxed "state III" poly(VPGVG) at 31 Å end-to-end extension. It is clear from this perspective that there is still the need to have the Val^4 side chains directed inward to fill the β spiral and displace the intraspiral water.

the stress/strain experiments on the cross-linked PPP samples where prolonged heating at 80°C converts the cross-linked poly(VPGVG) to a shortened state [8] in which Young's modulus is reduced by a factor of 3 after 24 h of heating at 80°C. As noted previously for state II, the rms fluctuation for "state III" is generally more prominent in the suspended segment than in the β turn.

In the process of the state II to state III transition, the sample is shortened while water is extruded from the PPP solution. This suggests that the pitch of the helix, i.e. axial rise per turn, is smaller for the totally relaxed state III. Thus the end-to-end distance is expected to be smaller in state III. Work to obtain the optimal structure at short end-to-end distance is in progress and a shortened state in Fig. 3 has been obtained.

Nuclear Overhauser-effect experiments using proton magnetic resonance on the poly(VPGVG) sample in states II and III are consistent with a decrease in the inter-turn distance in the "state III" β-spiral structure [25]. The change in the circular dichroism (CD) spectrum of poly(~~SPVG~~) in the state II→III transition are also consistent with the shortened pitch of the PPP β spiral. With regard to the nuclear Overhauser results for state III, there is a closer proximity of the $Val^1\gamma$-C<u>H</u>$_3$ hydrogens to the $Pro^2\beta$-c<u>H</u> (which is *cis* to the Pro α-C<u>H</u>) than occurs in state II. This proximity is very apparent in Fig. 3(A).

poly(VPGVG)

cap C

ACKNOWLEDGEMENTS

This work was supported in part by contract No. N00014-86-K-0402 from the Department of the Navy, Office of Naval Research, and by NIH grant No. HL29578.

REFERENCES

1 L. Sandberg, L. Lesile, C. Leach, V. Torres, A. Smith and D. Smith., Pathol. Biol., 33 (1985) 266.
2 L. Sandberg, N. Weissman and D. Smith, Biochemistry, 8 (1969) 2940.
3 H. Yeh, Orstein-Goldstein, Z. Indik, P. Sheppard, N. Anderson, J. Rosenbloom, G. Cicila, K. Yoon and J. Rosenbloom, Collagen Rel. Res., 7 (1987) 235.
4 D. W. Urry, Res. Dev., 30 (1988) 57.
5 D. W. Urry Res. Dev., 34 (1988) 72.
6 D. W. Urry, D. K. Chang, H. Zhang and K. U. Prasad, Biochem. Biophys. Res. Commun., 153 (1988) 832.
7 D. W. Urry, T. L. Trapane, M. Iqbal, C. M. Venatachalam and K. U. Prasad, Biopolymers, 24 (1985) 2345.
8 D. W. Urry, J. Protein Chem., 7 (1988) 1.
9 D. Volpin, D. W. Urry, I. Pasquali-Ronchetti and L. Gotte, Micron, 7 (1976) 193.
10 M. A. Khaled, V. Reunugopalakrishnan and D. W. Urry, J. Am. Chem. Soc., 98 (1976) 7547.
11 D. W. Urry, D. K. Chang, R. Kirshna, D. H. Huang, T. L. Trapane and K. U. Prasad, Biopolymers, ~~in press~~. 28 (1989) 819.
12 G. J. Thomas, Jr., B. Prescott and D. W. Urry, Biopolymers, 26 (1987) 921.
13 D. W. Urry and M. M. Long, CRC Crit. Rev. Biochem., 4 (1970) 1.
14 W. J. Cook, H. M. Einsphar, T. L. Trapane, D. W. Urry and C. E. Bugg, J. Am. Chem. Soc., 102 (1980) 5502.
15 F. Sciortino, M. U. Palma, D. W. Urry and K. U. Prasad, Biochem. Biophys. Res. Commun., ~~in press~~. 157 (1988) 1061.
16 C. M. Venkatachalam, M. A. Khaled and D. W. Urry, J. Am. Chem. Soc., 103 (1981) 2372.
17 D. W. Urry, C. M. Venkatachalam, M. M. Long and K. U. Prasad, in R. Srinivasan and R. H. Sarma (Eds.), Conformation in Biology, Adenine Press, New York, 1982, pp. 11-27.
18 D. W. Urry, C. M. Venkatachlam and K. U. Prasad, Int. J. Quantum Chem.: Quantum Biol. Symp., 10 (1983) 81.
19 D. K. Chang and D. W. Urry, Chem. Phys. Lett., 147 (1988) 395.
20 N. Go and H. A. Scheraga, Macromolecules, 6 (1973) 273.
21 C. M. Venkatachalam and D. W. Urry, J. Comput. Chem., 5 (1984) 64.
22 B. R. Brooks, R. E. Bruccoleri, B. O. Olafson, D. J. States, S. Swaminathan and M. Karplus, J. Comput. Chem., 4 (1984) 187.
23 D. K. Chang and D. W. Urry, J. Comput. Chem., ~~submitted~~ in press.
24 T. L. Hill, An Introduction to Statistical Thermodynamics, Addison-Wesley, Reading, MA, Chap. 1.
25 D. K. Chang, K. U. Prasad and D. W. Urry, in preparation.

Sciortino

Journal of Biomolecular Structure & Dynamics, ISSN 0739-1102
Volume 6, Issue Number 5 (1989), ©Adenine Press (1989).

Nuclear Overhauser Effect and Computational Characterization of the β-Spiral of the Polypentapeptide of Elastin

D.K. Chang[1], C.M. Venkatachalam[2], K.U. Prasad[1] and D.W. Urry[1]
[1]Laboratory of Molecular Biophysics
The University of Alabama at Birmingham
P.O. Box 300/University Station
Birmingham, Alabama 35294

[2]Polygen Corporation
100 Fifth Avenue, II Floor
Waltham, Massachusetts 02154

Abstract

The structure of the elastin polypentapeptide, poly(VPGVG), was studied by nuclear Overhauser effect experiments using perdeuterated Val^1 and Val^4 samples under the condition where intermolecular interactions are absent. More extensive interaction was found between the Val^1 γCH and Pro^2 βCH protons than between the Val^4 γCH and Pro^2 βCH protons. The Val^1 γCH_3 - Pro^2 βCH interaction does not occur within the same pentamer as previously shown experimentally and as expected from steric considerations. The results are incompatible with the presence of a random chain network in poly(VPGVG) at room temperature but are readily explicable in terms of interturn interactions in a β-spiral structure. More specifically, the results indicate that the β-spiral conformation with 2.9 pentamers/turn is more prevalent than that with 2.7 pentamers/turn. Using conformations developed by molecular mechanics calculations, molecular dynamics simulations were carried out to compare the relative energies of these two variants of this class of β-spiral structures. It was found in vacuo that the structure with 2.9 pentamers/turn is indeed more stable than that of 2.7 pentamers/turn by ~1 kcal/mole-pentamer.

Introduciton

The sequential polypeptide, $(L \cdot Val^1\text{-}L \cdot Pro^2\text{-}Gly^3\text{-}L \cdot Val^4\text{-}Gly^5)_n$ abbreviated poly (VPGVG), or simply PPP, which is the longest repeating sequence in bovine and porcine tropoelastins (1,2), has been under intensive physicochemical characterization in recent years (3-5). As previously reviewed (4), these characterizations include thermoelasticity, dielectric relaxation measurements, circular dichroism, microscopy, temperature-composition and NMR studies. Microscopic studies revealed that PPP self-assembles into fibers due to underlying parallel aligned twisted filaments with diameters of ~50Å (6,7). As such, PPP does not form a random chain

network. The twisted filament can be expected to be composed of supercoiled PPP β-spirals which are helical structures with about 3 pentamer units per turn. Recently, the conformation of PPP (MW > 50 kD) and of cyclo(VPGVG)$_3$ both in H_2O and in DMSO solutions have been studied by one and two dimensional ^{1}H NMR (8). This comparison is particularly relevant as the cyclopentadecapeptide has been shown to have a conformation very nearly identical to that of the linear PPP (9). It was observed, in addition to the characteristics of a Type II β-turn for VPGVG, that there is a Val^1 (or Val^4) γCH - Pro^2 βCH nuclear Overhauser effect interaction in DMSO and in D_2O at 5°C below the aggregation temperature for PPP but not for the cyclopentadecapeptide. Since it is not likely, therefore, to be due to the interaction (10) within the same pentapeptide unit, it would seem necessarily to arise from helical interturn yet intramolecular interactions. It is particularly significant that the cyclopentadecapeptide, cyclo(VPGVG)$_3$ which has no helical interturn interactions in solution, does not show this interaction (8).

This interturn interaction of PPP results from the hydrophobic effect of the side chains (i.e., those of Pro^2, Val^1 and Val^4). As a consequence of the hydrophobic effect, clathrate-like water molecules surrounding hydrophobic groups become bulk water and an inverse-temperature transition is observed in which there is an increase in order within the PPP due to hydrophobic side chain interactions, as the aqueous PPP solution is heated through the transition temperature. Of specific interest here is that the Val^1 γCH - Pro^2 βCH interaction would correspond to 2.9 pentamers per turn whereas the Val^4 γCH - Pro^2 βCH interaction would correspond to 2.7 pentamers per turn for a β-spiral with ~3 pentamer units per turn. A β-spiral, with approximately 3 pentamers/turn, is required from the comparative conformational studies of the cyclic analogs with the linear polymer (9). In the previous experiments (8), it was not possible to distinguish the interactions between Val^1 γCH$_3$ and Pro^2 βCH from Val^1 γCH$_3$ and Pro^2 βCH because the extensive overlap of γCH$_3$ resonance peaks of Val^1 and Val^4. In order to resolve the issue of either 2.9 or 2.7 pentamer units per turn for the β-spiral structure, perdeuterated Val^4- and perdeuterated Val^1-PPP were synthesized and nuclear Overhauser effect (NOE) experiments were performed. Also, the 2.9 and 2.7 pentamer per turn β-spiral structures were generated by previously described molecular mechanics computations and molecular dynamics simulations were then utilized to compare the relative energies of these two β-spiral structures at room temperature.

Materials and Methods

L · Valine (d_8) was obtained from Cambridge Isotope Laboratories and was 98% deuterated. The tert-butyloxycarbonyl (Boc) derivative was prepared by reacting Val with di-tert-butyl carbonate (11). The synthesis of the two monomers, Boc-Gly-Val-Gly-Val(d_8)-Pro-OBzl (benzyl ester) and Boc-Gly-Val(d_8)-Gly-Val-Pro-OBzl was carried out according to published procedures (12,13) to obtain the final Val^1(d_8)-PPP and Val^4(d_8)-PPP respectively. The benzyl ester was hydrogenated to the free acid and converted to the p-nitrophenyl ester (-ONp) using bis-(p-nitrophenyl) carbonate (14). After removing the Boc-group, the pentapeptide active ester was polymerized for 15 days, diluted with water and dialyzed against water using a 50 kD cut-off

dialysis tubing. The retentate was lyophilized. The PPP was treated with base to saponify any unreacted -ONp present on the polymer chains, redialyzed against water after acidification and lyophilized. All the peptide intermediates were checked by thin layer chromatography and by carbon-13 NMR for comparison with previous syntheses.

For NMR studies, 30 mg of each of Val^1-d_8 and Val^4-d_8 poly(VPGVG) samples (MW > 50,000 Daltons) were dissolved in 0.5 ml D_2O (99.96% deuterium, Stohler Isotope Co.). The NOE experiments were performed on a Bruker WH-400 spectrometer (9.4 Tesla) equipped with an Aspect 3000 computer. A temperature of 22°C, was chosen as this is 5°C lower than the onset of aggregation observed in turbidity experiments at the same concentration for these two polypentapeptide (PPP) solutions. As the intrapentamer and intrapentadecamer hydrophobic interactions have been previously discussed (8), these conditions allow identification of the hydrophobic intramolecular interturn interactions. In the truncated driven NOE experiments, a 0.15 s presaturation time was used in which the cross relaxation for a pair of protons was allowed to occur. Difference spectra were obtained by subtracting the spectrum of the PPP sample irradiated at the resonance peaks of Val^1 or Val^4 γCH from the spectrum with no irradiation at any resonance. 4000 scans were accumulated for each spectrum.

Generation of the atoms of the polypentapeptide helix and the energy minimization were carried out following molecular mechanics methods described earlier (15). Helix generation was achieved by imposing helical constraints using a modification of the cyclization method of Go and Scheraga (16). This modified procedure is described in detail by Venkatachalam and Urry (17). The molecular conformations were viewed on an Evans and Sutherland picture system using HYDRA graphics software and the plots were generated on a Hewlett Packard multi-pen plotter HP-7550A.

For the molecular dynamics computation, the IRIS 3130 Workstation (Silicon Graphics, Inc.) was employed using the software program CHARMm (version 20.3) which was developed by Karplus (18) and adapted by Polygen Corporation. Two 7-repeat polypentapeptides, $(VPGVG)_7$, one with 2.7 and a second with 2.9 pentamers per turn, were studied and the total internal energies at 27°C for these two structures were compared. Each step in the dynamics simulation corresponded to 10^{-3}ps. The heating rate was 0.05°C/step and 10ps (10^4 steps) were used for equilibration.

Results and Discussion

Figure 1 contains reference (A) and NOE (B and C) spectra of Val^4-d_8(Val^4 perdeuterated)-PPP. Figure 1B is the result of saturating the Val^1 γCH_3 resonance at higher field (0.89 ppm) whereas Figure 1C is that of saturating the Val^1 γCH_3 resonance at lower field (0.94 ppm). It is clear that the γCH_3 resonating at 0.94 ppm is closer to Pro^2 βCH. The results of the NOE experiment for Val^1-d_8-PPP are given in Figure 2. Of the two Pro^2 βCH protons, the one resonating at 1.89 ppm gives the greater NOE on irradiation of the Val^1 γCH_3. The NOE peak also is observed at 1.89 ppm when the Val^4 γCH resonance is saturated, but the intensity for the latter is about 30% of

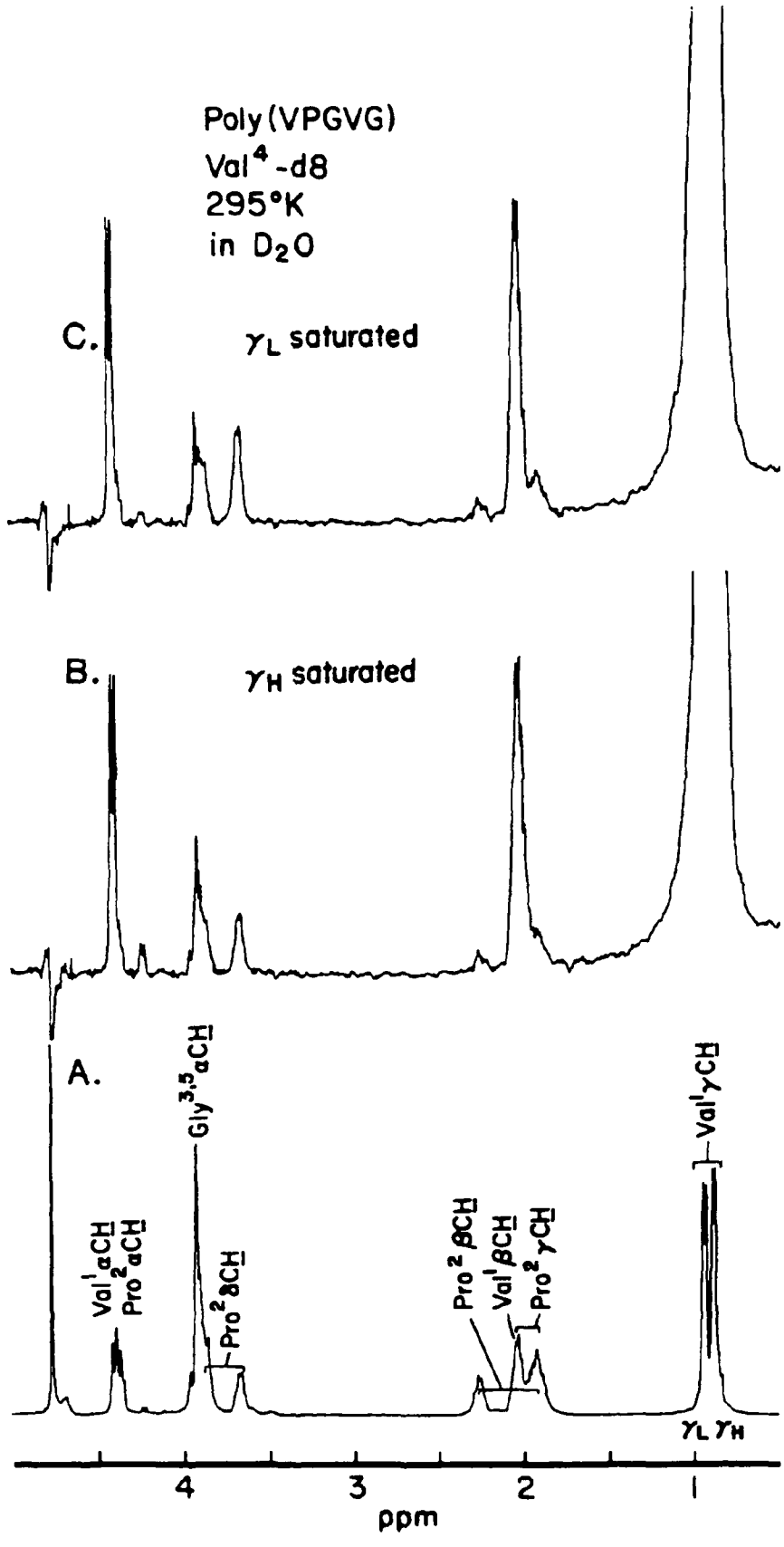

Figure 1: 400 MHz ^{1}H NOE difference spectra of Val^4-d_8 poly(VPGVG) in D_2O at 295°K: (A) reference, (B) difference spectrum with the resonance saturated at 0.94 ppm, (C) difference spectrum with the resonance saturated at 0.89 ppm.

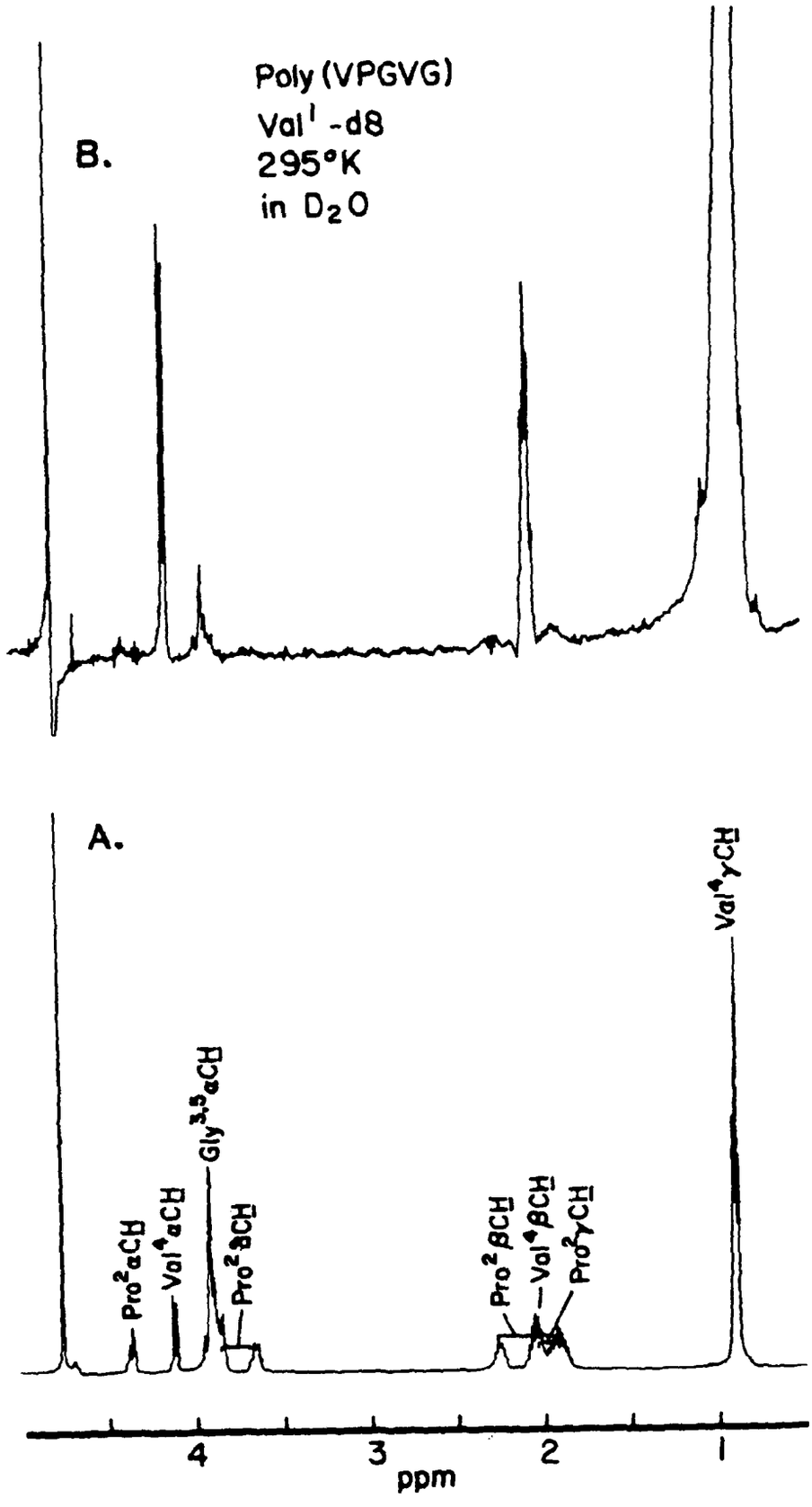

Figure 2: 400 MHz ^{1} NOE difference spectrum of Val^1-d_8 poly(VPGVG) in D_2O at 295°K: (A) reference, (B) difference spectrum with the resonance saturated at 0.90 ppm.

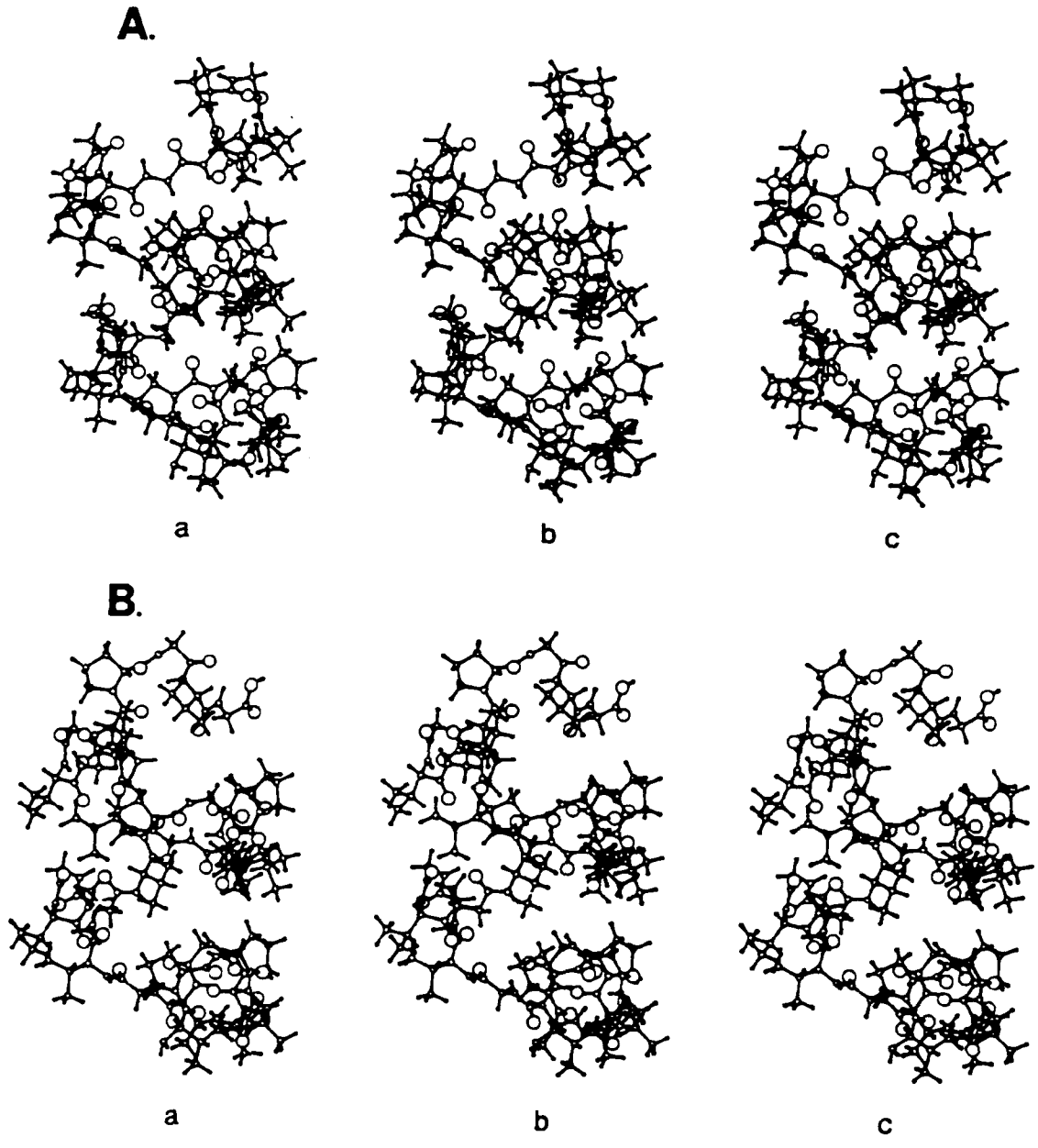

Figure 3: Two β-spirals of the polypentapeptide of elastin shown comprised of seven pentamers, i.e., $(VPGVG)_7$. **A.** A β-spiral with 2.7 pentamers per turn in which the interturn contacts involved pairwise hydrophobic interactions between the Val^4 γCH_3 moieties and the Pro^2 βCH_2 moieties. **B.** A β-spiral with 2.9 petamers per turn in which the interturn contacts involve hydrophobic associating Val^1 βCH_3 moieties with the Pro^2 βCH_2 moieties. The experimental data demonstrate this to be the preferred conformation in solution.

the former. The Pro^2 βCH NOE peak at 2.26 ppm is consistently weaker for both Val^1 and Val^4 perdeuterated samples.

Based on the concept of cyclic conformations with linear conformational correlates and on the comparative conformational studies of poly(VPGVG) with a series of cyclo$(VPGVG)_n$ where n = 1,2,3,4,5 and 6 (9), a family of β-spirals have been described with approximately three pentamers per turn (15). In Figure 3 are stereo views of two members of the family which differ in the details of the interturn hydrophobic contacts.

With the β-turns functioning as spacers between the turns of the β-spiral (6,15), there are two sets of interturn hydrophobic contacts possible. These are those involving the Val^4 γCH_3 moieties of one turn associating with the Pro^2 side chain in the adjacent turn as in Figure 3A where there are 2.7 pentamers per turn and those involving the Val^1 γCH_3 moieties in hydrophobic association with the Pro^2 side chain as in Figure 3B where there are 2.9 pentamers per turn. The NOE data of Figures 1 and 2 demonstrate that the structure in Figure 3B with 2.9 pentamers per turn is more prevalent in aqueous solutions at 22°C.

In addition to the general structural elucidation, further resonance assignment can be made from these two deuterated PPP samples which provides greater structured detail. By comparing Figures 1B and 1C, the Val^1 γCH resonating at 0.94 ppm (the lower field of the two γCH peaks) is closer to Pro^2 βCH resonating at 1.89 ppm. From the NOE data of regular PPP (8), the Pro^2 βCH proton resonating at lower field (2.26 ppm) is closer than the proton resonating at 1.89 ppm to the Pro^2 αCH, i.e., the Pro^2 βCH which resonates at 2.26 ppm is on the same side of the prolyl ring as the Pro^2 αCH. This means for the β-spiral structure that the Val^1 γCH_3 that is interacting with the Pro^2 βCH should be closer to the Pro^2 βCH on the side of the prolyl ring opposite to that defined by the Pro^2 αCH.

Neither structure in Figure 3 has a Val γCH_3 more proximal to the trans Pro^2 βCH, which is on the opposite side of the prolyl ring to the Pro^2 αCH, than to the cis Pro^2 βCH which is on the same side of the prolyl ring as the Pro^2 αCH. It is interesting, however, that a simple change in the prolyl ring pucker, from having the γ-carbon out of the prolyl plane on the αCH side to out of plane on the opposite side, would bring the Val^1 γCH_3 into closest proximity to the trans Pro^2 βCH as is evident from Figure 3B whereas this could not occur with the Val^4 γCH_3 of Figure 3A. Again the β-spiral with 2.9 pentamers per turn is in better accord with this detail of the experimental data.

Molecular dynamics simulations of $(VPGVG)_7$ were carried out to examine the relative stability of the two β-spiral structures. The computed energy is relative to the equilibrium values for bond length, bond angles and dihedral angles. After 50 ps of molecular dynamics simulation, E, the internal energy, for $(VPGVG)_7$ with 2.7 pentamer units per turn is 360 kcal/mole whereas E for $(VPGVG)_7$ with 2.9 pentamer units per turn is 353 kcal/mole. This means that the structure with 2.9 pentamer units per turn calculates to be more stable than that of 2.7 pentamer units per turn by about 1 kcal/mole-pentamer if the end effects for the limited size of $(VPGVG)_7$ are neglected. Since the Boltzmann distribution for various structures is inversely proportional to the exponential of energy, i.e., $e^{-E/RT}$, the ratio of population of 2.7 to 2.9 pentamer units per turn would be ~0.19 according to the *in vacuo* molecular dynamics simulation. The qualitative agreement with the NOE results where the value is approximately 0.3 is not discouraging considering the approximations made, namely, a) end effects are neglected, and b) the effects of solvent are assumed to be the same for these two structures. It will now become possible to determine independently the number of pentamer units per turn for the β-spiral structure by deuterating Val^4 and selectively deuterating Val^1 and Pro^2 at regular intervals in the polypentapeptide. This substantial and rather expensive synthetic effort is in progress.

Conclusions

The present studies demonstrate in PPP that the Val^1 γCH has a stronger NOE interaction than the Val^4 γCH with the Pro^3 βCH. The result indicates that the β-spiral with 2.9 pentamer units per turn is the dominant structure rather than the b-spiral with 2.7 pentamer units per turn. This conclusion utilizes the results of the study of the cyclic analogs where a helix of approximately 3 pentamers per turn was indicated (9). The NOE results for PPP in H_2O of course are inconsistent with the presence of a random chain network. Furthermore, the molecular dynamics simulation for $(VPGVG)_7$ at 300°K in vacuum corroborates qualitatively the NOE results, with the helical structure of 2.9 pentamers per turn being 1 kcal/mole-pentamer more stable than that of 2.7 pentamers per turn.

Acknowledgments

This work was supported in part by National Institutes of Health grant HL 29578 and Department of the Navy, Office of Naval Research contract N00014-86-K-0402. We thank Grant No. CA13148 to the Comprehensive Cancer Center, UAB, for the opportunity to use the NMR instrument at the rate of $15/hour in order to obtain the data in Figures 1 and 2.

References and Footnotes

1. Sandberg, L.B., Leslie, J.B., Leach, C.T., Torres, V.L., Smith, A.R., Smith and D.W., *Pathol. Biol. 33*, 266 (1985).
2. Yeh, H., Ornstein-Goldstein, N., Indik, Z., Sheppard, P., Anderson, N., Rosenbloom, J.C., Cicila, G., Yoon, K. and Rosenbloom, J., *Collagen and Related Research 7*, 235 (1987).
3. Thomas, Jr., G.J., Prescott, B. and Urry, D.W., *Biopolymers 26*, 921 (1987).
4. Urry, D.W.J., *Protein Chem. 7*, 1 (1988).
5. Guantieri, V., Jaques, A.M. and Serafini-Fracassini, A., *Biopolymers 26*, 1957 (1987).
6. Urry, D.W., *Ultrastruct. Pathol. 4*, 227 (1983).
7. Urry, D.W. and Long, M.M., *Elastin and Elastic Tissue*, (Sandberg, L.B., Gray, W.R., Franzblau, C., eds.) Plenum Press, New York, 685 (1977).
8. Urry, D.W., Chang, D.K., Krishna, R., Huang, D.H., Trapane, T.L. and Prasad, K.U., *Biopolymers*, in press.
9. Urry, D.W., Trapane, T.L., Sugano, H. and Prasad, K.U.J., *Am. Chem. Soc. 103*, 2080 (1981).
10. Noggle, J.H. and Schirmer, R.E., *The Nuclear Overhauser Effect - Chemical Applications*, Academic Press, New York (1971).
11. Tarbell, D.S., Yamamoto, Y. and Pope, B.M., *Proc. Natl. Acad. Sci. USA 69*, 730 (1972).
12. Prasad, K.U., Iqbal, M.A. and Urry, D.W., *Int. J. Pept. Protein Res. 25*, 408 (1985).
13. Urry, D.W. and Prasad, K.U., *Biocompatibility of Tissue Analogues*, (Williams, D.F., ed.) CRC Press, Inc., Boca Raton, Florida 89 (1985).
14. Weiland, Th., Heinke, B. and Vogeler, J., *Justus Liebigs Ann Der Chemie 655*, 189 (1961).
15. Venkatachalam, C.M. and Urry, D.W., *Macromolecules 14*, 1225 (1981).
16. Go, N. and Scheraga, H.A., *Macromolecules 6*, 273 (1973).
17. Venkatachalam, C.M. and Urry, D.W.J., *Comp. Chem. 5*, 64 (1984).
18. Brooks, B.R., Bruccoleri, R.E., Olafson, B.O., States, D.J., Swaminathan, S. and Karplus, M.J., *Comp. Chem. 4*, 187 (1983).

Date Received: November 29, 1988.

Communicated by the Editor R.H. Sarma

Journal of Protein Chemistry, Vol. 8, No. 2, 1989

Synthesis of 4% Glu-Containing Val[1] and Ile[1]-Polypentapeptides: Model Protein Systems for Demonstrating Mechanochemical Coupling

H. Zhang,[1] K. U. Prasad[1] and D. W. Urry[1,2]

Received August 19, 1988

The synthesis of 4% Glu-polypentapeptide (PPP) (i.e., 4 Glu residues per 100 amino acid residues) and 4% Glu-Ile[1]-PPP, in which Val[1] is substituted by a more hydrophobic Ile residue, is carried out by copolymerizing the p*-nitrophenyl-active esters of GE(OMe)GVP and GE(OMe)GIP with their parent pentamers GVGVP and GVGIP in 1.4 ratios, respectively. After removal of the methyl ester on the side chain of Glu, these polymers exhibited a remarkable* p*H dependence of the temperature for their inverse temperature transitions, which are followed as turbidity development at 300 nm. On* γ*-irradiation crosslinking, the elastomeric bands obtained exhibited a* p*H-mediated contraction and relaxation. Thus, for the first time, mechanochemical coupling is demonstrated in a synthetic polypeptide system. That the basic mechanism involves the hydrophobic effect (chemical modulation of an inverse temperature transition) and not ion–ion electrostatic repulsion is also discussed.*

KEY WORDS: peptide synthesis; sequential polypeptides; mechanochemical coupling; elastomeric peptides; chemical modulation of an inverse temperature transition.

1. INTRODUCTION[3]

A soluble precursor protein of elastin, tropoelastin, was isolated from copper-deficient procine aorta (Weissman *et al.*, 1963; Sandberg *et al.*, 1969). With sequencing work on this protein almost complete, the most striking feature that has emerged from this analysis was the presence of a pentapeptide sequence L·Val[1]-L·Pro[2]-Gly[3]-L·Val[4]-Gly[5], which repeats 11 times with one substitution in pig (Sandberg *et al.*, 1981, 1985). From bovine tropoelastin cDNA, the same sequence has been found

[1] Laboratory of Molecular Biophysics, University of Alabama at Birmingham, Birmingham, Alabama 35294.

[2] To whom correspondence should be addressed.

[3] Abbreviations used: Boc, tert.-butyloxycarbonyl; Bzl, benzyl; cDNA, Complementary DNA; CMR, carbon-13 nuclear magnetic resonance; DMF, Dimethylformamide; DMSO, dimethylsulfoxide; EtOAc, ethyl acetate; HOBt, 1-hydroxybenzotriazole; i-Boc-Cl, isobutylchloroformate; NMM, *N*-methylmorpholine; OMe, methyl ester; ONp, *p*-nitrophenyl ester; PBS, phosphate-buffered saline; Pd/C, palladium/carbon catalyst; PE, petroleum ether; PPP, polypentapeptide (L·Val[1]-L·Pro[2]-Gly[3]-L·Val[4]-Gly[5])$_n$; TFA, trifluoroacetic acid; TLC, thin-layer chromotography; Tos, *p*-toluenesulfonyl.

0277-8033/89/0400-0173$06.00/0

to repeat 11 times without a single substitution (Yeh *et al.*, 1987). The monomers, oligomers, and polymers of this repeating sequence have been synthesized, and their secondary and tertiary structures have been studied extensively in this laboratory. The most dominant secondary structural feature is the type II Pro^2-Gly^3 β-turn, which, on raising the temperature orders into a helical array, called a β-spiral (Urry, 1988*b*). One of the interesting properties common to tropoelastin, α-elastin (an oxalic acid treatment product of fibrous elastin) (Partridge *et al.*, 1955); and polypentapeptide (PPP), $(VPGVG)_n$, is the process of coacervation. All are miscible with water in all proportions below 20°C. On raising the temperature, the solutions turn turbid; on standing, a viscoelastic phase called the coacervate separates out at the bottom. The entire process is reversible. The composition of the PPP coacervate formed at 30°C has been determined to be about 38% protein and 62% water. This phenomenon is due to the hydrophobic effect, which involves the intra- and intermolecular association of the hydrophobic side chains of the amino acid residues in the protein; during this process, the clathrate-like water surrounding the hydrophobic side chains becomes bulk water. The process can be followed by determining the temperature profiles of turbidity formation ($TP\tau$) at 300 nm. The midpoint of $TP\tau$ for $(VPGVG)_n$, with n about 120, was determined to be 24.5°C. That this property is attributable to the hydrophobic effect can also be demonstrated by synthesizing a more hydrophobic peptide analog of PPP, the Ile^1-PPP, in which Val at position 1 is substituted with a more hydrophobic Ile residue. As expected, the midpoint of $TP\tau$ was lowered to about 10°C (Urry *et al.*, 1986*a*). Similarly the midpoint of $TP\tau$ can also be increased by preparing a less hydrophobic polypeptide; this has been demonstrated with $(VPGG)_n$, which has a midpoint of about 48°C (Urry *et al.*, 1986*b*). The PPP coacervate on γ-irradiation crosslinking forms an isoluble elastomeric matrix, and the hydrophobic effect can be demonstrated with this elastomeric matrix on raising the temperature from 20°C to 40°C as a shortening of the elastomeric band to about 45% of its original length.

This hydrophobic effect can be demonstrated further by yet another polypentapeptide model. The protonated (-COOH) and the unprotonated ($-COO^-$) forms of a carboxylic acid group can be considered, respectively, to make the peptide polymer more or less hydrophobic (Urry, 1988*c*). Thus, it becomes possible to alter the midpoint of $TP\tau$ of the polypentapeptide with carboxylic group in the side chain just by changing the *p*H value of the bathing solution. To demonstrate this effect experimentally, we report the synthesis (Figs. 1A and B), the characterization, and a few of the properties of two polypentapeptide models: 4% Glu-PPP (i.e., 4 Glu residues per 100 residues of amino acids) in which Val^4 is replaced occasionally with a Glu residue and the more hydrophobic 4% Glu-Ile^1-PPP. Contraction and relaxation have been observed on γ-irradiation crosslinked 4%-Glu containing polypentapeptide samples by changing the *p*H of the solution in which the elastomeric PPP strip is in equilibrium (Urry *et al.*, 1988*b*). Thus, mechanochemical coupling has been demonstrated for the first time with a synthetic polypeptide material (Urry *et al.*, 1988*b*). Since there is only a very low percentage of carboxyl groups in these copolymers, the effect observed here cannot be considered the result of electrostatic repulsion between ionizable carboxyl groups, but rather has been shown to arise from modulation of the hydrophobic effect by the protonated (more

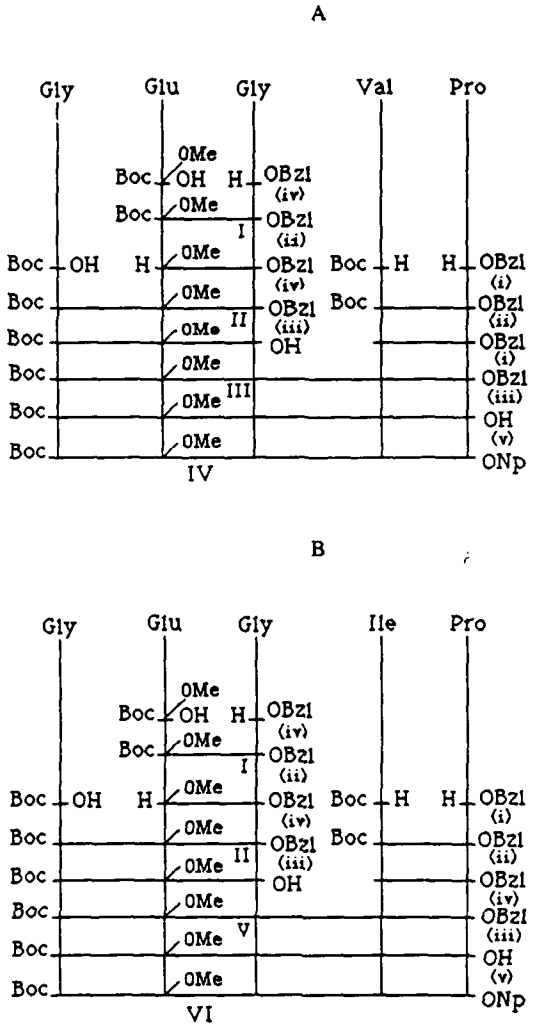

Fig. 1. Synthesis of (A) Boc-Gly-Glu(OMe)-Gly-Val-Pro-ONp, (B) Boc-Gly-Glu(OMe)-Gly-Ile-Pro-ONp. (I) i-Boc-Cl/NMM/HOBt. (II) HCl/dioxane. (III) H_2-Pd/C. (IV) i-Boc-Cl/NMM. (V) Bis(*p*-nitrophenyl)carbonate.

hydrophobic) and ionized (less hydrophobic) forms of carboxylic acid group (Urry *et al.*, 1988*a*).

2. EXPERIMENTAL PROCEDURE

The peptides were synthesized by classic solution methods. Elemental analyses were carried out by Desert Analytics (Tucson, Arizona), and amino acid analyses by the UAB/ARU Protein Chemistry Core (Birmingham, Alabama). The amino acid derivatives used in the syntheses were purchased from Bachem Inc. (Torrance, California). TLC on silica gel plates was performed in the following solvent systems: (1) EtOAc/EtOH/HOAc (90:10:10), (2) $CHCl_3/CH_3OH/HOAc$ (95:5:3), and (3) $CHCl_3/CH_3OH/HOAc$ (75:25:3).

Detection of the peptides on TLC plates was by ninhydrin spray and chlorine-toludine reagents. The melting points were determined with a Thomas Hoover Capillary melting point apparatus and are uncorrected. The temperature dependence for aggregation of the copolymers was followed by the development of turbidity at 300 nm, using a Cary 14 spectrophotometer.

2.1. Boc-Glu(OMe)-Gly-OBzl (I)

Boc-Glu(OMe)-OH (10.45 g, 40 mmoles) in acetonitrile (70 ml) was cooled to 0°C, and NMM (4.4 ml) was added. The solution was cooled to −15°C in a Dry Ice/MeOH bath, and i-Boc-Cl (5.2 ml) was added slowly under stirring while maintaining the temperature at approximately −12°C to −15°C. After stirring for 25 min at this temperature, a precooled solution of *p*-Tos-H-Gly-OBzl (12.82 g, 40 mmoles) and NMM (4.4 ml) in DMF (70 ml) was added slowly, and the reaction mixture was stirred overnight at room temperature. Solvents were removed under reduced pressure, and the residue was dissolved in EtOAc (500 ml) and H_2O (300 ml). The aqueous phase was extracted again with EtOAc (100 ml). The EtOAc layer was washed with 20% citric acid, water, saturated $KHCO_3$, and water and was dried over Na_2SO_4. The residue obtained by evaporation of the solvent was crystallized from EtOAc/PE. Yield: 15.3 g, 93.6%, m.p. 66–67.5°C. R_f^1, 0.93; R_f^2, 0.65; R_f^3, 0.94. Anal. Calc. for $C_{20}H_{28}N_2O_7$ (408.46): C 58.81, H 6.91, N 6.86%. Found: C 59:25, H 7.06, N 6.90%.

2.2. Boc-Gly-Glu(OMe)-Gly-OBzl (II)

Compound I (16.34 g, 40 mmoles) was deblocked with 5.1 N HCl/dioxane for 1.75 hr at room temperature. Excess HCl and dioxane were removed under reduced pressure, and the sample was triturated with ether and PE, filtered, washed with ether, and dried (yield: 100%). HCl-H-Glu(OMe)-Gly-O-Bzl was neutralized with NMM (4.4 ml) and dissolved in DMF (80 ml) and then coupled to Boc-Gly-OH (7 g, 40 mmoles) in acetonitrile (60 ml) and NMM (4.4 ml) using i-Boc-Cl (5.2 ml) and worked up as for I to obtain 17.9 g product (yield: 96.1%), m.p. 86–89°C. R_f^1, 0.76; R_f^2, 0.56; R_f^3, 0.89. Anal. Calc. for $C_{22}H_{31}N_3O_8$ (465.51): C 56.77, H 6.71, N 9.03%. Found: C 56.89, H 6.88, N 9.05%.

2.3. Boc-Gly-Glu(OMe)-Gly-Val-Pro-OBzl (III)

Compound II (14 g, 30.1 mmoles) was taken in HOAc (150 ml) and hydrogenated in the presence of 10% Pd/C (1.5 g) at 40 psi. After filtering the catalyst, the solvent was removed under reduced pressure and the residue was precipitated from ether and a large amount of PE, filtered, and dried to obtain 8.6 g product (yield: 76%). Boc-Gly-Glu(OMe)-Gly-OH obtained above (4.1 g, 10.92 mmoles) in acetonitrile (75 ml) and NMM (1.2 ml) was cooled to −15°C; i-Boc-Cl (1.42 ml) was added slowly. After stirring for 10 min at this temperature, HOBt (1.67 g, 10.92 mmoles) was added. The reaction mixture was stirred for an additional 15 min, and a precooled solution of HCl-H-Val-Pro-OBzl (Prasad *et al.*, 1985) (4.3 g, 12.6 mmoles) in DMF (50 ml) and NMM (1.39 ml) was added slowly. The reaction mixture was stirred overnight and worked up as for I to obtain 6.0 g product from EtOAc/PE recrystalization (yield: 83%), m.p. 130–131.5°C. R_f^1, 0.66; R_f^2, 0.42; R_f^3, 0.89. Anal. Calc. for $C_{32}H_{47}N_5O_{10}$ (661.76): C 58.08, H 7.16, N 10.58%. Found: C 58.31, H 7.26, N 10.70%.

2.4. Boc-Gly-Glu(OMe)-Gly-Val-Pro-ONp (IV)

Boc-Gly-Glu(OMe)-Gly-Val-Pro-OH (2.8 g, 4.9 mmoles) obtained from catalytic hydrogenation of III was dissolved in pyridine (20 ml) and reacted with bis(*p*-nitrophenyl)carbonate (2.98 g, 9.8 mmoles). The reaction mixture was stirred at room temperature for 2 days. Pyridine was moved under reduced pressure. The residue was precipitated from ether, filtered, and washed with ether several times. The solid was taken into EtOAc and washed with 10% citric acid, H_2O, $KHCO_3$ and H_2O. Compound IV, precipitated from EtOAc/PE, was chromatographed over a silica gel (200–325 mesh) column (2.5 × 30 cm). After initial washing with $CHCl_3$, 2.2 g of IV was obtained when eluted with 50% acetone in $CHCl_3$ (yield: 65%), m.p. 122–124.5°C. R_f^1, 0.69; R_f^2, 0.44; R_f^3, 0.88. Anal. Calc. for $C_{31}H_{44}N_6O_{12}$ (692.73): C 53.75, H 6.40, N 12.13%. Found: C 53.63, H 6.43, N 12.11%.

2.5. Boc-Gly(OMe)-Gly-Ile-Pro-OBzl (V)

Boc-Gly-Glu(OMe)-Gly-OH (4.3 g, 11.46 mmoles) in acetonitrile (75 ml) was coupled to HCl-H-Ile-Pro-OBzl (Urry *etal.*, 1986*a*) (4.47 g, 12.6 mmoles) in DMF (50 ml) and NMM (1.39 ml) using i-Boc-Cl (1.49 ml) and worked up as for III to obtain 6.0 g product (yield: 77.5%), m.p. 174–175.5°C. R_f^1, 0.58; R_f^2, 0.36; R_f^3, 0.90. Anal. Calc. for $C_{33}H_{49}N_5O_{10}$ (675.79): C 58.65, H 7.31, N 10.36%. Found: C 58.54, H 7.41, N 10.42%.

2.6. Boc-Gly-Glu(OMe)-Gly-Ile-Pro-ONp (VI)

Boc-Gly-Glu(OMe)-Gly-Ile-Pro-OH (1 g, 1.71 mmole) obtained from catalytic hydrogenation of V was reacted with bis(*p*-nitrophenyl)carbonate (1.04 g, 3.42 mmoles) in pyridine (20 ml) and worked up as for IV to obtain 0.79 g product (yield: 65.4%), m.p. 95–98°C. R_f^1, 0.63; R_f^2, 0.38; R_f^3, 0.88. Anal. Calc. for $C_{32}H_{46}N_6O_{12}$ (707.76): C 54.38, H 6.56, N 11.89%. Found: C 54.84, H 6.60, H 11.84%.

2.7. Synthesis of 4%-Glu–Polypentapeptide

Boc-GE(OMe)GVP-ONp (1.5 g, 2.16 mmoles) and Boc-GVGVP-ONp (5.61 g, 8.64 mmoles) were mixed, and the Boc group was removed by TFA (120 ml) treatment for 1 hr at room temperature. TFA was evaporated under reduced pressure, and the residue, precipitated with ether, was filtered, washed with ether, and dried. The TFA salts of the pentapeptide-ONp were copolymerized in DMSO (8 ml) for 4 weeks at room temperature in the presence of NMM (1.9 ml, 17.28 mmoles). The copolymer was taken into cold distilled water and dialyzed against water using a 3500-dalton cutoff dialysis tubing for 5 days and a 50-kD cutoff dialysis tubing for 6 days at 4°C, changing water twice a day. The retentate was lyophilized to give 3.08 g. The -OMe moieties on the side-chain carboxyl groups of Glu were removed by saponification (1 N NaOH) and once again dialyzed using 50-kD cutoff dialysis tubing to ensure removal of any breakdown products resulting from the base treatment and lyophilized to obtain 4%-Glu-polypentapeptide. The [^{13}C]-NMR (CMR) spectra are presented in Fig. 2. Amino acid ratios: Gly 10.0 (10.0), Glu 0.93 (1), Val 10.0 (10.0), Pro 5.0 (5.0).

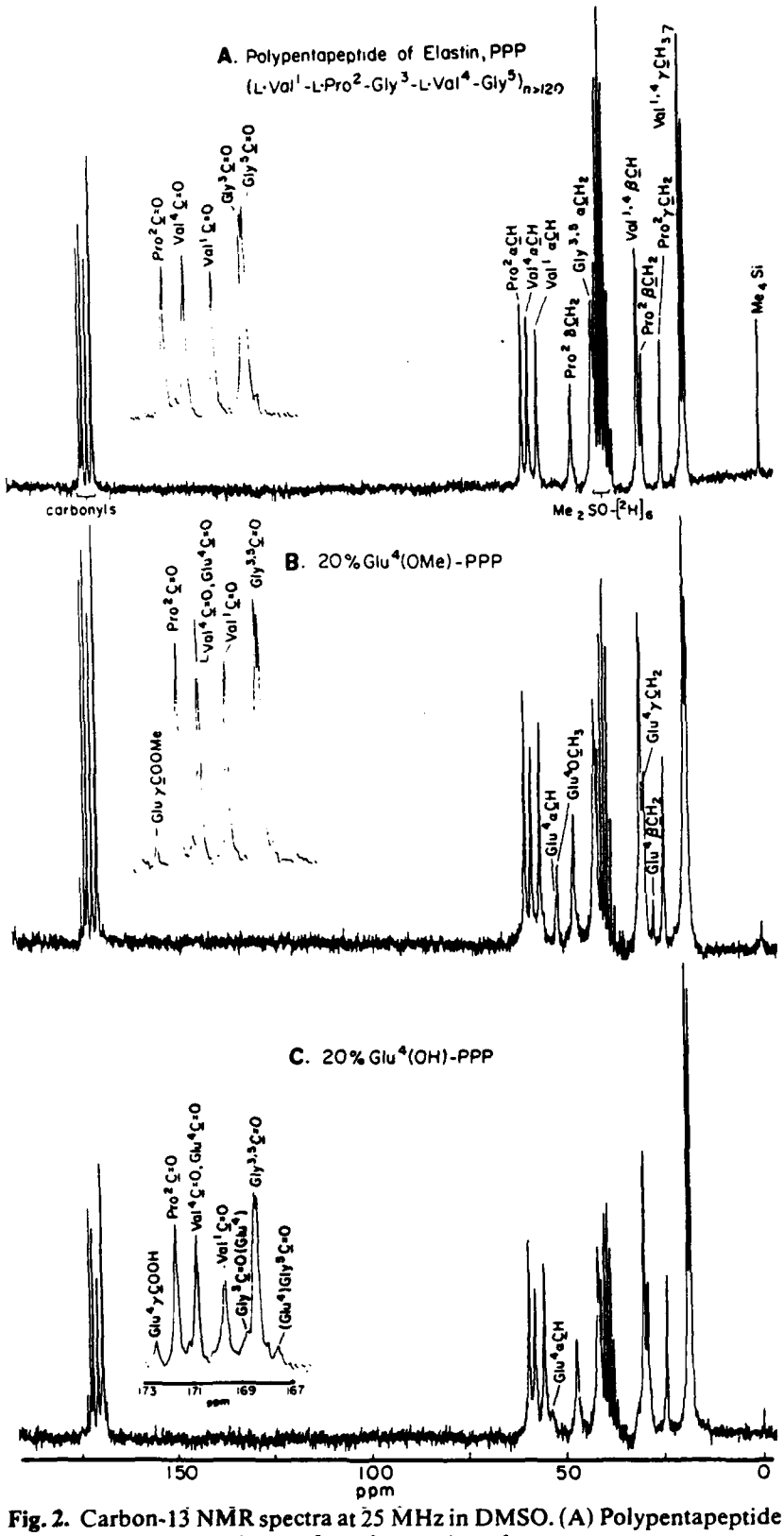

Fig. 2. Carbon-13 NMR spectra at 25 MHz in DMSO. (A) Polypentapeptide of elastin (PPP) $(L\text{-}Val^1\text{-}L\text{-}Pro^2\text{-}Gly^3\text{-}L\text{-}Val^4\text{-}Gly^5)_{n>120}$ with all assignments indicated. (B) The 4%-Glu^4(OMe)-polypentapeptide, where on the average one of five Val^4 residues is replaced by a Glu(OMe) residue with the assignments of the resonances of the guest residue indicated. (C) Upon removal of the methyl group, the 4%-Glu^4-polypentapeptide is obtained. The sharp Glu^4(OMe) peak of (B) is gone, and the Glu^4 αCH has shifted toward the Val^1 αCH resonance; the β and γ CH_2 resonances are buried under the higher field peaks.

2.8. Synthesis of 4%-Glu-Ile^1–Polypentapeptide

Boc-GE(OMe)GIP-ONp (0.708 g, 1 mmole) and Boc-GVGIP-ONp (2.65 g, 4 mmoles) were mixed, and the Boc group was removed by TFA (100 ml). The remaining workup was the same as for 4%-Glu-polypentapeptide. After lyophilization, 1.38 g copolymer was obtained. The [^{13}C]-NMR spectrum is presented in Fig. 3B. The OMe moieties on the side-chain carboxyl groups of Glu were removed by saponification (1 N NaOH) and dialyzed using a 50-kD cutoff dialysis tubing and lyophilized to give 4%-Glu-Ile^1-polypentapeptide. This CMR spectrum is presented in Fig. 3C. Amino acid ratios: Glu 1.17 (1), Gly 11.63 (10), Pro 4.81 (5), Val 4.03 (4), Ile 5.0 (5).

3. RESULTS AND DISCUSSION

The syntheses of the peptides were carried out by the classic solution methodology using a 3+2 approach. The side-chain carboxyl group of Glu was potected as methyl ester. The Boc-group was used for N^{α}-amino protection, and the α-carboxyl group was protected as benzyl ester. Boc-Gly-Glu(OMe)-Gly-OBzl was built by the mixed anhydride (Vaughan and Osato, 1952) method and hydrogenated to obtain the free acid. Boc-Val-Pro-Bzl (Prasad *et al.*, 1985) and Boc-Ile-Pro-OBzl were also synthesized by the mixed anhydride method as reported earlier (Urry *et al.*, 1986*b*). The tripeptide acid was then coupled to the deblocked dipeptide benzyl esters to obtain Boc-Gly-Glu(OMe)-Gly-Val-Pro-OBzl and Boc-Gly-Glu(OMe)-Gly-Ile-Pro-OBzl. After hydrogenation, the peptide acids were converted to *p*-nitrophenyl esters by reacting with bis(*p*-nitrophenyl)carbonate (Wieland *et al.*, 1962). Boc-GVGVP-ONp (Urry and Prasad, 1985) and Boc-GVGIP-ONp (Urry *et al.*, 1986*b*) were prepared as described previously. Boc-GE(OMe)GVP-ONp with Boc-GVGVP-ONp and Boc-GE(OMe)GIP-ONp with Boc-GVGIP-ONp were mixed in 1:4 ratios, deblocked with TFA, and copolymerized for 4 weeks in DMSO, with NMM as the base. The reaction mixtures were diluted with water, dialyzed against water first using a 3500-dalton cutoff dialysis tubing and then a 50-kD cutoff dialysis tubing for several days. The retentates were lyophilized. The methyl ester on the side chain of Glu was removed by base treatment and redialyzed using a 50-kD cutoff dialysis tubing to remove any breakdown peptides that might have formed during the base treatment. The purity of the intermediate products and the copolymers was checked by TLC, CMR spectra, and amino acid analysis.

The incorporation of Glu residues into the copolymers was clearly seen in the CMR spectra in Figs. 2 and 3. In Fig. 2, the PPP (A) is compared with 4% Glu(OMe)-PPP (B) and 4% Glu(OH)-PPP (C). The homogeneity of the products is clearly established with the assignment of all the peaks in the CMR spectra. The removal of methyl ester signal after the base treatment of the polymer is also clear. Similarly, the CMR spectra in Fig. 3 clearly demonstrate the purity of the 4% Glu-Ile^1-PPP. Amino acid analysis (as reported in Section 2. Experimental Procedure) also established the incorporation of Glu residues to the extent of 4%, as expected from the synthetic procedure.

From the dialysis experiments, it is understood that the molecular weight of the polymers should be more than 50 kD. The midpoint of TPτ is also indicative

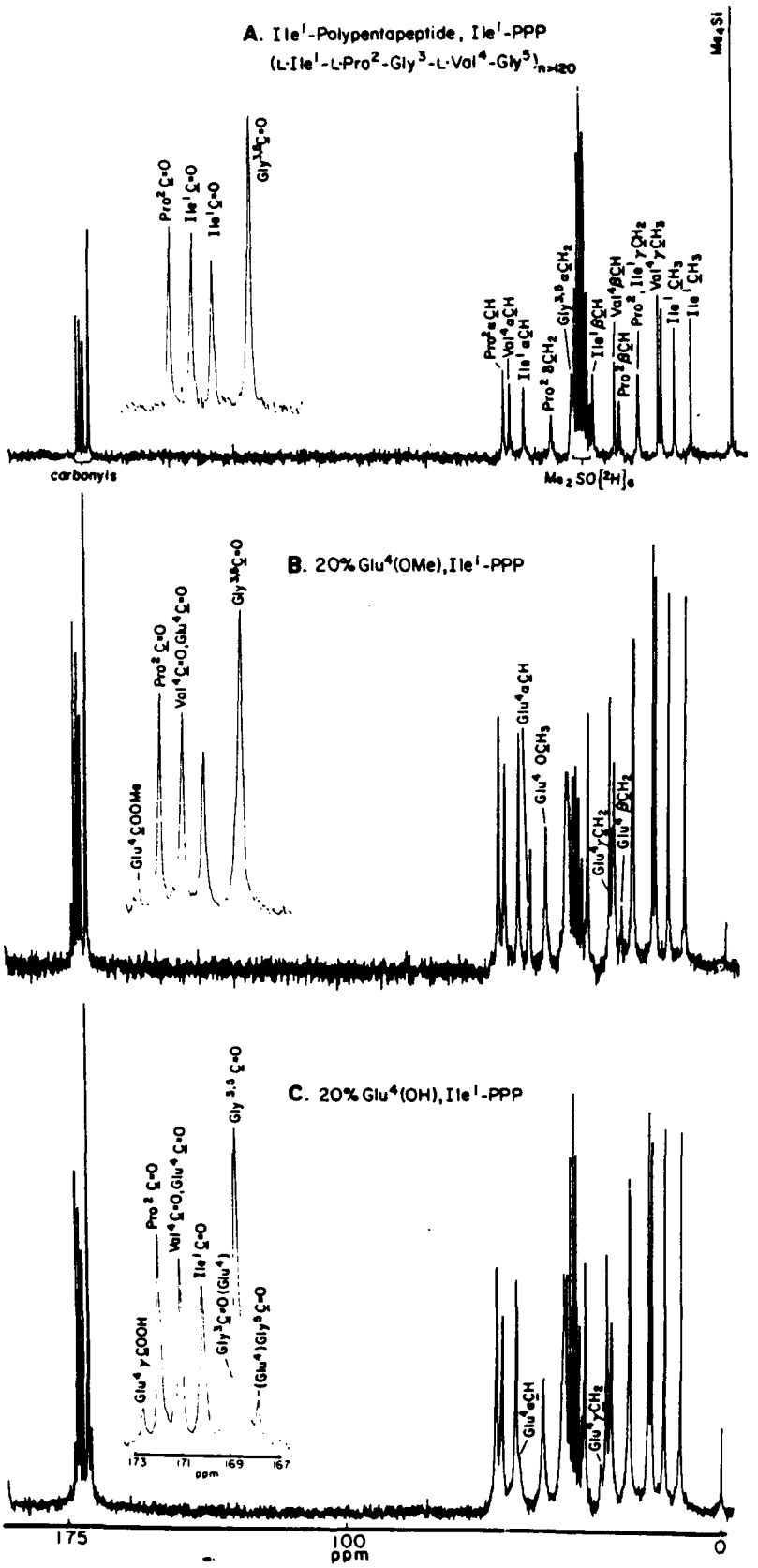

Fig. 3. Carbon-13 NMR spectra at 25 MHz in DMSO. (A) Ile[1]-polypentapeptide (Ile[1]-PPP), with all assignments indicated. (B) The 4%-Glu[4](OMe)-Ile[1]-polypentapeptide, where Val[1] is replaced by Ile[1] and where on the average one of five Val[4] residues is replaced by a Glu(OMe) residue. (C) Upon removal of the methyl group, the 4%-Glu[4]-Ile[1]-polypentapeptide is obtained.

of the molecular weight of the polymer; i.e., the higher the molecular weight, the lower the midpoint (Urry and Prasad, 1985). In the present studies, 4% Glu(OMe)-PPP has a midpoint of 25°C (Fig. 4A-b) as compared with PPP at 24.5°C (Fig. 4A-a) with an established molecular weight of more than 50 kD. The same thing is true with 4% Glu(OMe)-Ile^1-PPP (Fig. 4B-b) which has a midpoint of 12.6°C as compared with 9.9°C for Ile^1-PPP (Fig. 4B-a) with established molecular weight of more than 50 kD. After the base treatment, the midpoints of TPτ for both 4% Glu-PPP (Fig. 4A-c) and 4% Glu-Ile^1-PPP (Fig. 4B-c) have shifted remarkably to higher temperatures. The change of pH has no effect on the TPτ in the case of PPP and Ile^1-PPP, but in the case of 4% Glu-PPP and 4% Glu-Ile^1-PPP, a variation in the pH of the solution has a remarkable effect. While a pH change from 2 to 7 in phosphate-buffered saline (PBS) shifted the midpoint from 25°C to 70°C (Urry *et al.*, 1988*a*) in the case of 4% Glu-PPP a shift of about 20°C was observed from that of 4% Glu-Ile^1-PPP. From the determination of the midpoints of TPτ at varying pH values, the pK_a of 4% Glu-PPP was determined to be 4.4 and the pK_a of 4% Glu-Ile^1-PPP 5.4 (Urry *et al.*, 1988*a*). It has been suggested that the difference between the pK_a of 4% Glu-PPP and 4% Glu-Ile^1-PPP could be due to the hydrophobic effect (Urry *et al.*, 1988*a*). After γ-irradiation crosslinking, both 4% Glu-PPP and 4% Glu-Ile^1-PPP were observed to undergo pH-induced contraction and relaxation. The synthesis of these polymers has made it possible to observe mechanochemical coupling for the first time in synthetic polypeptide models. The

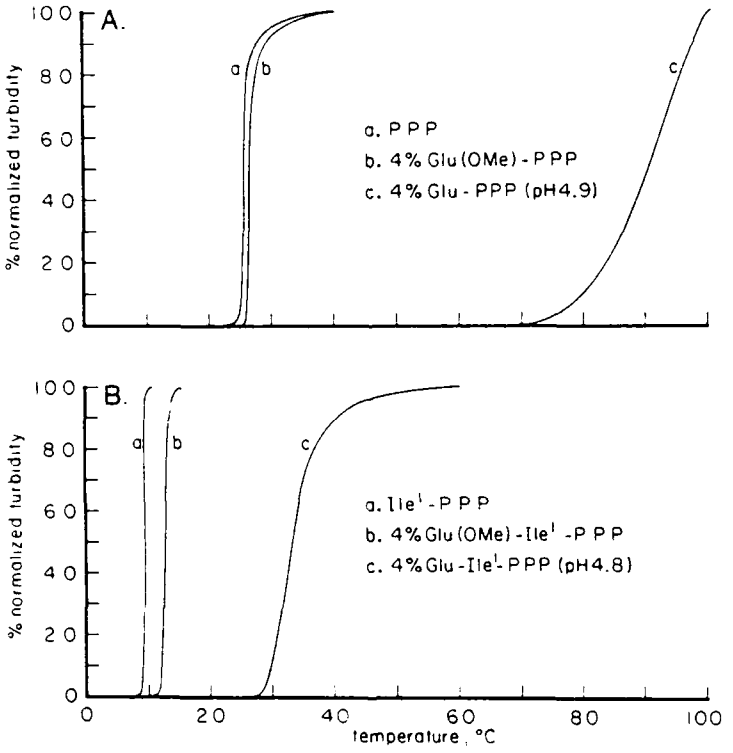

Fig. 4. (A) Temperature profiles of aggregation for PPP, 4%-Glu(OMe)-polypentapeptide and 4%-Glu-polypentapeptide. (B) Temperature profiles of aggregation for Ile^1-PPP, 4%-Glu(OMe)-Ile^1-polypentapeptide, and 4%-Glu-Ile^1-polypentapeptide.

*p*H dependence of the length at a fixed load and the *p*H dependence of a force at a constant length can be monitored using these polymers (Urry *et al.*, 1988*b*). Because of the presence of a very low percentage of the carboxyl groups, the *p*H dependence of these properties is expected to be attributable to the hydrophobic effect rather than to ion-ion electrostatic repulsion. This is demonstrated by the partial differential of chemical potential with respect to force at constant composition, i.e., $(\partial\mu/\partial_f)_n$, which is positive for charge-charge repulsion (Katchalsky *et al.*, 1960) and negative for the present anionic charge modulation of an inverse temperature transition (Urry, 1988*a*). These syntheses make possible for the first time the demonstration in a synthetic polypeptide system that a change in chemical potential can bring about a contraction in which work is performed.

ACKNOWLEDGMENTS

The authors would like to thank Marsha Waller for obtaining the [^{13}C]-NMR spectra of Figs. 2 and 3 and Dorothy Hains for obtaining the data of Fig. 4. This work was supported in part by grant HL 29578 from the National Institutes of Health and by contract N00014-86-K-0402 from the Department of the Navy, Office of Naval Research.

REFERENCES

Katchalsky, A., Lifson, S., Michaeli, I., and Zwick, M. (1960). *Size and Shape of Contractile Polymers: Conversion of Chemical Into Mechanical Energy* (Wasserman, A., ed.) Pergamon Press, New York, pp. 1-40.

Partridge, S. M., Davis, H. F., and Adair, G. S. (1955). *Biochem. J.* **61**, 11-21.

Prasad, K. U., Iqbal, M. A., and Urry, D. W. (1985). *Int. J. Peptide Protein Res.* **25**, 408-413.

Sandberg, L. B., Weissman, N., and Smith, D. W. (1969). *Biochemistry* **8**, 2940-2945.

Sandberg, L. B., Soskel, N. T., and Leslie, J. B. (1981). *N. Engl. J. Med.* **304**, 566-579.

Sandberg, L. B., Leslie, J. G., Leach, C. T., Alvarez, V. L., Torres, A. R., and Smith, D. W. (1985). *Pathol. Biol.* **33**, 266-274.

Urry, D. W., (1988*a*). *Int. J. Quantum Chem. Quantum Biol. Symp.* **15**, 235-245.

Urry, D. W. (1988*b*). *J. Protein Chem.* **7**, 1-34.

Urry, D. W. (1988*c*). *J. Protein Chem.* **7**, 81-114.

Urry, D. W., and Prasad, K. U. (1985). In *Biocompatibility of Tissue Analogues* (Williams, D. F., ed.), CRC Press, Boca Raton, Florida, pp. 89-116.

Urry, D. W., Long, M. M., Harris, R. D., and Prasad, K. U. (1986*a*). *Biopolymers* **25**, 1939-1953.

Urry, D. W., Harris, R. D., Long, M. M., and Prasad, K. U. (1986*b*). *Int. J. Petptide Protein Res.* **28**, 649-660.

Urry, D. W., Chang, D. K., Zhang, H., and Prasad, K. U. (1988*a*). *Biochem. Biophys. Res. Commun.* **153**, 832-839.

Urry, D. W., Haynes, B., Zhang, H., Harris, R. D., and Prasad, K. U. (1988*b*). *Proc. Natl. Acad. Sci. USA* **85**, 3407-3411.

Vaughan, J. R., Jr., and Osato, R. L. (1952) *J. Am. Chem. Soc.* **74**, 676-678.

Weissman, N., Shielfd, G. S., and Carnes, W. H. (1963). *J. Biol. Chem.* **238**, 3115-3123.

Wieland, T., Heinke, B., and Vogeler, K. (1962). *Justus Liebigs Ann. Chem.* **655**, 189-194.

Yeh, H., Ornstein-Goldstein, N., Indik, Z., Sheppard, P., Anderson, N., Rosenbloom, J. C., Cicila, G., Yoon, K., and Rosenbloom, J. (1987). *Collagen Rel. Res.* **7**, 235-247.

Two-Dimensional Proton NMR Studies on Poly(VPGVG) and Its Cyclic Conformational Correlate, Cyclo(VPGVG)$_3$

D. W. URRY, D. K. CHANG, *Laboratory of Molecular Biophysics;*
N. R. KRISHNA, D. H. HUANG, *Comprehensive Cancer Center;*
T. L. TRAPANE, and K. U. PRASAD, *Laboratory of Molecular Biophysics, The University of Alabama at Birmingham, Birmingham, Alabama 35294*

Synopsis

Two-dimensional nuclear Overhauser enhancement (2D NOESY) data are reported for the polypentapeptide of elastin, poly(VPGVG), and the cyclopentadecapeptide, cyclo(VPGVG)$_3$. In both, the repeating type II Pro^2-Gly^3 β-turn can be derived from the NOE data, providing confirmation of many previous studies. In addition, other through-space connectivities are detailed that also compare favorably with previously determined crystal and solution structures for cyclo(VPGVG)$_3$. Also, near identical data for the cyclopentadecapeptide and the polypentapeptide demonstrate the cyclic conformation-linear (helical) conformational correlate relationship between the two molecules. The 2D NOESY experiment is seen to be an effective means of establishing the presence or absence of a conformational relationship between a cyclic repeating sequence and its higher molecular weight linear counterpart. This is an approach of substantial practical value when developing the conformation of sequential polypeptides and when attempting to identify the presence of the conformation of a repeating peptide sequence within a more complex primary structure.

Having established the basic conformational relationship between a cyclic conformation and its linear helical counterpart, cross peaks present in the linear helical structure that are not present in the cyclic conformational correlate can provide information on the interactions between adjacent turns of the helix. In this connection, a ValγC$\underline{H}_3$ $\leftrightarrow$ ProβC$\underline{H}_2$ interaction is reported that can be the basis for determining the number of pentamers per turn of helix once it is determined whether it is dominantly the Val^1 or Val^4 γC$\underline{H}_3$ that is interacting with the Pro^2βC$\underline{H}_2$.

INTRODUCTION

The polypentapeptide, poly(VPGVG), also abbreviated as PPP, is the longest, most striking repeating sequence in tropoelastin, the single precursor protein of elastin fibers.[1-3] In porcine and bovine tropoelastin,[3,4] PPP occurs in the longest sequence between cross-links which are formed from lysine residues. In tropoelastin tryptic digestion, PPP cleaves on the carboxyl side of the Lys residues, giving as tryptic peptides the sequences between cross-links, with the exception of a single arginine residue. There are some 20 tryptic peptides in this approximately 800-residue protein, giving an average tryptic peptide length of about 40 residues. In the polypentapeptide containing tryptic peptide, the PPP is 57 residues in length in pig with but one substitution and the PPP is within an 81-residue tryptic peptide.[3] In bovine tropoe-

Biopolymers, Vol. 28, 819–833 (1989)

CCC 0006-3525/89/040819-15$04.00

lastin, the PPP is also 57 residues in length without a single substitution and it occurs in an equivalent 73-residue tryptic peptide.[4]

Tropoelastin,[5,6] α-elastin (a 70,000 molecular weight fragmentation product from oxalic acid treatment of elastin fibers),[7] and poly(VPGVG) are each soluble in water below 20°C, but on raising the temperature to the physiological range, aggregation occurs reversibly to form filamentous arrays observable by electron microscopy and to macroscopically form a viscoelastic phase called the coacervate,[8] which is about 60% water, and 40% peptide or protein.[9] When chemically or when γ-irradiation cross-linked in the coacervate state, the cross-linked PPP is elastomeric with an elastic modulus and temperature dependence of elastomeric force similar to that of elastin fibers.[10] Remarkably, in water, elastomeric force develops on raising the temperature from 20 to 40°C by means of an inverse temperature transition, and elastomeric force decreases on slowly raising the temperature above 60°C due to heat denaturation.[11,12]

Early conformational studies on the repeating pentamer have demonstrated the presence of a type II Pro^2-Gly^3 β-turn.[13,14] These findings were subsequently confirmed by demonstrating that cyclo(VPGVG)$_3$ has a nearly identical conformation to that of the linear polypentapeptide[15,16] and by the crystal structure of cyclo(VPGVG)$_3$, which exhibited the type II Pro^2-Gly^3 β-turn, as shown for the pentameric repeat in Fig. 1.[17]

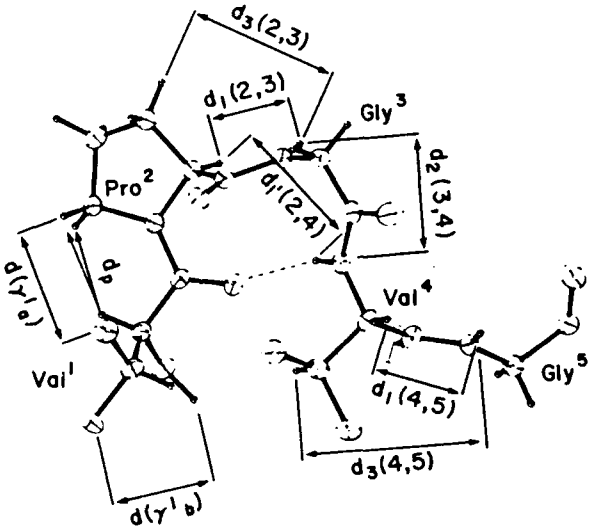

through space connectivities

d_1 (2,3): Pro^2 αCH — Gly^3 NH
d_1 (4,5): Val^4 αCH — Gly^5 NH
$d_{1'}$(2,4): Pro^2 αCH — Val^4 NH
d_2(3,4): Gly^3 NH — Val^4 NH
d_p: Val^1 αCH — Pro^2 δCH_2
$d(\gamma'_a)$: Val^1 $\gamma_a CH_3$ — Pro^2 δCH_2
$d(\gamma'_b)$: Val^1 $\gamma_b CH_3$ — Val^1 NH
d_3(4,5): Val^4 βCH — Gly^5 NH
d_3(2,3): Pro^2 βCH — Gly^3 NH

Fig. 1. Crystal structure of a pentamer segment of cyclo(VPGVG)$_3$, a conformational correlate of the linear high polymer of the pentapeptide of elastin. The Val^1CO ... HN Gly^3 hydrogen bond of the type II Pro^2-Gly^3 β-turn is shown as a dashed line. (Adapted with permission from Ref. 16.) The through-space connectivities observed for the molecule in solution are indicated by arrows on the structure and corresponding proton–proton interactions are given below.

The present effort begins two-dimensional nmr (2D nmr) studies[18-21] on peptides of elastin with two-dimensional nuclear Overhauser enhancement spectroscopy (2D NOESY) and correlation spectroscopy (2D COSY) data on poly(VPGVG) and on cyclo-$(VPGVG)_3$. The solvents used are dimethyl sulfoxide and water. The conformation of poly(VPGVG) is more developed in dimethyl sulfoxide than in water at temperatures below the inverse temperature transition, but the evidence is substantial that the conformation in dimethyl sulfoxide is very similar to that in water above the temperature of the inverse temperature transition[22] when elastomeric force is fully developed. Aggregation attending the inverse temperature transition precludes obtaining high-resolution proton nmr spectra directly on the elastomeric state in water, which is a state of 60% water and 40% peptide by weight at 40°C.[9] Fortunately, elasticity is retained in dimethyl sulfoxide and an elastomeric force has been reported for elastin fibers that is dominantly entropic in this solvent system,[23] just as it is dominantly entropic for elastin fibers in water.[24-26] Accordingly, the conformation of elastin peptides in dimethyl sulfoxide is directly relevant to the elastomeric state of elastin. Also, it is possible, as reported here, to obtain one-dimensional (1D) NOE data in water at a temperature just below the onset of the inverse temperature transition, which is relevant to incipient hydrophobic interactions.

MATERIALS AND METHODS

Syntheses

The syntheses and characterizations of PPP with a molecular weight of greater than 100,000 daltons and cyclo$(VPGVG)_3$ were as previously described.[15,27]

NMR EXPERIMENTS:

Samples of the cyclo$(VPGVG)_3$ and the PPP were dissolved in dimethyl-$[^2H]_6$-sulfoxide (DMSO-d_6 99.96% ^2H, Merck Isotopes, Montreal, Canada) at concentrations of 0.064*M*. Proton nmr experiments were performed at ambient temperature (22–23°C) on a Bruker WH-400 (9.4 T) spectrometer equipped with an Aspect 2000 computer, external pulse programmer, and Diablo 31 disk drive. Proton chemical shifts were referenced to internal tetramethylsilane (0 ppm). The 2D NOESY nmr experiments in DMSO-d_6 were performed in the phase-sensitive[28-31] and quadrature detection modes with 1024 points in the t_2 dimension (spectral width = 4000 Hz) and with 256 t_1 experiments. A mixing time of 150 or 200 ms was used. Prior to Fourier transformation, the data in the t_2 domain were multiplied by an unshifted sine bell window function, while the data in the t_1 domain were multiplied by a shifted sine bell function.

For the studies in water, 2D COSY and NOESY results were obtained from a solution of 0.4*M* PPP (MW > 50 kdal) in 85% H_2O and 15% D_2O at 294 K. The solvent peak was suppressed by selective presaturation of the peak during pulse delay between two consecutive acquisitions. Sixteen and 144 transients were collected for COSY and NOESY, respectively, for each of 256 t_1 experiments with 1 K data points in t_2 dimension and 4000 Hz spectral width.

For 1D NOE experiments, samples of the cyclo$(VPGVG)_3$, poly$(VPGVG)_{12}$, and poly$(VPGVG)_n$ (50 kdal < MW < 100 kdal) were dissolved in 99.96% D_2O

(Stohler Isotope Chemicals) to make final solutions of 0.1*M* in pentamer units. The 1D spectra were collected on a Bruker WH-400 spectrometer equipped with an Aspect 3000 computer. Truncated driven NOE experiments were employed for 1D NOE measurements. In these experiments, a 0.15 s presaturation time in which magnetization is allowed to transfer was used selectively to saturate resonances of valyl γ-methyl protons. The observed proton–proton through-space contacts are expected to involve distances up to about 3.5 Å.

RESULTS AND DISCUSSION

The 2D NOESY maps are given in Figs. 2 and 3 for cyclo(VPGVG)$_3$ and for PPP, respectively, in DMSO. They are seen to be very nearly identical, with the obvious exception that the lower molecular weight cyclopentadecapeptide exhibits a finer structure. Also, while overlapping in the 1D spectra, the $Gly^3N\underline{H}$ and $Gly^5N\underline{H}$ resonances are seen to be very slightly shifted in the 2D maps, with the order interchanged for the cyclic and linear peptides. Both peptides show the same small fraction of *cis* Val-Pro, as seen most readily by the small doublet in the 1D spectrum near 4.6 ppm. This small occurrence of *cis* does give rise to some minor cross peaks. The assigned 2D COSY (upper half) and 2D NOESY (lower half) maps with connectivities indicated are given in Fig. 4 for PPP.

Details of the β-turn: As sketched in the lower half of Fig. 4, all four d_1 connectivities ($\alpha C\underline{H}_i \leftrightarrow N\underline{H}_{i+1}$) are observed in DMSO, and they are also apparent in water in the 2D NOESY map of Fig. 5, where $d_1(3,4)$ and $d_1(5,1)$ overlap. The d_1 connectivity of particular interest for the β-turn is $d_1(2,3)$, i.e., the $Pro^2\alpha C\underline{H} \leftrightarrow Gly^3N\underline{H}$ through-space NOE; it is particularly prominent in water (Fig. 5). This proton–proton distance is a function of the ψ^2 torsion angle. In the crystal structure of the cyclopentadecapeptide the value is 140°,[17] whereas in the methanol solution structure the value obtained using nmr and conformational energy minimization was 118°.[16] From Fig. 2 of Billeter et al.,[32] these angles are in the minimal distance range near 2.3 Å. Proximity of the $Pro^2\alpha C\underline{H}$ and $Gly^3N\underline{H}$ protons demonstrated over a decade ago by NOE[14] was the initial basis for concluding a type II β-turn in the pentamer t-Boc-VPGVG-OCH_3. The primary d_2 connectivity most readily identified in DMSO (Fig. 4) but also present in water (Fig. 5) is the intense $d_2(3,4)$, i.e., $Gly^3N\underline{H} \leftrightarrow Val^4N\underline{H}$. This proton–proton distance is a function of ϕ^3 and ψ^3. From the crystal structure[17] the values are, respectively, 80° and −7°, whereas the structure derived using conformational energy calculations and nmr-derived constraints from solution gave values of 111° and −58°, respectively.[16] The proton–proton distance for the former would be 2.5 Å, whereas for the latter it would be about 3.2 Å. One proton–proton proximity apparent in Figs. 2–4 that is particularly constraining for the β-turn is the $Pro^2\alpha C\underline{H} \leftrightarrow Val^4N\underline{H}$ through-space connectivity labeled $d_1'(2,4)$ in Fig. 1; it is most apparent in DMSO in Fig. 4. These two protons separated by seven bonds are within the 3.5-Å distance for the expected cutoff in these studies. This proximity is facilitated by the nonlinearity of the $Val^1C{-}O \ldots H\underline{N}\ Val^4$ hydrogen bond of the β-turn and requires the appropriate three torsion angles for ψ^2, ϕ^3, and ψ^3. This connectivity provides an interesting demonstration of the β-turn in water at temperatures just below the onset of the inverse

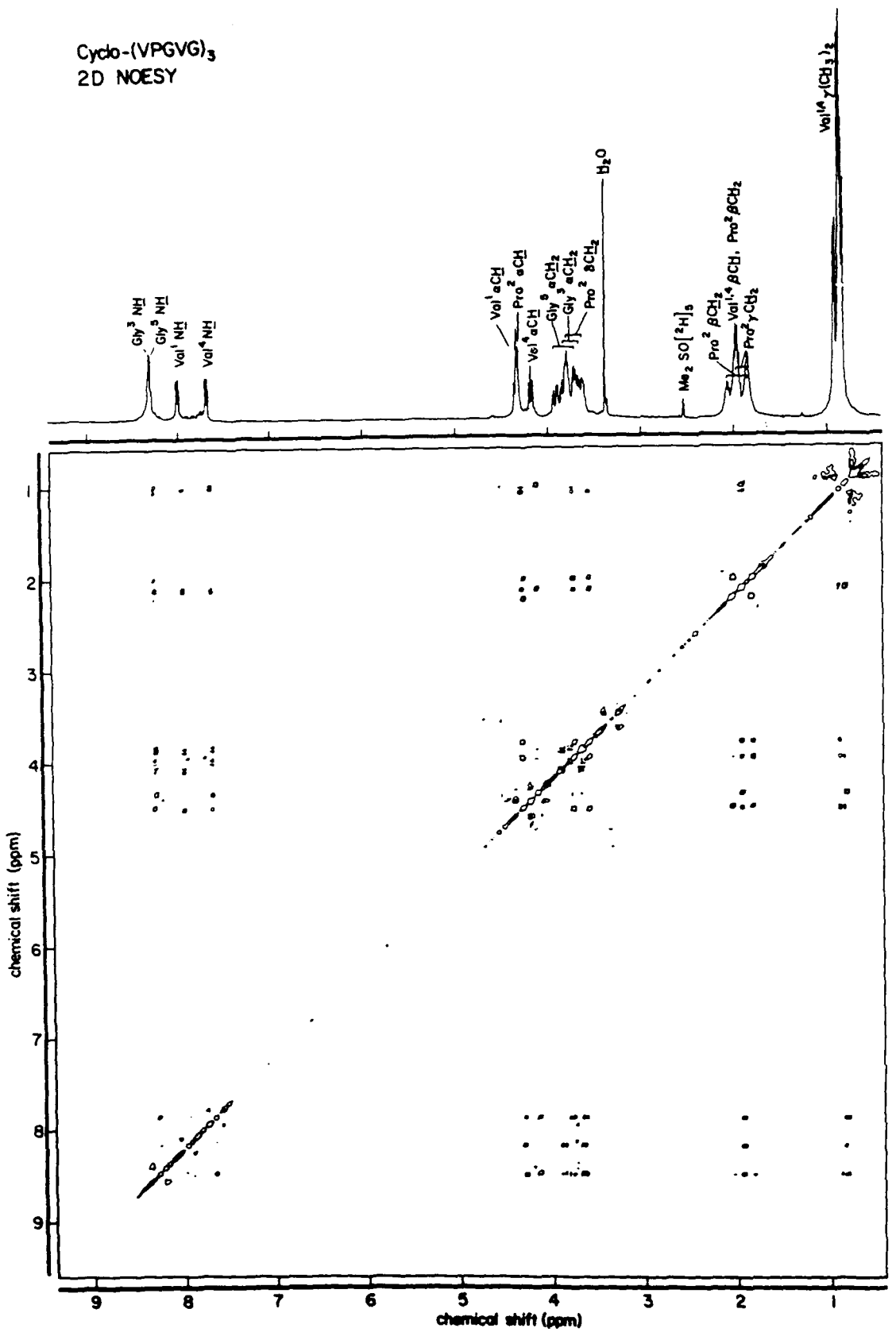

Fig. 2. Two-dimensional proton homonuclear NOE contour plot for the cyclopentadecapeptide, cyclo(VPGVG)$_3$, in dimethyl-[$^2H_6$]-sulfoxide at 400 MHz and 23°C. The concentration of pentapeptide is 0.064*M*. The corresponding 1D spectrum is given above the map with all of the proton resonances assigned.

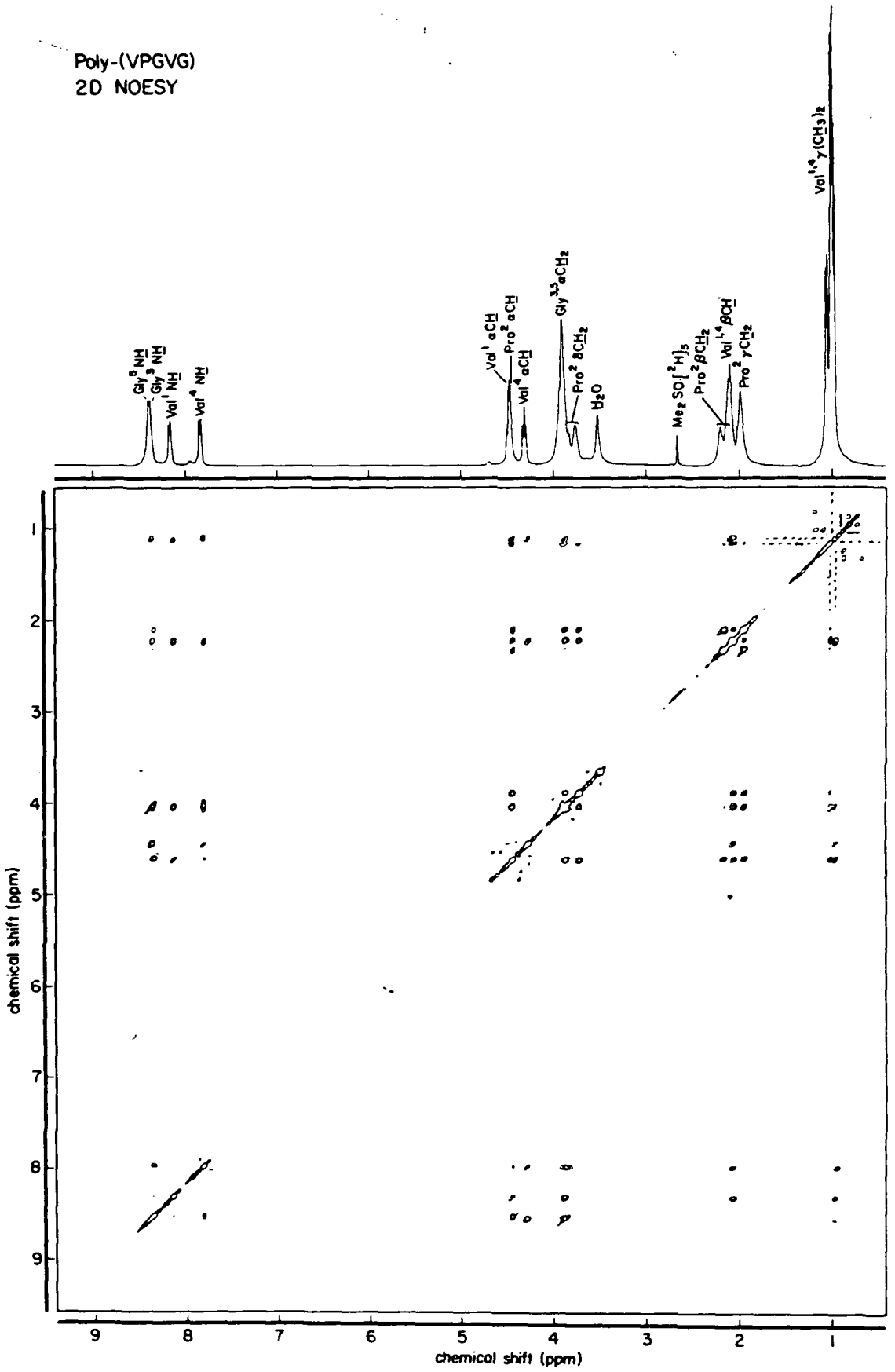

Fig. 3. Two-dimensional proton homonuclear NOE contour plot for the greater than 100,000 dalton molecular weight polypentapeptide of elastin, PPP, in dimethyl-[$^2H_6$]-sulfoxide at 400 MHz and 23°C. The concentration of pentapeptide is 0.064*M*. Assignments are given on the corresponding 1D spectrum, which is above the plot. Note that the map for the linear high polymer is strikingly similar to the map for the cyclic conformational correlate, cyclo(VPGVG)$_3$ (Fig. 2).

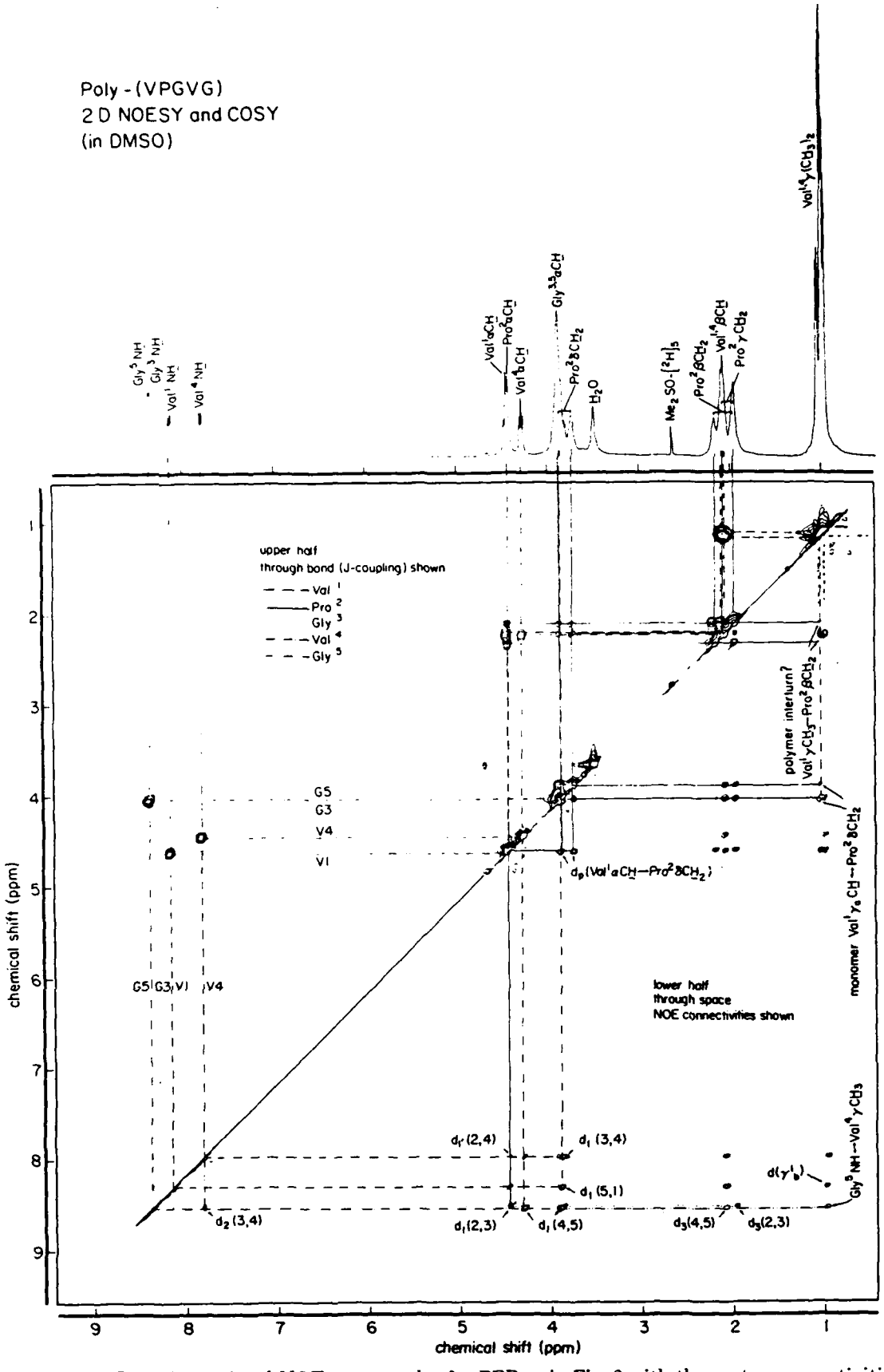

Fig. 4. Two-dimensional NOE contour plot for PPP as in Fig. 3 with the proton connectivities outlined. In the upper half of the map are shown the connectivities for the through bond (J coupled) protons. In the lower half are shown the through-space connectivities for the pentamer as diagrammed in Fig. 1.

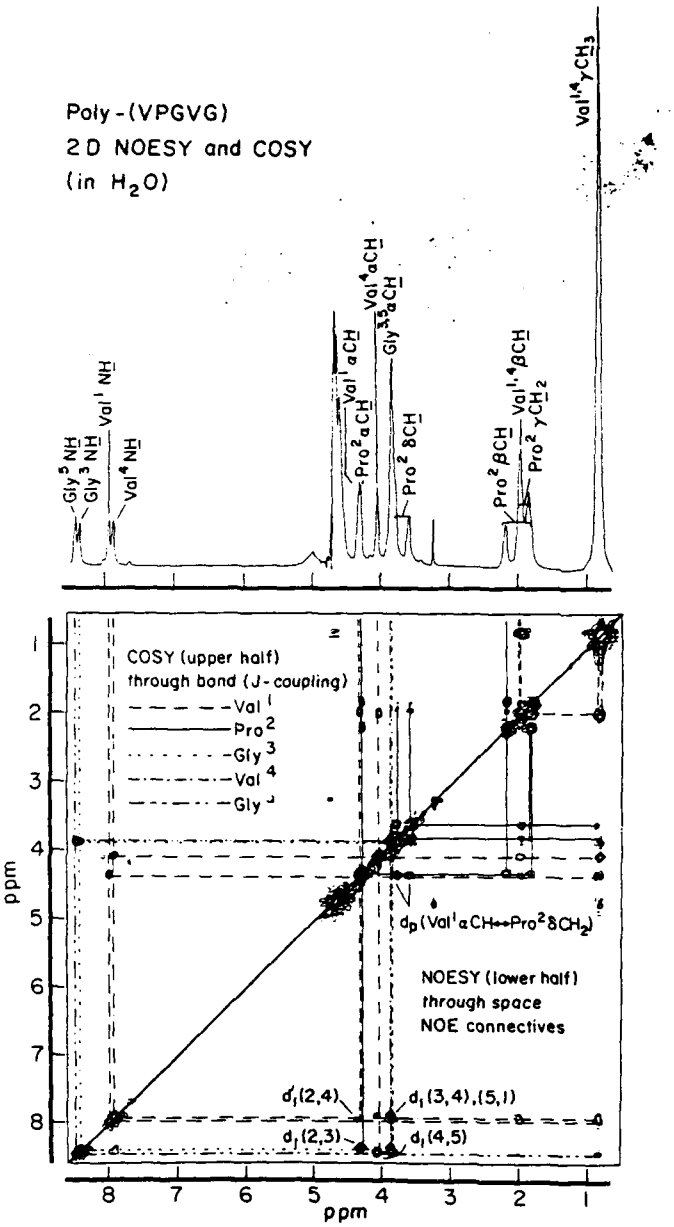

Fig. 5. Four hundred megahertz ^1H 2D COSY (upper left) and 2D NOESY (lower right) contour maps of PPP in 85% H_2O and 15% D_2O solution at 294 K, pH 2.7. The concentration of polypentapeptide is 0.4*M*; the mixing time for NOESY experiment is 0.15 s. The residue designation is the same as that in Fig. 4.

temperature transition as has also been recently demonstrated by Raman spectroscopy.[33]

The particular β-turn utilizing the tetrapeptide sequence VPGV has additional unique proton–proton proximities. The $Val^1\alpha C\underline{H} \leftrightarrow Pro^2\delta C\underline{H}_2$ through-space connectivity indicated as d_p in Fig. 1 is very apparent in the central region of the 2D NOESY maps of cyclo$(VPGVG)_3$ and PPP. This further demonstrates the presence of the unique β-turn structure in solution and places constraints on ψ^1 near 120°, i.e., 129° in the crystal,[17] and 115° in the solution-derived structure[16] Another set of connectivities that are apparent in the 2D maps and in Fig. 1 involves the $Val^1\gamma C\underline{H}_3$ moieties. Following

he low-field $\gamma C\underline{H}_3$ doublet from the 1D spectra in DMSO in Figs. 3 and 4, this is seen to uniquely interact through space with the $Pro^2\delta C\underline{H}_2$; it is identified as $\gamma C\underline{H}_3$ of the Val^1 residue and indicated as the $Val^1\gamma_a C\underline{H}_3$. Another $Val\gamma CH_3$ within the major $C\underline{H}_3$ peak interacts through space with the $Val^1N\underline{H}$; it is indicated as the $Val^1\gamma_b C\underline{H}_3 \leftrightarrow Val^1N\underline{H}$ connectivity. This latter interaction is most apparent in Fig. 2 and may be verified in Fig. 3. Significantly, these connectivities identify the Val^1 residue as the source of the low-field $\gamma C\underline{H}_3$ resonance. The identification of the $Val^1\gamma C\underline{H}_3$ resonances can be useful in consideration of interturn interactions in the polypentapepide β-spiral (see below). In aqueous systems with lower molecular weight PPP, the $Val^1\gamma C\underline{H}_3 \leftrightarrow Pro^2\delta C\underline{H}_2$ interaction was earlier demonstrated to be markedly enhanced by raising the temperature from 20 to 40°C and directly demonstrated the increased hydrophobic association attending an inverse temperature transition in water.[34]

The d_3 connectivities, $d_3(2,3)$ for $Pro^2\beta C\underline{H}_2 \leftrightarrow Gly^3N\underline{H}$ and $d_3(4,5)$ for $Val^4\beta C\underline{H} \leftrightarrow Gly^5N\underline{H}$, are also apparent in DMSO. The relevant torsion angles are ψ^2 and ψ^4 as well as the χ_1 angles for each of the residues. These connectivities are of interest for different reasons. As seen in Figs. 2–4, the $d_3(2,3)$ connectivity is most significant to the upfield component of the $Pro^2\beta C\underline{H}_2$ doublet. Looking at Fig. 1, it is apparent that this is the radial proton, whereas the axial $Pro^2\beta C\underline{H}$ proton is at a greater distance. The radial hydrogen therefore is responsible for the high-field component of the ^2J doublet and the axial hydrogen for the low-field component. In particular, the most proximal $Pro\beta C\underline{H}_2$ proton is sufficiently close (near 3.5 Å) to give a weak interaction, whereas the most distal gives only a slight dot both for cyclo$(VPGVG)_3$ and PPP. This allows the qualitative sense that the chosen mixing time is such as to give contacts for distances up to 3.5 Å when the conformation is relatively well defined.

For more dynamic structures or for a more dynamic part of these structures, the situation is more complex, as is apparent for the second d_3. Referring to Fig. 1, it is apparent that $d_3(4,5)$, i.e., $Val^4\beta C\underline{H} \leftrightarrow Gly^5N\underline{H}$, is a relatively long distance with χ_1^4 at an angle giving a near maximal distance between the two hydrogen nuclei. For a ψ^4 of 119° for the cyrstal and near 100° for the solution-derived structure, depending on the value of χ_1^4, the distance ranges from 3.5 to 4.5 Å. With ψ^4 and χ^4 as given in Fig. 1, the distance is near the maximal value of 4.5 Å. Thus in order to have a significant NOE, some structural flexibility is required in the peptide segment not in the β-turn, which has been referred to as the dynamic suspended segment.[10,11] If χ_1^4 were such as to give the closest distance, even here the distance of 3.5 Å is near the cutoff. This is not likely because the $^3J(Val^4\alpha C\underline{H}\text{-}\beta C\underline{H})$ coupling constant is 9.0 Hz that, while indicating some flexibility, requires a significant preference for the *trans* orientation of Fig. 1. The $Val^4\beta C\underline{H} \leftrightarrow Val^4N\underline{H}$ cross peak of Figs. 2 and 3 further demonstrate the χ_1^4 *trans* orientation of Fig. 1. Another source of flexibility would be for the peptide moiety to rock, i.e., to librate. As shown for the proposed β-spiral conformation of PPP, the torsion angles, ψ_4 and ϕ_5, are coupled and can undergo librational motions, within a 2 kcal/mole residue cutoff energy, of up to 160° without affecting the positions of the Val^1 α-carbons.[10] This would bring the $Gly^5N\underline{H}$ and the $Val^4\beta C\underline{H}$ hydrogens to within 2.5 Å of each other and is a much more effective way to

achieve the proximity indicated by the 2D NOESY data. The peptide libra tions in the pentamer–water system, proposed as a source of entropy change on stretching, have been observed by means of dielectric relaxation data for PPP[35] as well as for packed crystallites of cyclo(VPGVG)$_3$ (Henze and Urry, unpublished data). The librations obviously are much more damped in the crystallites. Peptide librations within the Val^4-Gly^5-Val^1 suspended segment are facilitated by the inherent flexibility of the β-turn. This is consistent with the observation of all d_1 connectivities as the maximal $\alpha C\underline{H}_i - N\underline{H}_{i+1}$ distance is 3.55 Å, which occurs at ψ_i of $-60°$.[32]

Accordingly, the 2D nmr data confirm in substantial detail the previous studies and proposals for this pentapeptide system, and they contain a most interesting means of demonstrating the conformational relationship between cyclic and linear analogs. Of particular interest would be to obtain information unique thus far to the 2D nmr approach, that is, to learn of interrepeat interactions not present in cyclo(VPGVG)$_3$ but present in PPP. In going from a cyclic structure to a helical conformational correlate, i.e., the β-spiral, interactions that could be unique to PPP would be the interturn interactions. As noted above, the two 2D NOESY maps are almost identical for the cyclic and linear polymers. One difference seen in DMSO, where there are weak cross peaks in the PPP data that are not present in the cyclo(VPGVG)$_3$ data, has to do with interactions with the Pro$^2\beta C\underline{H}_2$ protons. The low-field $\gamma C\underline{H}_3$ protons that have been identified above with the Val^1 residue may have an interaction with the Pro$^2\beta C\underline{H}_2$ protons that is not present in the cyclopentadecapeptide. Care must be taken that these are not the result of streaking from the $\gamma C\underline{H}_3$ region. However, their absence in cyclo(VPGVG)$_3$ even at very low contour levels and when unsymmetrized, and the absence of other cross peaks from the more intense higher field $\gamma C\underline{H}_3$ peak, allow the possibility that this is a unique interturn hydrophobic association, which in water would be responsible in part for the inverse temperature transition leading to increased intramolecular order concommitantly with aggregation to form the viscoelastic coacervate state. Two possible interturn interactions are shown in unrolled perspective[36] in Fig. 6. In part A the interturn Val–Pro interactions involve the Val^4 side chain. This is the interaction that was derived in the *in vacuo* molecular mechanics development of the polypentapeptide β-spiral[37] from the cyclic conformational correlate, the cyclopentadecapeptide. The plotted β-spiral was considered to be one of a class of related conformations. In Fig. 6(B) is a second possible interturn interaction where the Val^1 methyl protons would be interacting with the Pro$\beta C\underline{H}_2$ protons. The latter could be consistent with the minor cross peaks under consideration. Along the bonding network this would be a distance of likely more than 40 bonds without the aid of hydrogen bonds to hold a pair of helical turns of polypeptide chain together. Such an NOE would necessarily be weak. Studies in water with lower molecular weight polypentapeptide to limit the aggregation and with very high molecular weight polypentapeptide are reported below to further consider this question of interturn hydrophobic interactions, which would be responsible for the intramolecular component of the inverse temperature transition in water.

To explore the weak NOE between Pro$\beta C\underline{H}_2$ and Val^1 (or Val^4) methyl protons [as suggested in 2D NOE map for PPP in Fig. 3 and putatively

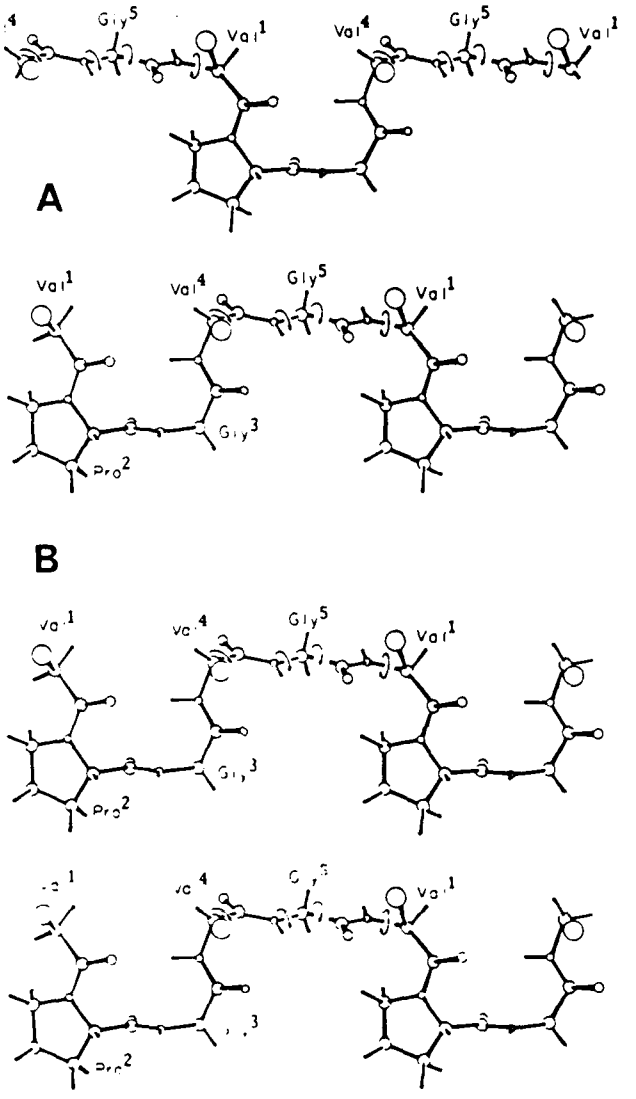

Fig. 6. Unrolled perspective of two turns of a PPP β-spiral showing possible interturn interactions. (A). Interturn interactions where the Val^4 side chain of a pentamer would interact with the $Pro^2\beta$ and γCH_2 protons of another pentamer. (B) Interturn interactions where the Val^1 side chain of one pentamer would interact with the $Pro^2\beta$ and γCH_2 protons of another pentamer. Adapted with permission from Ref. 34.

labeled in Fig. 4], 1D NOE experiments were performed in which valyl methyl protons were saturated. The reason for using the 1D NOE technique is as follows: Since, in processing 2D nmr data, a weighting function is always used for each dimension to enhance the spectral resolution, weak NOE peaks are often more difficult to detect than in the 1D NOE experiment for a particular proton pair. In addition, t_1 ridges due to the presence of strong diagonal peaks such as the one observed for Val$\gamma C\underline{H}_3$ protons, make it more difficult to ascertain the NOE peaks due to Val$\gamma C\underline{H}_3$–Pro$\beta C\underline{H}_2$ interactions. These connectivities, suggesting possible interturn interactions, were not observed in the 2D NOESY map in water (see Fig. 5) perhaps for the above reasons. Because of this and because the hydrophobic contacts have greatest significance in water, the 1D NOE experiments were carried out on aqueous solutions. The turbidity experiments for samples with the same concentration in H_2O solution as used in nmr measurements indicate that cyclo$(VPGVG)_3$

does not aggregate at temperatures below 313 K, $(VPGVG)_{12}$ begins aggregation at 313 K, and $(VPGVG)_n$ (50 kdal < MW < 100 kdal) begins aggregation at 298 K. For cyclo$(VPGVG)_3$ at 294 K, negative NOE peaks are found for Val^1 and $Val^4\alpha C\underline{H}$, for Val^1 and $Val^4\beta C\underline{H}$, and for $Pro^2\delta C\underline{H}$ [see Fig. 7(E)]. These are interactions between $Val\gamma C\underline{H}_3$ protons and protons of the same pentamer unit. There are no $Pro\beta C\underline{H}_2$ NOE peaks observable for this peptide. In contrast, $Pro\beta C\underline{H}_2$ NOE peaks can be detected, for poly$(VPGVG)_n$ where $n = 12$ at 307 K [see Fig. 7(A)]. As no aggregation should occur at this temperature for $(VPGVG)_{12}$ at the concentration used in the present study, the negative NOE peaks of $Pro\beta C\underline{H}_2$ have to be due to intramolecular

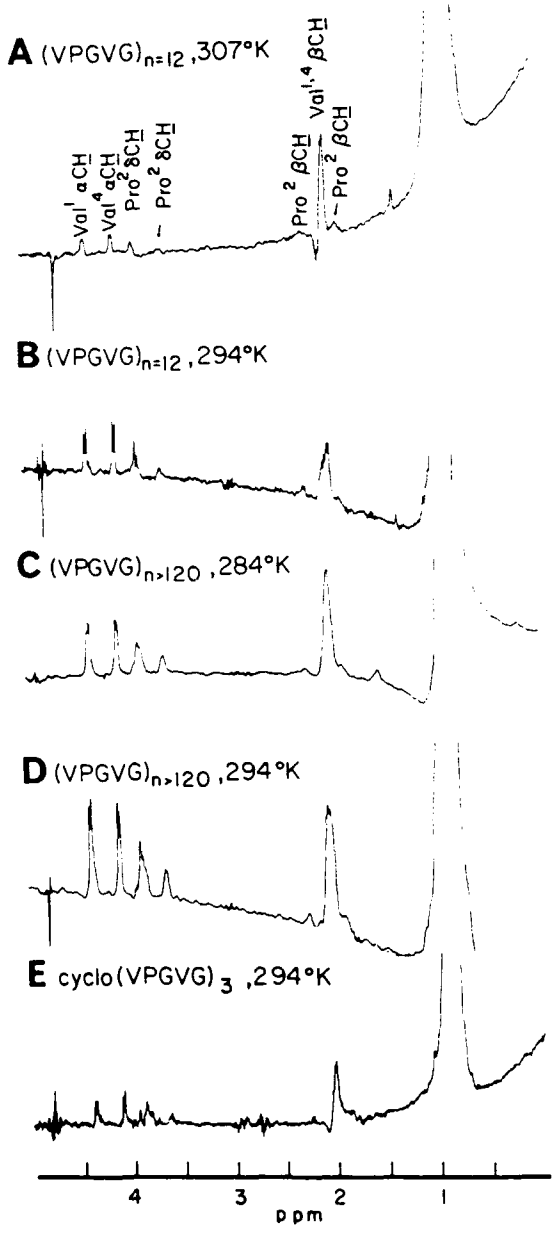

Fig. 7. The 1D NOE difference spectra on saturation of the $Val\gamma C\underline{H}_3$ resonances of 0.1*M* $(VPGVG)_{12}$ in 99.96% D_2O solution at 307 K (A) and 294 K (B) of $(VPGVG)_{n>120}$ in 99.96% D_2O solution at 284 K (C) and 294 K (D), and of cyclo$(VPGVG)_3$ in D_2O solution at 294 K (E). Sweep width = 4000 Hz, presaturation time = 0.15 s.

interactions and in particular due to the interactions between protons that belong to different pentamer units.

Upon lowering the temperature to 294 K, the ratio of the NOE peak intensity of ProβC$\underline{H}_2$ peaks to other NOE peaks decreases [Fig. 7(B)]. Based on the fixed geometry alone, lowering the temperature should increase the negative NOE effect, because the NOE intensity is approximately proportional to $1/r^6$ and $f(\tau_c)$ where

$$f(\tau_c) = \frac{5 + \omega^2\tau_c^2 - 4\omega^4\tau_c^4}{10 + 23\omega^2\tau_c^2 + 4\omega^4\tau_c^4}$$

and τ_c is the effective correlation time for the ^{1}H-^{1}H dipolar interaction under consideration.[38,39] Instead, the decrease in negative NOE intensity for ProβC$\underline{H}_2$ can be explained by loss of intramolecular hydrophobic interactions within the β-spiral structure at 294 K for the $(VPGVG)_{12}$ solution, which is 20 K below the temperature for the set of intermolecular hydrophobic interaction, and consequently there is a loss of the intramolecular interturn proton–proton interaction. Distinct ProβC$\underline{H}_2$ NOE peaks are also observed for $(VPGVG)_{n>120}$ with MW between 50 kdal and 100 kdal at 294 K, at a temperature 4° below that at which aggregation occurs for this solution [see Fig. 7(D)]. It seems apparent that interturn ValγC$\underline{H}_3$...ProβC$\underline{H}_2$ hydrophobic contacts have been observed. Further, NOE studies using $[(Val^1(d_8)\text{-}Pro^2\text{-}Gly^3\text{-}Val^4\text{-}Gly^5)_n$ and $(Val^1\text{-}Pro^2\text{-}Gly^3\text{-}Val^4(d_8)\text{-}Gly^5]_n$ with $n > 120$ have shown that it is the Val$^1\gamma$C$\underline{H}_3$ that is preferentially interacting with the Pro$^2\beta$C$\underline{H}_2$ as occurs in Fig. 6(B) and not in Fig. 6(A) (in preparation).

CONCLUSIONS

A β-turn is specified by appropriate restriction of the ϕ_{i+1}, ψ_{i+1}, ϕ_{i+2}, and ψ_{i+2} torsion angles. In the sequence $(Val^1\text{-}Pro^2\text{-}Gly^3\text{-}Val^4\text{-}Gly^5)$, ϕ_{i+1}, which is ϕ_2, is appropriately restricted by the proline ring. An intense Pro$^2\alpha$C$\underline{H}$ ↔ Gly^{3}N$\underline{H}$ is necessary for a type II β-turn and this is observed, but it is the Pro$^2\beta$C$\underline{H}$ (equatorial) ↔ Gly^{3}N$\underline{H}$ interaction that quite definitively establishes the correct $\psi_{i+1} = \psi_2$ and $\phi_{i+2} = \phi_3$ torsion angle ranges for the Pro^2-Gly^3 type II β-turn. This latter interaction, being significantly more intense for the equatorial Pro$^2\beta$C$\underline{H}$ proton than for the axial Pro$^2\beta$C$\underline{H}$ proton, confirms conformational constraint and confirms the experimental parameters chosen to give an approximate maximal contact distance of 3.5 Å, and it indicates the absence of significant spin diffusion, which is also apparent as the t_1 values for this polypentapeptide are greater than 1 s.[40,41] Finally, the values of both $\phi_{i+2} = \phi_3$ and $\psi_{i+2} = \psi_3$ are those required of a β-turn (as in a 3_{10}-helix), as shown by the intense Gly^{3}N$\underline{H}$ ↔ Val^{4}N$\underline{H}$ interaction. Thus all of the torsion angles required to specify a Pro^2-Gly^3 β-turn are appropriately restricted. Finally, the observation of the NOE between the Pro$^2\alpha$C$\underline{H}$ ↔ Val^{4}N$\underline{H}$ protons (which are separated by seven bonds) provides further demonstration of this β-turn. The Pro^2-Gly^3 type II β-turn can be derived directly from the NOE data.

The reported 2D NOE derivation of the β-turn is confirmatory of much previous work. Demonstrated for the first time, however, are the utility of 2D NOE in using more readily solvable cyclic conformations of repeating peptide sequences to derive conformations of the related linear helical conformation and the capacity to utilize proton–proton interactions not present in the cyclic conformation to deduce helical interturn interactions in sequential polypeptides. Furthermore, this analysis of the 2D NOE of PPP provides the basis for determining whether or not this repeating sequence in a more complex primary structure occurs in the same conformation as in the isolated sequential polypeptide.

This work was supported in part by National Institutes of Health grant HL 29578, the NMR Core Facility NCI grant CA 13148, the Department of the Navy, Office of Naval Research contract N00014-86-K-0402, and the National Science Foundation grant DMB-8502666.

References

1. Foster, J. A., Bruenger, E., Gray, W. R. & Sandberg, L. B. (1973) *J. Biol. Chem.* **248** 2876–2879.

2. Sandberg, L. B., Soskel, N. T. & Leslie, J. B. (1981) *N. Engl. J. Med.* **304**, 566–579.

3. Sandberg, L. B., Leslie, J. B., Leach, C. T., Alvarez, V. L., Torres, A. R. & Smith, D. W. (1985) *Patho. Biol.* **33**, 266–274.

4. Indik, Z., Yoon, K., Morrow, S. D., Cicila, G., Rosenbloom, J. C., Rosenbloom, J. & Ornstein-Goldstein, N. (1987) *Connect. Tissue Res.* **16** 197–211.

5. Smith, D. W., Weissman, N. & Carnes, W. H. (1968) *Biochem. Biophys. Res. Commun.* **31**, 309–315.

6. Sandberg, L. B., Weissman, N. & Smith, D. W. (1969) *Biochemistry* **8**, 2940–2945.

7. Thomas, J., Elsden, D. F. & Partridge, S. M. (1963) *Nature* **200**, 651–652.

8. Urry, D. W. (1982) *Methods Enzymol.* **82**, 673–716.

9. Urry, D. W., Trapane, T. L. & Prasad, K. U. (1985) *Biopolymers* **24** 2345–2356.

10. Urry, D. W. (1984) *J. Protein Chem.* **3**, 403–436.

11. Urry, D. W. (1985) in *Biomolecular Stereodynamics III*, Sarma, R. H. & Sarma, M. H., Eds., Adenine Press, Guilderland, NY, pp. 173–196.

12. Urry, D. W. (1987) in *Advances in the Molecular Biology of Connective Tissue Fibrous Proteins*, Professor S. M. Partridge Festschrift Volumn, Gotte, L. Ed., Scottish Academic Press, Edinburgh, pp. 25–50.

13. Urry, D. W., Cunningham, W. D. & Ohnishi, T. (1974) *Biochemistry* **13**, 609–615.

14. Khaled, M. A. & Urry, D. W. (1976) *Biochem. Biophys. Res. Commun.* **70** 485–491.

15. Urry, D. W., Trapane, T. L., Sugano, H. & Prasad, K. U. (1981) *J. Am. Chem. Soc.* **103**, 2080–2089.

16. Venkatachalam, C. M., Khaled, M. A., Sugano, H. & Urry, D. W. (1981) *J. Am. Chem. Soc.* **103**, 2372–2379.

17. Cook, W. J., Einspahr, H. M., Trapane, T. L., Urry, D. W. & Bugg, C. E. (1980) *J. Am. Chem. Soc.* **102**, 5502–5505.

18. Wider, G., Macura, S., Kumar, A., Ernst, R. R. & Wüthrich, K. (1984) *J. Magn. Reson.* **56**, 207–234.

19. Wüthrich, K., Wider, G., Wagner, G. & Braun, W. (1982) *J. Mol. Biol.* **155**, 311–319.

20. Wagner, G. & Wüthrich, K. (1982) *J. Mol. Biol.* **155**, 347–366.

21. Wider, G., Lee, K. H. & Wüthrich, K. (1982) *J. Mol. Biol.* **155**, 367–388.

22. Urry, D. W. & Long, M. M. (1976) *CRC Crit. Rev. Biochem.* **4**, 1–45.

23. Mistrali, F., Volpin, D., Garbaldo, G. B. & Ciferri, A. (1971) *J. Phys. Chem.* **75**, 142–149.

24. Hoeve, C. A. J. & Flory, P. J. (1958) *J. Am. Chem. Soc.* **80**, 6523–6526.

25. Hoeve, C. A. J. & Flory, P. J. (1974) *Biopolymers* **13** 677–686.

26. Dorrington, K. L. & McCrum, N. C. (1977) *Biopolymers* **16** 1201–1222.

27. Urry, D. W. & Prasad, K. U. (1985) in *Biocompatibility of Tissue Analogues*, Williams, D. F., Ed., CRC Press, Inc., Boca Raton, FL, pp. 89–116.

28. Aue, W. P. I., Bartholdi, D., & Ernst, R. R. (1976) *J. Chem. Phys.* **64**, 2229.
29. Nagayama, K., Kumar, A., Wüthrich, K. & Ernest, R. R. (1980) *J. Mag. Reson.* **40**, 321–334.
30. Bax, A. & Freeman, R. (1981) *J. Mag. Reson.* **44**, 542.
31. States, D. J., Haberkorn, R. N. & Ruben, D. J. (1982) *J. Mag. Reson.* **48** 286–292.
32. Billeter, M., Braun, W. & Wüthrich, K. (1982) *J. Mol. Biol.* **155**, 321–346.
33. Thomas, G. J., Prescott, J. B. & Urry, D. W. (1987) *Biopolymers* **26**, 921–934.
34. Urry, D. W., Khaled, M. A., Rapaka, R. S. & Okamoto, K. (1977) *Biochem. Biophys. Res. Commun.* **79**, 700–706.
35. Urry, D. W., Henze, R., Harris, R. D. & Prasad, K. U. (1984) *Biochem. Biophys. Res. Commun.* **125**, 1082–1088.
36. Urry, D. W. (1983) *Ultrastruct. Pathol.* **4**, 227–251.
37. Vankatachalam, C. M. & Urry, D. W. (1981) *Macromolecules* **14** 1225–1229.
38. Balaram, P., Bothner-By, A. A. & Dadok, J. (1972) *J. Am. Chem. Soc.* **94**, 4015–4017.
39. Solomon, I. (1955) *Phys. Rev.* **99**, 559–565.
40. Urry, D. W., Trapane, T. L., Iqbal, M., Vankatachalam, C. M. & Prasad, K. U. (1985) *Biochemistry* **24**, 5182–5189.
41. Urry, D. W., Trapane, T. L., McMichens, R. B., Eqbal, M., Harris, R. D. & Prasad, K. U. (1986) *Biopolymers* **25**, S209–S228.

Received November 2, 1987
Accepted July 12, 1988

Vol. 153, No. 2, 1988 BIOCHEMICAL AND BIOPHYSICAL RESEARCH COMMUNICATIONS
June 16, 1988 Pages 832-839

pK SHIFT OF FUNCTIONAL GROUP IN MECHANOCHEMICAL COUPLING DUE TO HYDROPHOBIC EFFECT: Evidence for an apolar-polar repulsion free energy in water

Dan W. Urry, Ding-Kwo Chang, Hong Zhang and Kari U. Prasad

Laboratory of Molecular Biophysics, School of Medicine
University of Alabama at Birmingham, P. O. Box 300/UAB Station
Birmingham, Alabama 35294

Received May 9, 1988

In the sequential polypeptide poly[4(VPGVG),(VPGEG)] and its more hydrophobic analog poly[4(IPGVG),(IPGEG)] when the material is γ-irradiation cross-linked to form an elastomeric matrix, mechanochemical coupling occurs on changing the pH, that is, motion and mechanical work are achieved by a change in proton chemical potential. The temperature dependence of aggregation at different pH values in phosphate buffered saline demonstrates the pK to be shifted approximately one pH unit higher for the more hydrophobic sequential polypeptide. The pH dependence of contraction or relaxation for each elastomer shows a similar shift. Data are reviewed and 2D-NMR data are presented which argue that the pK shift is not due to different conformations of the polypentapeptides. Specifically it is proposed that there exist a competition between carboxylates and hydrophobic side chains for mutually incompatible water structures; this results in an apolar-polar repulsion free energy in water with the difference in free energy reflecting the difference in the Ile and Val hydrophobicities.

The hydrophobic effect is the basis of inverse temperature transitions exhibited in water by polypeptides with hydrophobic side chains (1-3). The polypeptide becomes more-ordered on raising the temperature through the transition while more-ordered clathrate-like water surrounding hydrophobic side chains at temperatures below the transition becomes less-ordered bulk water at temperatures above the transition. The hydrophobic side chains form intra- and interpolypeptide contacts as the result of the transition.

The polypentapeptide of elastin (4-6), $(L\text{-}Val^1\text{-}L\text{-}Pro^2\text{-}Gly^3\text{-}L\text{-}Val^4\text{-}Gly^5)_n$ or simply $(VPGVG)_n$ with n>120, undergoes such a transition as demonstrable by an increase in order both intra- and intermolecularly on raising the temperature from 20° to 40°C (7). $(VPGVG)_n$ is soluble in water in all proportions at 20°C and the result of the transition is the formation of a viscoelastic phase, called the coacervate, which is approximately 40% peptide and 60% water by weight at 40°C (8). Further demonstration of the inverse temperature transition is achieved by analogs of the polypentapeptide. When the Val^1 residue is replaced by Ile^1 to give $(IPGVG)_n$ with n>120, this makes the polypentapeptide more hydrophobic, and the transition

0006-291X/88 $1.50

occurs at lower temperatures, between 0° and 20°C (9). When an analog is made which is less hydrophobic, e.g., $(VPGG)_n$, the transition occurs at a higher temperature, between 40° and 60°C (10). Also hydroxylation of the proline residue shifts the transition to higher temperatures (11). When the coacervate states of the sequential polypeptides are γ-irradiation cross-linked to form insoluble matrices, a process in which the elastomeric product is essentially indistinguishable by NMR from the coacervate (12,13), the inverse temperature transition can be seen as an elastic contraction on raising the temperature from 20° to 40°C. The contraction at 40°C is to less than one-half of the 20°C length (7).

Since a change in hydrophobicity can change the temperature of the inverse temperature transition, a change in hydrophobicity at fixed temperature can bring about a contraction or relaxation (14). In these terms a carboxyl group can be considered to be more hydrophobic than the carboxylate anion and by this mechanism a change in pH could be used to bring about contraction or relaxation (11). This new mechanism of mechanochemical coupling has recently been demonstrated on poly[4(VPGVG):(VPGEG)] which had been γ-irradiation cross-linked to form an elastomeric matrix (14). For simplicity, this elastomeric matrix is designated with the prefix X^{20}- as a 20 Mrad cross-linking dose was used.

In the present report curves for the pH dependence of transition temperatures for poly[4(VPGVG),(VPGEG)] and for the more hydrophobic poly[4(IPGVG),(IPGEG)] are seen to differ by about one pH unit and the pH dependence of length for the 20 Mrad cross-linked polymers under similar load are similarly shifted with the more hydrophobic sequential polypeptide exhibiting the higher pH values. The results are interpreted to indicate the occurrence of a solvation mediated apolar-polar repulsion free energy arising from the mutual incompatibility of clathrate-like and ion solvation water structures. The difference in repulsion free energies reflects the difference in hydrophobicities of the Ile and Val residues.

MATERIALS AND METHODS

Polypentapeptides: The detailed synthesis of poly[4(VPGVG),(VPGEG)] and of poly-[4(IPGVG),(IPGEG)] will be presented elsewhere (H. Zhang, K.U. Prasad and D.W. Urry, in preparation). The verification of each synthesis is, however, contained in the 2D NMR data presented below. These polymers were dialyzed against 50,000 D cut-off membranes such that both polypentapeptides have values of n which are greater than 120.

The pH dependence for the temperature of aggregation: Poly[4(VPGVG),(VPGEG)] and poly[4(IPGVG),(IPGEG)] (40 mg/ml phosphate buffered saline) are soluble at low temperatures. On raising the temperature aggregation begins which is followed by the development of turbidity at 300 nm. The difference between the two sequential polypeptides is one additional CH_2 moiety per pentamer in the Ile containing polypentapeptide.

Elastomer preparation: The coacervates were cross-linked by means of a 20 x 10^6 radiation absorbed dose (20 Mrad) of cobalt 60 γ-irradiation to form elastomeric bands as previously described (14).

pH dependence of elastomer length at fixed load: Both elastomers, are stretched with a load of approximately 1 gm/mm^2 cross-sectional area and the length is measured as a function of pH as previously described (14).

Two dimensional nuclear Overhauser enhancement spectroscopy (2D-NOESY) measurements: The experiments were carried out on a Bruker WH-400 spectrometer using a standard pulse sequence (15). 256 t_1 experiments were performed with a sweep width of 4000 Hz and a mixing time of 0.185 sec. An unshifted sine bell function was used for 2D-data processing, and the HOD peak was suppressed by selectively saturating the HOD resonance while performing the pulse sequences.

RESULTS AND DISCUSSION

When the temperature dependence of aggregation (coacervation) is monitored by turbidity development as a function of temperature at different values of pH, the pK_a for poly[4(VPGVG),(VPGEG)] is found to be 4.4 and that for poly[4(IPGVG),(IPGEG)] is 5.4. This is shown in Figure 1A. What is apparent is that the pK_a of the Glu in the Ile^1 analog is shifted approximately 1 pH unit higher than that of the Glu in the Val^1 analog. As shown in Figure 1B curve a, on lowering the pH from 7 to 3 in phosphate buffered saline (0.15 N NaCl, 0.01 M phosphate), the cross-linked elastomer contracts from a length of 8.7 mm to 4.2 mm. The midpoint of this pH dependence of length curve at a constant load of approximately 1 gm/mm^2 occurs at a pH of 4.6 for X^{20}-poly[4(VPGVG),(VPGEG)] and at 5.4 for X^{20}-poly[4(IPGVG):(IPGEG)].

Shown in Figure 2A and B are the two dimensional nuclear Overhauser enhancement spectroscopy (2D-NOESY; 15,16) data for poly[4(VPGVG),(VPGEG)] and poly[4(IPGVG),(IPGEG)], respectively, at pH 2.5 and at temperatures 5°C below the onset of the inverse temperature transition as defined in Figure 1A. The dotted lines denote the connectivities arising from non-regular residues (i.e., those residues that are adjacent to the Glu^4 residue). In Figure 2A, the chemical shift changes due to replacement of Val^4 by Glu^4 (the signs + and - represent downfield and upfield shifts, respectively) are Gly^3 N$\underline{H}$ (+0.1 ppm), Val^1 N$\underline{H}$ (+0.11 ppm), Gly^5 N$\underline{H}$ (-0.26 ppm) and Gly^5 αC$\underline{H}$ (-0.03 ppm). In Figure 2B, the chemical shift changes due to replacement of Val^4 by Glu^4 are Gly^3 N$\underline{H}$ (+0.1 ppm), Ile^1 N$\underline{H}$ (+0.07 ppm), Gly^5 N$\underline{H}$ (-0.26 ppm) and Gly^5 αC$\underline{H}$ (-0.09 ppm). The resolution was ±0.01 ppm. The type II β-turn (17) is preserved in the pentapeptide unit containing Glu^4 for both polypentapeptides as evidenced by a strong $d_1(2,3)$ NOE peak for the Pro^2 αC$\underline{H}$ - Gly^3 N$\underline{H}$ preceding Glu^4. A strong NOE interaction between Glu^4 γC$\underline{H}$ at 2.33 ppm and Gly^5 N$\underline{H}$ at 8.25 ppm for both polypentapeptides suggests that the side chain of Glu^4 is leaning toward the

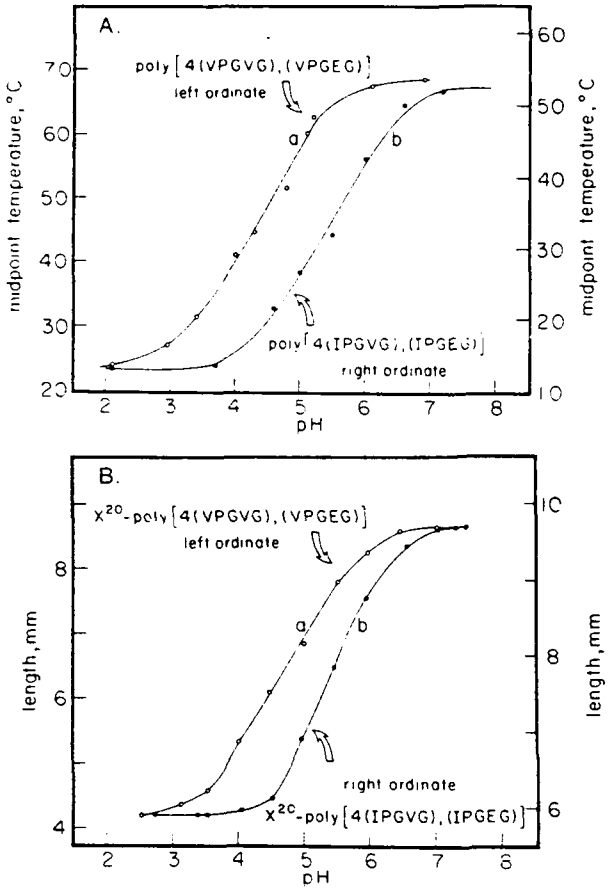

FIGURE 1 A. pH dependence for the temperature at which coacervation is initiated. The difference between the two sequential polypeptides is one additional CH_2 moiety per pentamer in the Ile containing polypentapeptide. The temperature at which coacervation occurs depends on pH and defines the pK of the carboxyl functional group. The pK_a for the more hydrophobic polypentapeptide is raised by one pH unit. B. pH dependence of length for γ-irradiation cross-linked matrices of X^{20}-poly[4(VPGVG),(VPGEG)] and X^{20}-poly[4(IPGVG),(IPGEG)] in phosphate buffered saline. On lowering the pH from a value near 7, the elastomers are found to shorten, i.e., to contract, effectively lifting weights that can be of the order of one-thousand times their own weight. This is mechanochemical coupling first demonstrated in synthetic polypeptides by these sequential polypeptides. Significantly, the curve is shifted to higher values in the case of the more hydrophobic sequential polypeptide.

carbonyl, instead of the NH, side of the Glu residue. The mean of the chemical shift differences, when comparing those of one polypentapeptide with those of the other, is 0.025 ppm with the largest difference being 0.06 ppm. Since conformational differences are commonly reflected by differences in chemical shifts of the order of 1.0 ppm (17), the differences observed here are more than an order of magnitude smaller. The similarity of chemical shift change and NOE interaction patterns for these two polypentapeptides demonstrate essentially identical conformations in the protonated form of the Glu side chain.

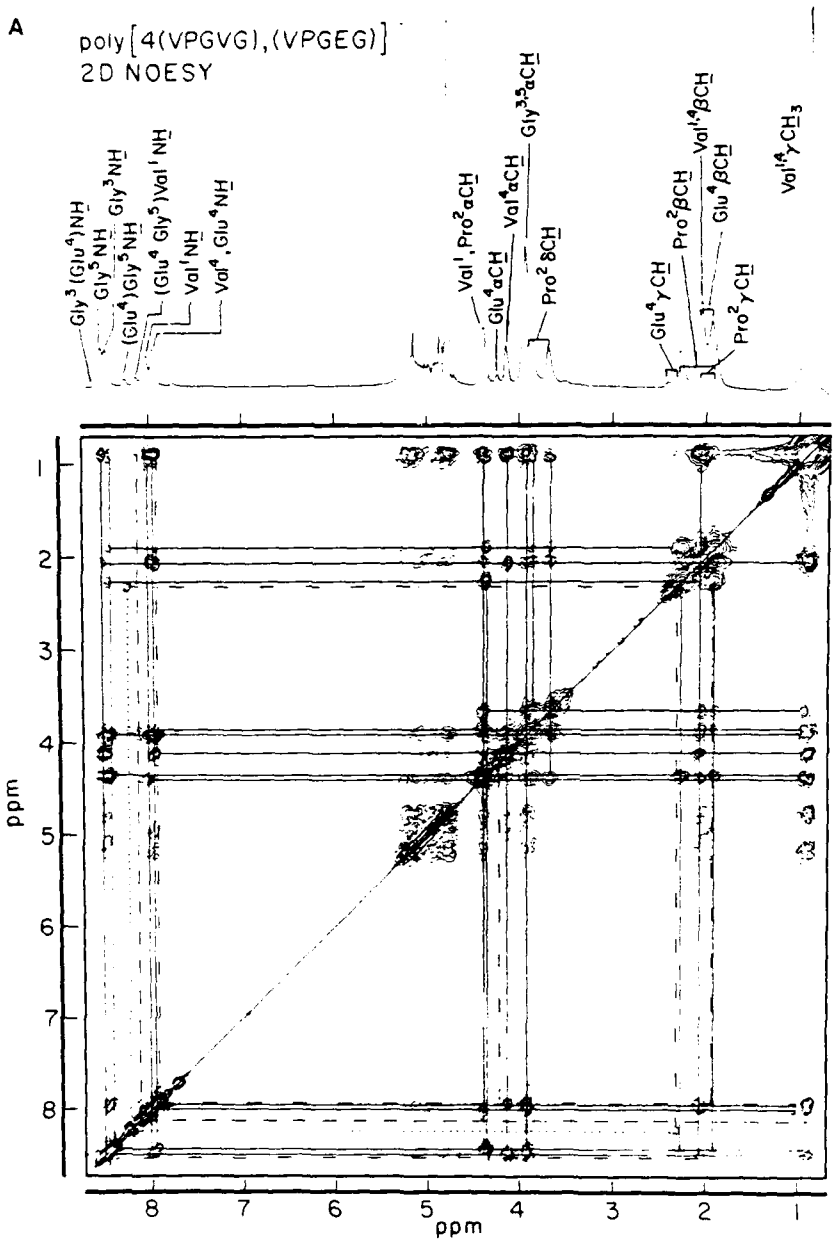

FIGURE 2 Two dimensional proton homonuclear NOE (NOESY) contour plots in 90% H_20, 10% D_20 (to provide for an internal lock) for A. poly[4(VPGVG),(VPGEG)] at 295°K and B. poly[4(IPGVG),(IPGEG)] at 282°K with both in phosphate buffered saline at pH 2.5 and at concentrations of 80 mg in 0.4 ml. Analysis of this data (see text) demonstrates essentially identical conformations for the two polypentapeptides.

This is much as expected. Since both Val and Ile have β-branched side chains, the steric effects on the polypeptide backbone must also be essentially identical. Furthermore, circular dichroism (CD) spectra of both polypentapeptides change remarkably toward an increase in

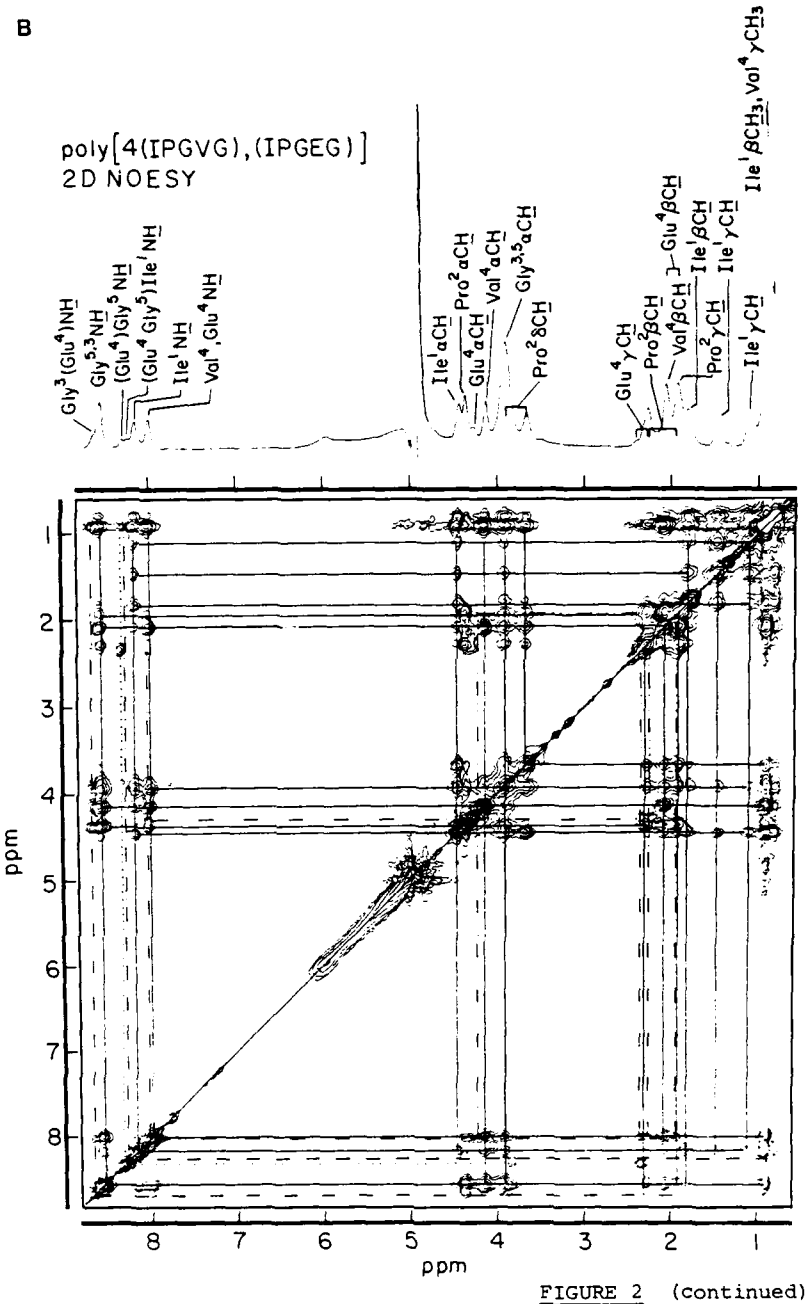

FIGURE 2 (continued).

intramolecular order (to a recurring β-turn CD pattern) as a result of the inverse temperature transition, and poly(VPGVG) and poly(IPGVG) have essentially identical conformations as demonstrated by indistinguishable CD spectra before and after the transition.

What then, is the source of the shift in pK_a? When considering protein mechanisms where a shift from the normal pK of a functional group is observed, the cause is commonly

considered to be due to electrostatic interactions (18), for example, due to the proximity of charges within the protein which change the energy of the ionized state or perhaps due to a conformation in which intramolecular hydrogen bonding is favored. In the present case, each polypeptide exhibits essentially identical conformations and contains the same number of Glu residues which are the only ionizable groups. Thus, neither a difference in conformation nor in the number of chargeable species in the polypeptides is the source. Accordingly the question arises as to whether the hydrophobic effect could be responsible, i.e., whether the differences in water structure within the matrix could be involved.

In general two possibilities would be considered, 1) that the more favorable formation of clathrate-like water around the Ile of poly[4(IPGVG),(IPGEG)] results in hydrogen bonding between clathrate-like water and carboxyl which stabilizes the protonated state of the Glu side chain, or 2) that the greater propensity for clathrate-like water formation in poly[4(IPGVG),(IPGEG)] results in a less favorable free energy for anion formation in the matrix. The first possibility is not consistent with the conformational studies whereas the second possibility is supported by two additional experimental findings. Firstly, increasing the concentration of salt solution in which X^{20}-poly(VPGVG) is bathed at an appropriate temperature can cause the stretched elastomer to contract (19). The rationale is that the greater ionic strength decreases the stability of the clathrate-like water and drives the system toward greater intramolecular hydrophobic interaction (19). Secondly, the pH dependence of length of X^{20}-poly[4(VPGVG),(VPGEG)] depends on the load on the elastomeric band, that is, the curve shifts to higher pH values as the load is increased (20). As increased load stretches the elastomer and exposes more hydrophobic side chains, this forced exposure of hydrophobic side chains and the shift toward formation of more clathrate-like water leads to a decreased free energy of the more polar carboxylate anion in the matrix. Thus both destabilization of clathrate-like water by increasing salt concentration and destabilization of the carboxylate anion by increased exposure of hydrophobic groups have been observed.

In the present example, therefore, it would seem that the increased hydrophobicity of the Ile^1-polypentapeptide over that of the Val^1-polypentapeptide is responsible. If this be the case, then the shift in pK_a could possibly be a measure of the difference in hydrophobicities. Since, in the concentration range of interest, $pH=-\log[H^+]$ and the proton chemical potential $\mu=2.3RT\log[H^+]$, then the change in chemical potential due to a change from Val to Ile becomes

$\Delta\mu=-2.3RT\Delta pK_a$. With a ΔpK_a of one as seen in Figure 1A, near physiological temperatures $\Delta\mu\cong1400$ cal/mole. Interestingly, this is the difference between the approximate hydrophobicities of Val (-1500 cal/mole and Ile (-2900 cal/mole) according to the Nozaki and Tanford (21) scale as listed in Table 1 of Bull and Breese (22). Thus there is evidence for a solvation mediated apolar-polar repulsion free energy. Simply stated hydrophobic side chains require one type of water structure whereas anions require a different kind of water structure and the two are mutually incompatible.

ACKNOWLEDGEMENT:

The authors wish the thank D. Hains, B. Haynes and J. Jaggard for their technical assistance in obtaining the data of Figure 1 and Richard Knight, R. Gilchrist and W. L. Alford of the Auburn University Nuclear Science Center for carrying out the γ-irradiation cross-linking. This work was supported in part by the Department of the Navy, Office of Naval Research contract N00014-86-K-0402. One of us (D.W.U.) wishes to acknowledge stimulating discussions with Professors M. U. Palma and M. B. Palma-Vittorelli.

REFERENCES:

1. Frank, H. S. and Evans, M. W. (1945) *J. Chem. Phys.* **13**, 493-507.
2. Kauzmann, W. (1959) *Adv. Protein Chem.* **14**, 1-63.
3. Tanford, C. (1973) in *The Hydrophobic Effect: Formation of Micelles and Biological Membranes* , John Wiley and Sons, Inc., New York.
4. Sandberg, L. B., Soskel, N. T. and Leslie, J. B. (1981) *N. Engl. J. Med.* **304**, 566-579.
5. Sandberg, L. B., Leslie, J. G., Leach, C. T., Alvarez, V. L., Torres, A. R. and Smith, D. W. (1985) *Pathol. Biol.* **33**, 266-274.
6. Yeh, H., Ornstein-Goldstein, N., Indik, Z., Sheppard, P., Anderson, N., Rosenbloom, J. C., Cicila, G., Yoon, K. and Rosenbloom, J. (1987) *Collagen Rel. Res.* **7**, 235-247.
7. Urry, D. W. (1988) *J. Protein Chem.* **7**, 1-34.
8. Urry, D. W., Trapane, T. L. and Prasad, K. U. (1985) *Biopolymers* **24**, 2345-2356.
9. Urry, D. W., Long, M. M., Harris, R. D. and Prasad, K. U. (1986) *Biopolymers* **25**, 1939-1953.
10. Urry, D. W., Harris, R. D., Long, M. M. and Prasad, K. U. (1986) *Int. J. Pept. Protein Res.* **28**, 649-660.
11. Urry, D. W. (1988) *J. Protein Chem.* **7**, 81-114.
12. Urry, D. W., Trapane, T. L., Iqbal, M., Venkatachalam, C. M. and Prasad, K. U. (1985) *Biochemistry* **24**, 5182-5189.
13. Urry, D. W., Trapane, T. L., McMichens, R. B., Iqbal, M., Harris, R. D. and Prasad, K. U. (1986) *Biopolymers* **25**, S209-S228.
14. Urry, D. W., Haynes, B., Zhang, H., Harris, R. D. and Prasad, K. U. *Proc. Natl. Acad. Sci. USA* (in press).
15. Jeener, J., Meier, B. H., Bachman, P. and Ernst, R. R. (1979) *J. Chem. Phys.* **71**, 4546-4553.
16. Wider, G., Macura, S., Kumar, A., Ernst, R. R. and Wüthrich, K. (1984) *J. Magn. Reson.* **56**, 207-234.
17. Urry, D. W. and Long, M. M. (1976) *CRC Crit. Rev. Biochem.* **4**, 1-45.
18. Tanford, C. (1962) *Adv. Protein Chem.* **17**, 69-165.
19. Urry, D. W., Haynes, B., Thomas, D. and Harris, R. D., *J. Am. Chem. Soc.* (in press).
20. Urry, D. W., (1988) *Int. J. Quantum Chem.: Quantum Biol. Symp.* (in press).
21. Nozaki, Y. and Tanford, C. (1971) *J. Biol. Chem.* **246**, 2211-2217.
22. Bull, H. B. and Breese, K. (1974) *Arch. Biochem. Biophys.* **161**, 665-670.

MOLECULAR DYNAMICS CALCULATIONS ON RELAXED AND EXTENDED STATES OF THE POLYPENTAPEPTIDE OF ELASTIN

D.K. CHANG and D.W. URRY

Laboratory of Molecular Biophysics, School of Medicine, University of Alabama in Birmingham, P.O. Box 300/University Station, Birmingham, AL 35294, USA

Received 22 February 1988; in final form 8 April 1988

Reported are the first molecular dynamics calculations on the elastomeric polypentapeptide of elastin as $(VPGVG)_7$. The salient points are that (1) there is little change in internal energy on extension; (2) a trajectory of 50 ps is insufficient to reflect the primary structural periodicity in rms displacements of torsion angles, but does show librational processes and their damping on extension; and (3) the recurring β-turn structure is retained.

1. Introduction

The study of the structure and mechanism of elasticity of biological elastin has been an active, albeit controversial, area of research [1–8]. One of the structural characteristics of bovine and porcine elastin is that it has a long repeating pentapeptide sequence, i.e. $(L\text{·}Val^1\text{–}L\text{·}Pro^2\text{–}Gly^3\text{–}L\text{·}Val^4\text{–}Gly^5)_n$ with $n=11$ [9]. As a result, physical properties of the synthetic polypeptide, poly(VPGVG), have been extensively investigated. From experiments on the thermoelasticity of elastin at constant length and volume, Hoeve and Flory [2] concluded that the internal energy component of force accounts for a negligible fraction of the total elastomeric force. Recently, Urry and co-workers studied the thermoelastic behavior of γ-irradiated cross-linked poly(VPGVG) and reached the same conclusion, that is, that the entropy change of the polypeptide with increasing length is the major source of the retractive force. The origin of the entropic mechanism for the elastic peptide is different, however, according to these two groups. Flory and co-workers consider that the entropy decrease on stretching is due to the change in the distribution of end-to-end distance between cross-linking points of peptide chains. The internal degrees of freedom, such as changes in bond angles and torsion angles, are taken into account only in the context of end-to-end distance of peptide chains. A damping of the amplitudes of correlated motions of torsion angles (librations) is considered to be a major source of the entropy decrease on elongation of the polypeptide elastic fiber according to Urry and co-workers, that is, the damping of backbone librational processes of peptide chains upon stretching is taken to be the primary source of entropy decrease. The primary differences between these two theories are: (1) each individual internal degree of freedom (torsion angles, in particular) is taken into consideration by Urry et al., and (2) the distribution of end-to-end distance of a collection of chains is not central to the mechanism proposed by Urry et al. This means that entropic elastic force can be generated by a single peptide chain segment and can occur in a regular, non-random, albeit dynamic, structure. The helically recurring β-turn structure of poly(VPGVG) is called a β-spiral.

Stereo pair plots of the β-spiral of poly(VPGVG) for seven pentamers with 2.7 pentamers per turn is given in figs. 1A (axis view) and 1B (side view), and in figs. 1C (relaxed) and 1D (extended) are three pentamers, approximately one turn, with a central pentamer unit showing the range of librational processes that can occur within a 2 kcal/mole residue cut-off energy. In these conformational energy calculations there is seen to be a damping of the amplitude of librations on extension [6]. The calculation was done on a pentadecapeptide.

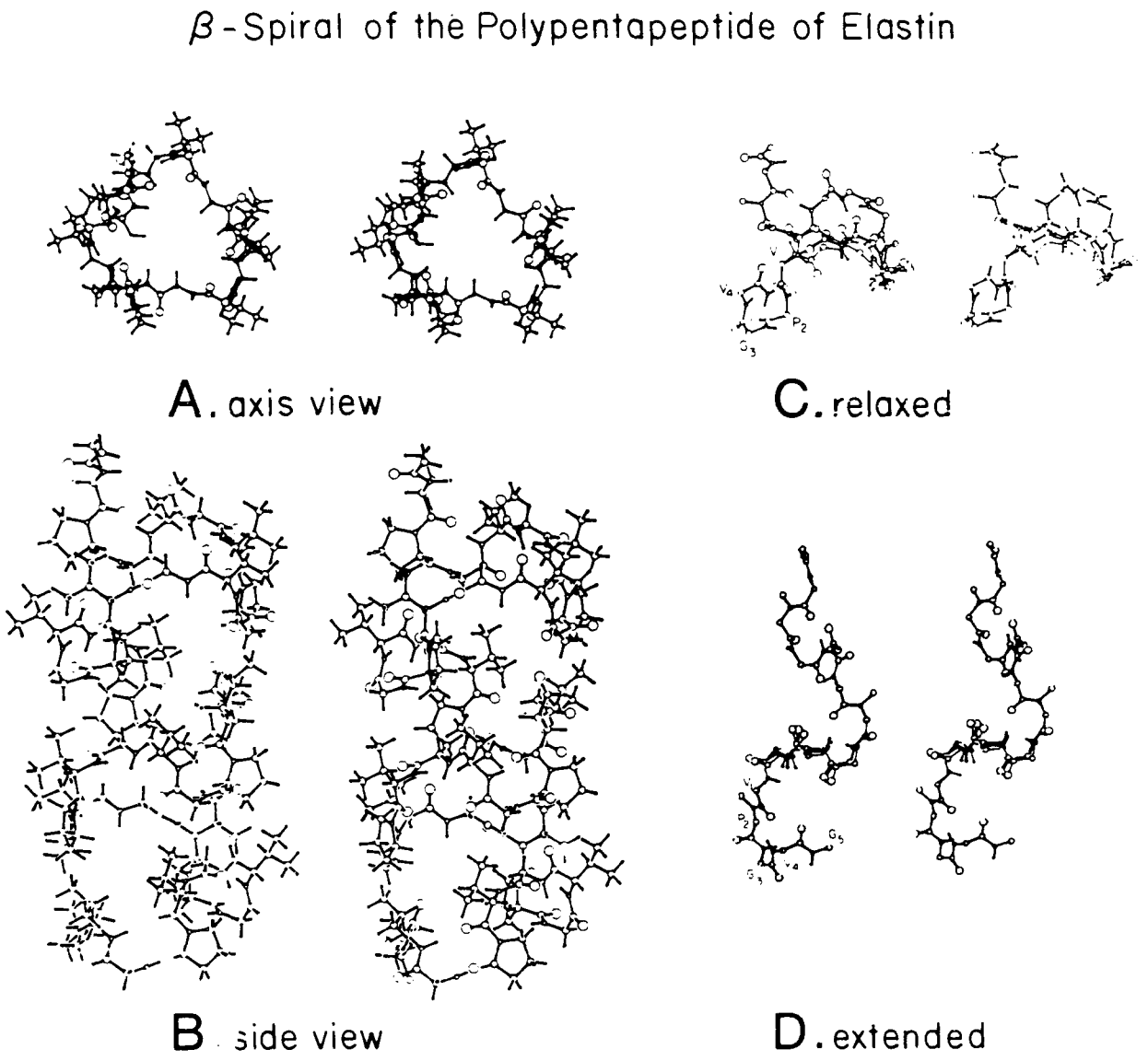

Fig. 1. β-spiral of the polypentapeptide of elastin, $(VPGVG)_n$, with $n=7$ in A and B and with $n=3$ for C in the relaxed and for D in a state at 130% extension.

$(VPGVG)_3$, and the damping of libration upon 130% elongation was observed in the (suspended) segment containing the correlated torsion angle pairs $\psi(Val^4)$–$\phi(Gly^5)$ and $\psi(Gly^5)$–$\phi(Val^1)$. The number of accessible states was enumerated by using different cut-off energies above the minimized energy conformation. The entropy change was found to be essentially independent of the value of the cut-off energy. Experimentally, a dielectric relaxation near 10 MHz for the PPP coacervate was observed and interpreted as arising from peptide backbone libration [10].

Since the aforementioned computation was static in nature, i.e. the structure was minimized without explicitly taking account of atomic thermal energy, in the present effort it is of interest to apply molec-

ular dynamics simulation to the polypentapeptide and to address the problem of the correlation (or relaxation) time for the librational processes observed in the MHz frequency range, to assess the presence of structural features and to determine the effect of extension on internal energy.

2. Methods

The software package, CHARMm (version 20.3), developed by Karplus and co-workers and adapted by Polygen, Inc., was used in the calculation. The potential energy functions and parameters were as described by Brooks et al. [11]. The harmonic approximation was employed in the energy terms of bond lengths, bond angles and improper torsional potentials. $E_\sigma = k_\sigma[1+\cos(no-\delta)]$ was used for the dihedral (torsion) angle energy term and the Lennard-Jones 6–12 potential was used for van der Waals interactions. Since intramolecular interturn interactions are considered to be important in the formation of the β-spiral structure as the result of an inverse temperature transition [12], a polypeptide with seven repeating pentamer units, $(VPGVG)_7$, was used in the molecular dynamics (MD) simulation. For both relaxed and extended states of the β-spiral, a structure with 2.7 pentamer units per turn was used. The axial rise was 9.45 Å per turn in the relaxed state and 21.6 Å per turn in the extended state, corresponding to 130% extension. In the simulation, the amide nitrogen atom of residue one, i.e. Val^1, and the carbonyl carbon atom of residue 35, i.e. Gly^{35}, were fixed in space. Each step in the simulation corresponds to 10^{-15} s. Both structures were thermalized to 300 K with 0.05 °C rise per step. The structures were then equilibrated for 25 ps. Finally, the systems were allowed to undergo 50 ps of a molecular dynamics production stage. The algorithm used for integrating the equations of motion adopted in CHARMm was proposed by Verlet [13]. The root-mean-square (rms) fluctuations of backbone torsion angles as well as internal energy (sum of kinetic and potential energy) were noted during the production period.

3. Results and discussion

The average values of total energy and various potential energy terms are presented in table 1, for 50 ps of molecular dynamics production time for both relaxed and extended states of $(VPGVG)_7$. The total energy is lower by 15 kcal/mole for the relaxed state than for the extended state. The primary source for the difference is obviously the van der Waals term, which is lower by 17 kcal/mole for the relaxed state. The difference arises from the interactions between the side chains of peptide residues which are absent or much weaker in the extended state. It has been reported that the extension of elastin fiber immersed in water is an exothermic process with its magnitude four times as large as the elastic work performed on the elastin sample [3]. Since the internal energy of

Table 1
Internal energy components of $(VPGVG)_7$ in relaxed and extended states resulting from a 50 ps molecular dynamics simulation [a,b]

	Relaxed	Extended	Δ(extended − relaxed)
total energy	352	367	15
total potential energy	37	56	19
van der Waals	−56	−39	17
bond length	68	68	0
bond angle	209	206	−3
dihedral angle	88	86	−2
improper torsional angle	22	21	−1
electrostatic terms	−295	−287	8

[a] Values are rounded off to the nearest kcal/mole.

[b] The potential energies listed are relative to the minimum value of the potential functions with respect to the given internal coordinates. Total energy is defined as the sum of total potential energy and total kinetic energy, with 0 K used as the reference for zero atomic kinetic energy.

the peptide is lower for this relaxed state, it can be deduced from our results that the heat of hydration, or heat of hydrophobic interaction due to the exposure of hydrophobic groups to the solvent upon elongation, overcomes the loss in van der Waals interactions. It is also interesting to note that the heat generated upon extension of the elastin fiber decreases as the polarity of the solvent decreases [3]. For example, the heat decreases to zero in the 3:7 ethylene glycol/water mixed solvent. The heat also decreases when solvent is changed from pure water to 2 M methanol to 2 M ethanol to 2 M propanol to pure formamide. This can be rationalized by noting that the heat of solvation is less for the less polar solvents which more closely compensate for the loss of van der Waals interactions of the peptide chains when they are stretched.

Accordingly, for such an elastic system where the chains become solvated on extension, when examining results of an in vacuo calculation for the change in internal energy on extension, it is perhaps more appropriate to delete the van der Waals term. In this regard it is seen that the change in internal energy due to changes in bond lengths, bond angles, dihedral angles and improper torsional angles are equal in magnitude but opposite in sign to the change in

Table 2
Root-mean square (rms) fluctuation of torsion angles (ϕ and ψ) of (VPGVG)$_7$ after 25 ps of equilibration time and 50 ps of molecular dynamics simulation

	Torsion angle	Relaxed	Extended		Torsion angle	Relaxed	Extended
	ψ_1	43.9	29.7		ψ_{18}	*9.5*	*7.8*
	ϕ_2	14.6	13.4		ϕ_{19}	*9.0*	*7.1*
	ψ_2	49.3	47.8	suspended segment	ψ_{19}	*9.1*	*8.7*
	ϕ_3	29.6	10.3		ϕ_{20}	*11.7*	*12.2*
	ψ_3	32.4	14.2		ψ_{20}	*40.0*	*11.8*
	ϕ_4	9.2	9.7		ϕ_{21}	*23.7*	*11.8*
	ψ_4	10.1	10.9		ψ_{21}	*11.2*	*7.4*
	ϕ_5	7.7	8.8		ϕ_{22}	16.2	8.6
	ψ_5	8.2	11.8		ψ_{22}	14.7	13.2
	ϕ_6	11.2	26.2		ϕ_{23}	9.7	10.0
	ψ_6	9.7	22.2		ψ_{23}	9.2	10.7
	ϕ_7	9.5	6.8		ϕ_{24}	9.6	7.9
	ψ_7	9.7	17.4		ψ_{24}	10.5	8.9
	ϕ_8	12.4	10.4		ϕ_{25}	8.6	9.2
	ψ_8	10.1	28.2		ψ_{25}	9.8	8.9
	ϕ_9	9.9	9.4		ϕ_{26}	13.4	29.2
	ψ_9	15.3	10.9		ψ_{26}	13.1	10.9
	ϕ_{10}	14.3	7.8		ϕ_{27}	11.5	11.1
	ψ_{10}	9.6	11.1		ψ_{27}	36.0	12.7
	ϕ_{11}	11.8	30.0		ϕ_{28}	53.8	8.4
	ψ_{11}	12.1	12.6		ψ_{28}	37.3	12.7
	ϕ_{12}	10.0	6.9		ϕ_{29}	9.1	8.5
	ψ_{12}	14.3	9.8		ψ_{29}	11.4	12.3
	ϕ_{13}	8.6	8.2		ϕ_{30}	10.2	8.2
	ψ_{13}	10.1	8.5		ψ_{30}	11.0	12.7
	ϕ_{14}	8.9	10.7		ϕ_{31}	13.1	23.3
suspended segment	ψ_{14}	*10.1*	*10.0*		ψ_{31}	10.5	17.5
	ϕ_{15}	*15.6*	*14.3*		ϕ_{32}	9.5	6.0
	ψ_{15}	*12.5*	*10.6*		ψ_{32}	30.0	11.6
	ϕ_{16}	*9.7*	*12.2*		ϕ_{33}	36.4	10.2
	ψ_{16}	*7.2*	*9.7*		ψ_{33}	10.3	27.8
	ϕ_{17}	*7.3*	*8.8*		ϕ_{34}	8.9	19.4
	ψ_{17}	*9.6*	*10.1*		ψ_{34}	17.1	82.6
	ϕ_{18}	*8.4*	*8.0*		ϕ_{35}	78.8	58.5

the electrostatic interaction terms. The perspective therefore for the polypentapeptide β-spiral becomes one of little or no change in internal energy on extension when in an appropriate solvent.

Table 2 gives the 50 ps MD simulation of $(VPGVG)_7$ in terms of rms displacements of backbone torsion angles in both relaxed and extended states. The polypeptide chain end effects are evident from the magnitude of $\Delta\psi_1^2$ and $\Delta\phi_{35}^2$. A significant point is the lack of pentamer periodicity of rms displacements for the torsion angles in the same position in each pentapeptide, i.e. $\Delta\phi_i^2 \neq \Delta\phi_{i+5}^2$ or $\Delta\psi_i^2 \neq \Delta\psi_{i+5}^2$. This is most likely due to the fact that the 50 ps of molecular dynamics production time used in the present study is too short because the experimental correlation time is in the range of 10 ns as determined by both nuclear magnetic resonance [14] and dielectric relaxation measurements [10]. In the latter case the measured correlation time is not an average of many different correlation times, but rather it is a discrete relaxation of the Debye type indicating that the net dipole moment of each pentamer is rocking at the same frequency; the relaxation is due to a pentameric peptide librational mode.

Table 2 is also characterized by the correlated rms fluctuation values for adjacent torsion angles, i.e. when $\Delta\psi_i^2$ is large, $\Delta\phi_{i+1}^2$ or $\Delta\phi_i^2$ is correspondingly large. For example, $\Delta\psi_{15}^2$, $\Delta\phi_{16}^2$ and $\Delta\psi_{20}^2$, $\Delta\phi_{21}^2$ in the relaxed state; $\Delta\phi_6^2$, $\Delta\psi_6^2$ and $\Delta\phi_{31}^2$, $\Delta\psi_{31}^2$ in the extended state. This corresponds to localized peptide librational or rocking segmental motion. In general, the amplitude of librational motion is larger for suspended segments in the β-spiral structure. In a 35-residue helical structure with 2.7 pentamer repeats per turn, the true internal sequence not subject to end effects involves residues 14 through 21. This sequence is italicized in table 2 and includes two putative suspended segments, which are the two sets of four torsion angles ψ_{14}, ϕ_{15}, ψ_{15}, ϕ_{16} and ψ_{19}, ϕ_{20}, ψ_{20}, ϕ_{21}. It is apparent that these suspended segments experience the largest amplitude displacements in both relaxed and extended states and that the displacements are damped on extension.

While the trend of damping of librational motion upon elongation can be observed, it will be necessary to achieve trajectories with times of the order of magnitude of the 10 ns correlation time for peptide libration as measured from the dielectric relaxation studies and to do so in water before a truly satisfactory molecular dynamics characterization is achieved. Nevertheless this initial effort clearly provides much valuable insight.

It is significant to note that the β-turns of $(VPGVG)_7$ are retained after bringing the temperature to 300 K, after 25 ps of equilibration period, and after 50 ps of molecular dynamics production time both for relaxed and for extended states of polypentapeptide. Specifically, for the relaxed state, the average C_i–N_{i+3} distance is equal to 4.05 ± 0.10 Å for the static minimum energy structure before equilibration, 4.30 ± 0.15 Å after equilibration and 4.30 ± 0.3 Å after 50 ps of production time. For the extended state, the average C_i–N_{i+3} distance is equal to 4.20 ± 0.90 Å before equilibration, 4.45 ± 0.90 Å after equilibration and 4.25 ± 1.2 Å after 50 ps of production time. Furthermore using the pentadecapeptide the β-turns were maintained after 0.12 ns of trajectory time. Therefore the recurring β-turn, from which the β-spiral derives its name, is a structural feature of the elastomeric polypentapeptide of elastin in both the earlier molecular mechanics and now the molecular dynamics characterizations. As circular dichroism [15], nuclear magnetic resonance [16] and Raman spectroscopic studies [17] demonstrate the recurring β-turn in solution, the in vacuo calculations demonstrating the same structural feature are demonstrably of relevance to the solution state.

This elastomeric polypeptide system takes an added significance with recent studies. When high-molecular-weight polypentapeptide, i.e. $n > 120$, is synthesized and γ-irradiation cross-linked, the elastomeric matrix exhibits mechanochemical coupling in response to changes in salt concentration [18]. Furthermore, when there are four glutamic acid residues included per 100 residues of polypeptide in place of Val^4, the elastomeric matrix exhibits mechanochemical coupling in response to changes in *pH* [19]. This is the first synthetic polypeptide system to exhibit mechanochemical coupling and the process involves a newly described mechanism of chemical modulation of an inverse temperature transition [20].

4. Summary

In this first report of molecular dynamics simulations of the elastomeric polypentapeptide of elastin represented by $(L\text{-}Val^1\text{-}L\text{-}Pro^2\text{-}Gly^3\text{-}L\text{-}Val^4\text{-}Gly^5)_7$, it is demonstrated that (1) when the in vacuo van der Waals interaction terms are neglected, the change in internal energy on extension is small as required for a dominantly entropic elastomer; (2) the rms displacements for the backbone torsion angles do not reflect the periodicity of the primary structure indicating that 50 ps is an insufficient trajectory time; (3) the magnitudes of the rms displacements for the backbone torsion angles tend to be greater in the suspended segments defined as the peptide segment from the Val^4 α-carbon of the ith repeat to the Val^1 α-carbon on the $(i+1)$st repeat; (4) the rms displacements of the suspended segments are damped on extension; (5) there is a correlation in the magnitude of the rms displacements of the torsion angles on each side of a peptide moiety reflecting librational processes, and (6) the β-turn, defined as the $Val_iC...NVal_{i+3}$ distance, within a pentamer remains throughout the molecular dynamics simulation both in the relaxed and extended states.

Acknowledgement

This work was supported in part by National Institutes of Health grant HL 29578 and the Department of Navy, Office of Naval Research contract N00014-86-K-0402.

References

[1] C.A.J. Hoeve and P.J. Flory, J. Am. Chem. Soc. 80 (1958) 6523.
[2] C.A.J. Hoeve and P.J. Flory, Biopolymers 13 (1974) 677.
[3] T. Weis-Fogh and S.O. Andersen, Nature 227 (1970) 718.
[4] J.M. Gosline, Biopolymers 17 (1978) 677.
[5] D.W. Urry, C.M. Venkatchalam, M.M. Long and K.U. Prasad, in: Conformation in biology, eds. R. Srinivasan and R.H. Sarma (Adenine Press, Schenectady, 1982) p. 11.
[6] D.W. Urry and C.M. Venkatachalam, Intern. J. Quantum Chem. Quantum Biol. Symp. 10 (1983) 81.
[7] W.R. Gray, L.B. Sandberg and J.A. Foster, Nature 246 (1973) 461.
[8] K.L. Dorrington and N.H. McCrum, Biopolymers 16 (1977) 120.
[9] J.A. Foster, E. Bruenger, W.R. Gray and L.B. Sandberg, J. Biol. Chem. 248 (1973) 2876.
[10] D.W. Urry, R. Henze, R.D. Harris and K.U. Prasad, Biochem. Biophys. Res. Commun. 125 (1984) 1082.
[11] B.R. Brooks, R.E. Bruccoleri, B.O. Olafson, D.J. States, S. Swaminathan and M. Karplus, J. Comput. Chem. 4 (1983) 187.
[12] H.G. Bungenberg de Jong and H.R. Kruyt, Proc. Kon. Ned. Akad. Wet. 32 (1929) 849.
[13] L. Verlet, Phys. Rev. 159 (1967) 98.
[14] D.W. Urry, T.L. Trapane, R.B. McMichens, M. Iqbal, R.D. Harris and K.U. Prasad, Biopolymers 25 (1986) S209.
[15] D.W. Urry, M.M. Long, B.A. Cox, T. Ohnishi, L.W. Mitchell and M. Jacobs, Biochim. Biophys. Acta 371 (1974) 597.
[16] D.W. Urry, D.K. Chang, N.R. Krishna, D.H. Huang, T.L. Trapane and K.U. Prasad, Biopolymers, submitted for publication;
D.W. Urry and M.M. Long, CRC Crit. Rev. Biochem. 4 (1976) 1.
[17] G.J. Thomas Jr., B. Prescott and D.W. Urry, Biopolymers 26 (1987) 921.
[18] D.W. Urry, R.D. Harris and K.U. Prasad, J. Am. Chem. Soc., to be published.
[19] D.W. Urry, B. Haynes, H. Zhang, R.D. Harris and K.U. Prasad, Proc. Natl. Acad. Sci. US, to be published.
[20] D.W. Urry, J. Protein Chem. 7 (1988) 81.

ree Energy (Chemomechanical) Transduction in Elastomeric Polypeptides by Chemical Potential Modulation of an Inverse Temperature Transition

DAN W. URRY

Laboratory of Molecular Biophysics, School of Medicine, University of Alabama, P.O. Box 300/UAB Station, Birmingham, Alabama 35294, USA

"The isothermal conversion of chemical metabolic energy into mechanical work underlies the motility of all living organisms."

A. Katchalsky

Abstract

Data and analyses are presented on the first synthetic polypeptide system to exhibit mechanochemical coupling; the mechanochemical coupling can also be demonstrated to be both polymer-based and solvent-based with respect to where the result of the change in the chemical potential is focused. Both polymer-based and solvent-based processes are the result of chemomechanical transduction in which the change in chemical potential results in a change in the temperature at which an inverse temperature transition occurs. In the polymer-based process, the contraction/relaxation occurs due to a change in the chemical nature of the polypeptide; in the solvent-based process there is no change in the chemical nature of the polypeptide on contraction or relaxation, but rather the change in chemical potential changes the state of hydration of the polypeptide. The new mechanochemical system provides an experimental system with which to clarify and to quantitate what may be called aqueous mediated apolar–polar interaction energies in polypeptides and proteins with hydrophobic groups that may be variously exposed to the aqueous solution or buried within the folded polypeptide or protein. Furthermore, it is noted that any conformational change exhibited by ›lypeptide or protein that is the result of a binding of a chemical moiety, the change in chemical na of a bound moiety or the change in chemical potential of the medium can be viewed in terms of mechanochemical coupling or chemomechanical transduction.

Introduction

One year ago at the 1987 Sanibel Symposium was presented the concept that it should be possible to achieve mechanochemical coupling by chemical modulation of the hydrophobicity of elastomeric polypeptides that undergo reversible, thermally induced contraction at transition temperatures that could be varied by changing the hydrophobicity of the polypeptide [1]. The parent elastomeric polypeptide was the polypentapeptide of elastin, $(\text{L} \cdot \text{Val}^1\text{–L} \cdot \text{Pro}^2\text{–Gly}^3\text{–L} \cdot \text{Val}^4\text{–Gly}^5)_n$, also called PPP, which, when γ-irradiation crosslinked with $n > 120$ form elastomeric matrices in water which contract to less than one-half the 20°C length on raising the temperature to 40°C. When the polypentapeptide was made more hydrophobic, as in $(\text{L} \cdot \text{Ile}^1\text{–L} \cdot \text{Pro}^2\text{–Gly}^3\text{–L} \cdot \text{Val}^4\text{–Gly}^5)_n$, also called Ile^1–PPP, and γ-irradiation crosslinked, the contraction occurred between 0 and 20°C [2]. When the sequential polypeptide

International Journal of Quantum Chemistry: Quantum Biology Symposium, 15, 235–245 (1988)

CCC 0360-8832/88/01010235-11$04.00

was made less hydrophobic by removal of the Val^4 residue to give $(L \cdot Val^1\text{–}L \cdot Pro^2\text{–}Gly^3\text{–}Gly^4)_n$, also called PTP, and similarly crosslinked, the contraction occurred between 40 and 60°C [3]. These data are schematically shown in Figure 1. Therefore, the proposal was that if the sequential polypentapeptide were made with inclusion of a residue containing a functional side chain that could, by a reversible chemical process, be made more and less hydrophobic, i.e., more or less polar, then it should be possible by changes in chemical potential to achieve contraction and relaxation [1]. This has been achieved by the simple expediency of including 4 glutamic acid residues/100 residues of polypentapeptide with the substitution being at residue four [4]. The formal description is poly [(VPGVG), (VPGEG); 4:1] where V, P, G, and E stand for Val, Pro, Gly, and Glu, respectively. The structure is referred to as 4% Glu–PPP and when 20 Mrad γ-irradiation crosslinked, the elastomeric matrix is labelled X^{20}–4% Glu–PPP. When in phosphate buffered saline (PBS), which is 0.15*N* NaCl and 0.01*M* phosphate and when at 37°C, the elastomeric matrix contracts on lowering the pH and relaxes near neutral pH; this is shown in Figure 2. The elastomeric matrix is capable of lifting and setting down weights that are 1000 times its own dry weight. This represents the first synthetic polypeptide or model protein system to exhibit mechanochemical coupling and the mechanism, chemical modulation of an inverse temperature transition, represents a new process for achieving mechanochemical coupling. The following constitutes a brief review of the past year's progress in achieving and characterizing this new mechanism, which is viewed as being relevant to protein mechanisms in general. It will begin, however, by describing and delineating between the two presently demonstrated mechanisms for mechanochemical coupling: charge–charge repulsion and chemical modulation of an inverse temperature transition.

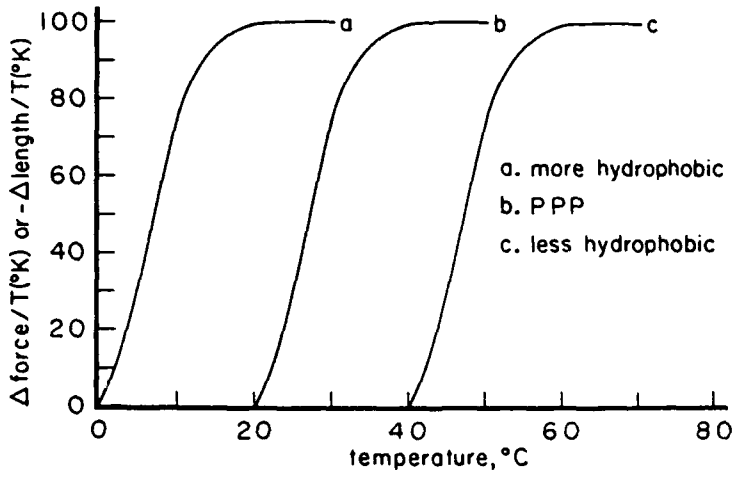

Figure 1. Schematic representation of the development of force/*T* (K) at constant length or the decrease in length/*T* (K) at constant force as a function of temperature (°C). Curves a, b, and c are representative of Ile^1–PPP, PPP and PTP, respectively. See text for the structural formulae. The temperature of the inverse temperature transition giving rise to force development or contraction is inversely dependent on the hydrophobicity of the polypeptide with curve (a) for the more hydrophobic, curve (b) for an intermediate hydrophobicity, and curve (c) for the less hydrophobic.

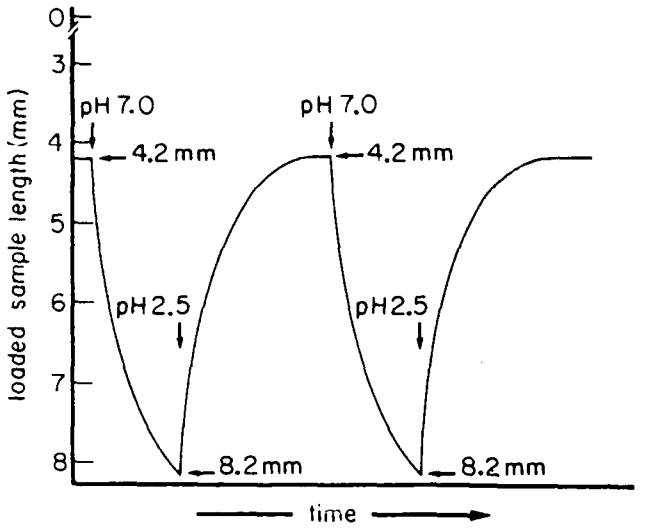

Figure 2. Mechanochemical coupling of X^{20}–4% Glu–PPP shown by a pH-elicited contraction on addition of a phosphate buffered saline (PBS) solution at pH 2.5 and a relaxation on addition of a PBS solution at pH 7. The load on the sample was 0.13 kg/cm^2 and the length changed from 4.2 mm (contracted) to 8.7 mm (relaxed).

Mechanisms of Mechanochemical Coupling

In polymer-based mechanochemical coupling a chemical couple is utilized. It can be two states of a functional side chain of an amino acid residue or of a covalently attached functional moiety, or the couple could be an empty and an occupied binding site. In the present analysis, the carboxyl/carboxylate anion chemical couple will be initially considered. In mechanochemical coupling in general, a change in chemical potential brings about either a change in length, or a change in force, or both in a cr inked elastic polymer. In the example of the carboxyl/carboxylate couple, the change in chemical potential is a change in proton potential which changes the ratio of [COOH] to [COO^-]. Of particular interest in delineating mechanisms, is the sign of the partial differential of chemical potential with respect to force at constant polymer composition, which could be stated as at constant degree of ionization, i.e., $(\partial\mu_i/\partial f)_{n_j}$ where μ_i and f are the chemical potential and force, respectively, and the partial differential is at constant composition, n_i. The sign of the partial differential is reversed depending on whether the mechanism for the carboxyl/carboxylate couple involves charge-charge repulsion or a new mechanism described as chemical modulation of an inverse temperature transition which may, with some license, be termed apolar-polar repulsion in an aqueous system. This will be briefly analyzed in what immediately follows and experimental data for the letter new mechanism will be given in the subsequent section.

The Charge–Charge Repulsion Mechanism of Mechanochemical Coupling

The charge-charge repulsion mechanism of mechanochemical coupling was first described by Katchalsky and Kuhn and colleagues [5, 6], using the polymer polymethacrylic acid,

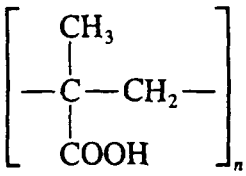

When this mechanochemical system is approximately 20% ionized, it is largely contracted to an extent limited by the repulsion between anions. On stretching, due to an increase in applied force, there is an increase in the mean distance between anions which relieves the repulsion between anions and allows more carboxyls to release their protons in the formation of more anions [7]. There is an increase in the acidity of the surrounding solution due to a decrease in the pK_a of the chemical couple. Equivalently, if the solution is made more acidic by an increase in the chemical potential of protons or addition of HCl, i.e. $\Delta\mu_i$ is positive, then the carboxylate anions become protonated lowering the charge-charge repulsion and the elastomer will contract with the development of force such that Δf is also positive. Accordingly, $(\partial\mu_i/\partial f)_{n_i}$ is positive [6].

An Apolar–Polar Repulsion Mechanism of Mechanochemical Coupling in Water

The present polypeptide mechanism is not based on repulsion of like charges but rather it may be described as a water mediated apolar–polar repulsion. It is based on the antagonism in an aqueous system of polar and nonpolar (hydrophobic) chemical moieties; it is a particular expression of the well-known salt effect on the solubility of hydrophobic solutes [8, 9], and it has its expression in polypeptides or proteins as the chemical modulation of the temperature of inverse temperature transitions. An inverse temperature transition involves, of course, the folding of a polypeptide or protein in such a way as to maximize hydrophobic contacts, that is, to remove hydrophobic groups from aqueous interaction. Its basis is the hydrophobic effect [10–12]. If the mechanochemical system involves an elastic matrix of a folded relatively hydrophobic polypeptide with occasional glutamic acid residues, e.g., 2–4/100 residues, then stretching the elastomer results in exposure of hydrophobic side chains and increases the free energy of carboxylate anions with the result of a shift toward protonation. On stretching, therefore, such a matrix would take up protons rather than release protons and the pK_a would increase as the result of the increase in force of stretching. An increase in pK_a means a decrease in proton potential. In terms of the interesting partial differential there is a decrease in the chemical potential of protons with an increase in force, that is $(\partial\mu_i/\partial f)_{n_i}$ is negative. Using the same chemical couple, the sign is exactly opposite for a mechanism involving apolar–polar repulsion than for a mechanism of charge–charge repulsion. This provides a diagnostic means for determining the dominant mechanism in a contractile polypeptide or protein as will be shown below for the carboxyl/carboxylate anion couple.

It should be noted for a chemical couple involving a protonated cationic species as in the imidazole/imidazolium couple of histidine that the sign would be reversed for both mechanisms with respect to the chemical potential of protons. It should also be appreciated that the chemical modulation of the temperature of an inverse temperature transition, i.e., the so-called apolar–polar repulsion mechanism, can utilize the entire polarity scale from the most hydrophobic to the most hydrophilic.

Carboxyl/Carboxylate Modulation of Contraction/Relaxation: The 4% Glu–Polypentapeptides

When the sequential polypeptide, poly[(VPGVG), (VPGEG); 4:1], is synthesized, there are 4 Glu residues/100 residues of polypentapeptide. The most ready characterization of pH dependence of the temperature of the inverse temperature transition is to scan temperature while following solution turbidity starting from low temperature where the polypeptide is soluble in PBS (phosphate buffered saline: 0.15*N* NaCl, 0.01*M* phosphate). A set of such scans, called temperature profiles of turbidity formation or TPτ's, are given in Figure 3(A). A remarkable pH dependence is seen for

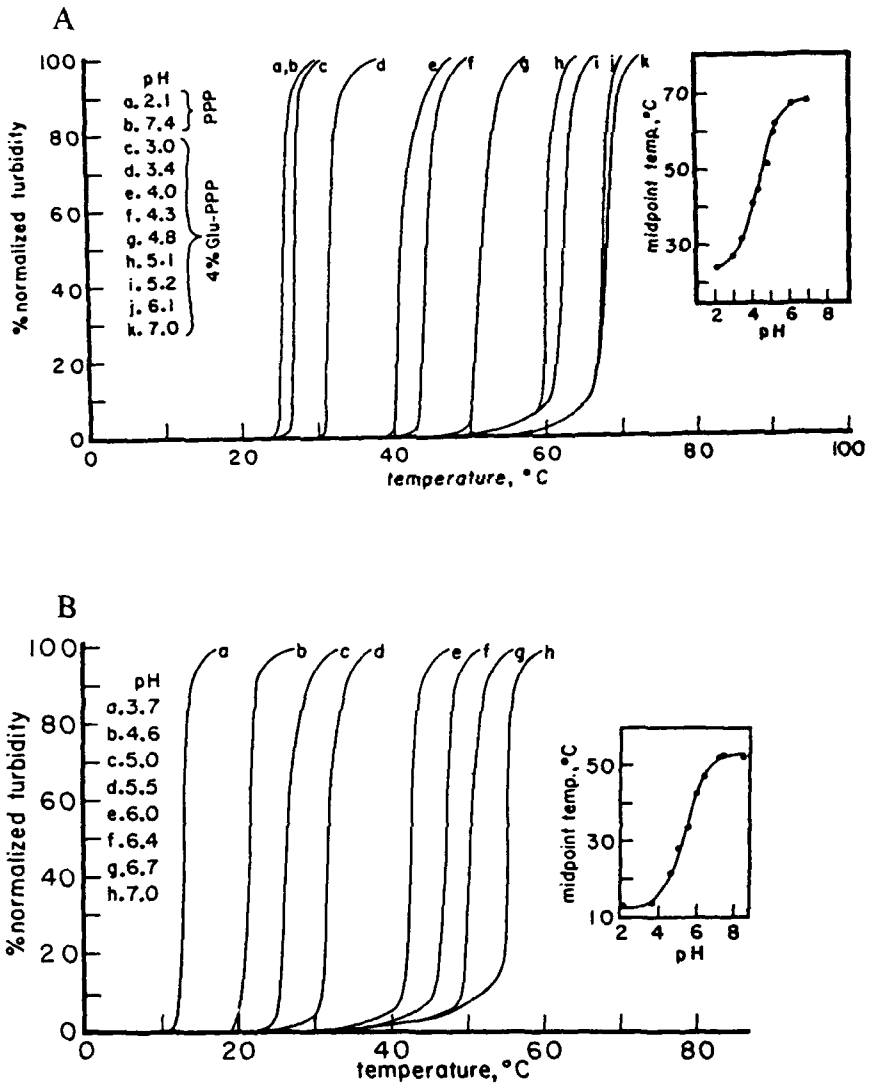

Figure 3. Temperature dependence of the inverse temperature transition for 4% Glu–polypentapeptides as followed by the turbidity development on aggregation. Part (A) is for 4% Glu–PPP and part (B) is for the more hydrophobic 4% Glu–Ile^1–PPP. There is a dramatic increase in the temperature of the transition on increasing the pH. The pK_a values can be estimated from the insets giving transition temperature versus pH; the values are 4.4 for 4% Glu–PPP and 5.4 for 4% Glu–Ile^1–PPP. Increased hydrophobicity causes an increase in the pK_a of the Glu side chain carboxyl/carboxylate couple and, of course, the transition temperatures for the more hydrophobic polypentapeptide are shifted to lower temperatures.

this measure of the temperatures at which the inverse temperature transitions occur; the temperature for the onset of the transition shifts from a low of 25°C at low pH (2.5) to a high of 70°C at high pH (7.0). The curves of Figure 3(A) approximate, after the polypentapeptide is crosslinked, for a given pH the temperature over which contraction occurs [4].

A Hydrophobicity-Induced Shift in pK_a

When the more hydrophobic sequential polypeptide, poly[(IPGVG), (IPGEG); 4:1] where I is Ile, is prepared, the temperature for the inverse temperature transition for a given pH, as expected for a more hydrophobic polypeptide, is shifted to a lower temperature [see Fig. 3(B)]. Also, very significantly for understanding mechanism, as is most readily seen from the inserts of Figures 3(A) and (B), the plots of temperature of the inverse temperature transition versus pH are displaced for the Val^1 and Ile^1 4% Glu–polypentapeptides. Using the midpoint of the curve to estimate pK_a, for 4% Glu–PPP the pK_a is 4.4, whereas, for the more hydrophobic 4% Glu–Ile^1–PPP, the pK_a is 5.4. For the more hydrophobic polypentapeptide the pK_a is raised by 1 pH unit. When the study utilizes the γ-irradiation crosslinked elastomers and measures, at a similar force per cross-sectional area for each of the elastomers, the length versus pH, the same result is obtained [see Fig. 4(A)]. The pK_a is raised for the more hydrophobic elastomer by ca. 1 pH unit [13]. Therefore, either the carboxyl moiety is more stabilized or the carboxylate anion is destabilized in the more hydrophobic elastomer.

Both polypentapeptides have the same number of Glu residues, per 100 residues of polypeptide, and the two-dimensional nuclear Overhauser enhancement spectroscopy (2D-NOESY) data for both show no differences in conformation [13]. Also, both parent polypentapeptides exhibit the same circular dichroism pattern before the transition and, though the CD patterns change after the transition, they are again the same for both polypentapeptides [2]. Therefore, the pK_a shift is not due to some difference in hydrogen bonding of the Glu side chain to the polypeptide backbone. It appears necessary to seek an explanation for the pK_a shift in terms of the change in hydrophobicity *per se*. This perspective will be confirmed below where the evidence is for an increase in the free energy of the more polar species in situations where there is more expression of hydrophobicity by the polypeptide.

A Stretch-Induced Shift in pK_a

The contracted elastomer results from the optimization of hydrophobic interactions within the matrix both intramolecularly and intermolecularly. Thus on stretching the elastomer, there is necessarily an exposure of hydrophobic groups to the aqueous medium. The hydrophobic side chains become solvated in an exothermic reaction resulting in clathrate-like water surrounding the hydrophobic groups. The question being addressed here is whether or not this exposure of hydrophobicity and formation of clathrate-like water affects the pK_a of the Glu residues in the matrix. The data is given in Figure 4(B). With a small load on the elastomer of 1.2×10^4 dyne/cm^2, the apparent pK_a is 4.1. When the load is increased to 1.3×10^5 dyne/cm^2, the apparent pK_a becomes 4.6. Therefore, in the same X^{20}–4% Glu–PPP matrix the pK_a increases

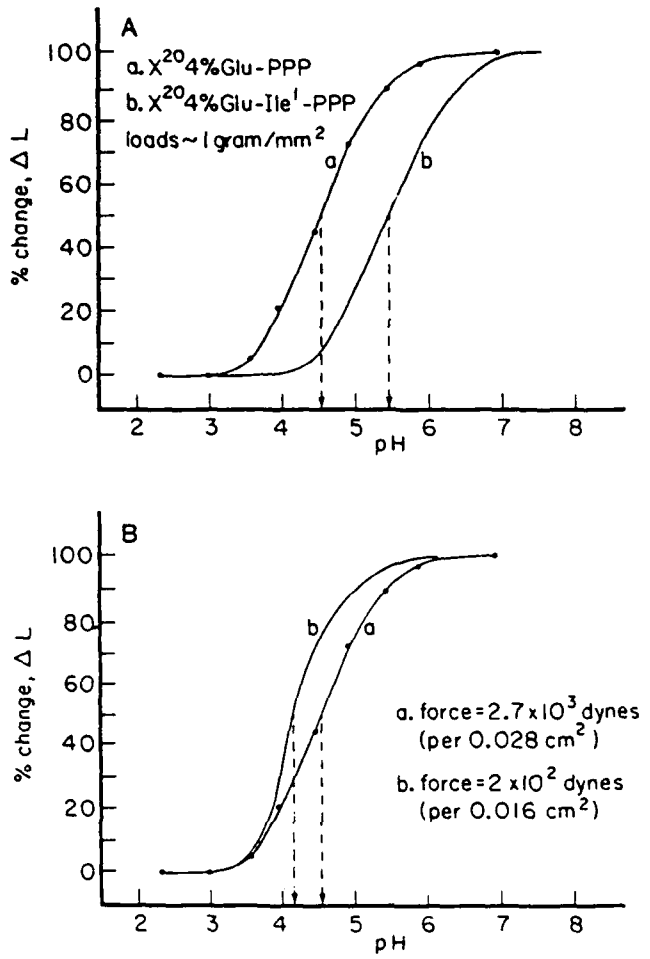

Figure 4. Dependence of pK_a on the expression of elastomeric matrix hydrophobicity. (A) The more hydrophobic elastomeric matrix, X^{20}–4% Glu–Ile^1–PPP, exhibits a higher pK_a for the pH elicited contraction than does X^{20}–4% Glu–PPP even though both have the same number of Glu residues per total number of residues. (B) On stretching the elastomeric matrix, X^{20}–4% Glu–PPP, there is an increase in the pK_a of the pH elicited contraction due to the increased exposure of hydrophobic groups on extension.

on stretching. This is exactly the opposite of what happens in the polymethacrylic acid system where charge-charge repulsion is the mechanism and reflects what may, by analogy, be called an apolar–polar repulsion exhibited in an aqueous system. In particular, from the data in Figure 4(B) $(\partial\mu_i/\partial f)_{n_i}$ is negative and is approximately -1×10^7 cm/mol [15]. In what follows it will be shown that the apolar–polar repulsion can be described as an increase in the free energy of ionic species on increasing the expression of hydrophobicity of the elastomeric polypeptide system.

Ionic Strength Modulation of Contraction/Relaxation

When the parent polypentapeptide, $(VPGVG)_n$, is γ-irradiation crosslinked to form simply X^{20}–PPP, it has been shown that the temperature for the inverse temperature transition is lowered on going from pure water to PBS as schematically shown with the thermoelasticity curves of Figure 5 [16]. This means that increased salt solution

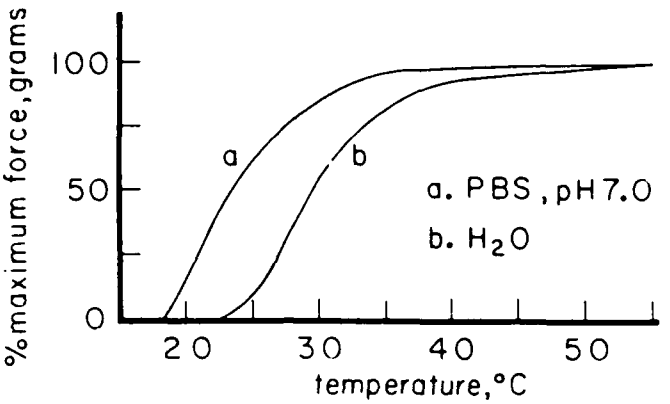

Figure 5. Schematic representation of the increase in force at constant length of X^{20}–PPP for both a pure water medium and for phosphate buffered saline. Phosphate buffered saline (PBS) is seen to shift the transition to lower temperatures; this shift is independent of the pH of the buffer. By choosing an intermediate temperature such as 25°C, PBS can be shown to cause a contraction and changing to water causes relaxation. Thus, mechanochemical coupling is demonstrated without any change in the chemical nature of the polypeptide chain; the mechanism is due to an antagonism between ions in solution and the expression of hydrophobicity by the elastomeric matrix. This was also demonstrated in Figure 4 (A) and (B) where a more hydrophobic elastic matrix exhibited a raised pK_a and where stretching, which results in the exposure of hydrophobic groups, causes an increase in pK_a. What is observed in all three cases is an aqueous mediated apolar–polar repulsion mechanism.

shifts the equilibrium to the folded state where expression of hydrophobicity is minimized. At an intermediate temperature say 25°C, the elastic matrix relaxes and lengthens in the presence of pure water and it contracts on addition of the salt solution. Thus, there is a solvent-based mechanochemical coupling which demonstrates that the structural transition can be entirely solvent mediated; in this case there is no change in the chemical nature of the polymer, but there is a change in the free energy of solvation. Most significantly, the result directly demonstrates the antagonism between the presence of polar ions and the expression of hydrophobicity. Therefore, it can be concluded that the pK_a shifts, which are observed on increasing the hydrophobicity of the matrix either by Val^1 replacement by Ile^1 or by stretching, are due to an increase in the free energy of the carboxylate anion.

Generalization and Extrapolations

General Considerations

The elastomeric strips that can now be prepared and are now being characterized provide an experimental system with which to clarify and to quantify what are here referred to as apolar–polar interaction energies in an aqueous environment. Thus by changing the hydrophobicity of the polypeptide the free energy of the anionic species changes as can be measured by the change in pK_a with $\mu = -2.3\ RTpK_a$. Analogously, by applying a force to the elastomer and measuring the shift in pK_a, it becomes possible to assess the hydrophobicity change. (In fact the polymers provide the opportunity to develop a hydrophobicity scale covering essentially the complete polarity scale.) This data supplemented with direct calorimetric measurements of the

heats and temperatures of the transitions along with temperature dependence of pK_a for relaxed and loaded states will provide a thermodynamic characterization of these mechanochemical systems. Also, of great interest, will be the equivalent Carnot cycle in the force versus length plane, e.g., where it will be possible to determine the efficiency with which these elastomeric strips may function as reversible mechanochemical engines.

Of further significance is that these mechanochemical systems may be operated using functional groups ranging in polarity from the most hydrophobic to the most hydrophilic. In place of the carboxyl/carboxylate couple could be any acid/base couple. More generally, it could be any chemical couple which involved a change in hydrophobicity, e.g., a redox couple. The chemical potential change could be used to drive a mechanochemical engine, or by putting in the mechanical energy of stretching the mechanochemical system could be used to develop concentration gradients, to achieve separations of the two states of the couple and to prepare chemical species.

Biological Relevance

In general proteins tend to fold with their hydrophobic side chains in the interior away from exposure to the aqueous milieu at physiological temperatures. Whether a particular polypeptide chain is so folded depends on the mean hydrophobicity of the interacting moieties and on the binding of any chemical species that would be antagonistic (more polar) or synergistic (less polar) to that folding. Phosphorylation would force an unfolding whereas dephosphorylation would force the folding. The reduction (making less polar) of a bound co-factor or prosthetic group would enhance the folded state, whereas oxidation would favor the unfolded state. The binding of any chemical species which altered the mean hydrophobicity would shift the equilibrium in a predictable way if the hydrophobicities were well calibrated. (Incidentally, these elastomeric sequential polypeptides provide an excellent system with which to achieve the calibration.) Accordingly this apolar–polar repulsion mechanism in aqueous systems is proposed to be a fundamental driving force in protein mechanisms.

It has already been demonstrated that the oxidation of elastin causes the elastin fibers to unfold or unwind, increasing their length and causing loss of elastic recoil [17]. This chemically irreversible step is proposed to be part of the pathology of the elastic fiber central to the development of pulmonary emphysema. Phosphorylation of muscle proteins whether it be of myosin, actin, titin, etc., by this mechanism can be expected to cause relaxation of force and, where relevant, to bring about disassembly. This would be the case with phosphorylation functioning in the polymer-based mode whereas conceivably based on the ionic strength modulation effect the opposite could happen should the phosphate function in the solvent-based mode with the structural transition occurring in an adjacent chain or filament. These are but a few of the examples of relevance to biology.

Summarizing Remarks

This article reports on the first demonstration of mechanochemical coupling in synthetic polypeptides. The demonstration was achieved not by copy of a known contractile protein, but rather by a design based on a principle of contraction derived

independent of a known contractile protein. The principle is one in which a change in chemical potential shifts the temperature of an inverse temperature transition ıe new mechanism was demonstrated using the carboxyl/carboxylate couple and has been experimentally delineated from a polymethacrylic acid,

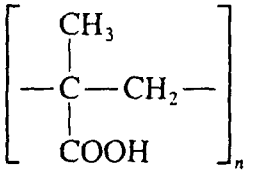

mechanochemical system where contraction was due to a mechanism in which protonation relieved a charge-charge repulsion, i.e., in which $(\partial\mu_i/\partial f)_{n_i} > 0$. By contrast, for the polypeptide mechanochemical system, $(\partial\mu/\partial f)_{n_i} < 0$. Accordingly, the mechanism is called an aqueous mediated apolar–polar repulsion. On applying force to the elastomer comprised of polymethacrylic acid, the pK_a of the carboxyl/carboxylate couple decreases whereas for the Glu containing hydrophobic polypeptide the application of force causes an increase in the pK_a. Importantly the apolar–polar repulsion mechanism does not require ionic species but rather can utilize the entire polarity scale from the most hydrophobic to the most hydrophilic.

The aqueous mediated apolar–polar repulsion mechanism is considered relevant to modulation of protein structure and function, in general. The elastomeric polypeptides under study provide an opportunity to quantitate the apolar–polar repulsion energies. Furthermore, any conformational change can be viewed as an expression of mechanochemical coupling when it is induced by: (1) the binding of a chemical moiety, (2) the change in polarity of an attached chemical moiety, or (3) a change in chemical potential of the medium that alters the thermodynamics of clathrate-like water formation. In general in biology, free energy transduction [18] could be viewed as conformational changes altering function as the result of either chemomechanical or electromechanical transduction. And these may be viewed as modulations of temperatures for conformational changes that may be called thermomechanical transduction.

Finally the point should be made that these elastomeric polypeptides provide the basis for numerous reversible mechanochemical and possibly electromechanical engines that could by means of chemical or electrical work achieve mechanical work, e.g., to power a rotary drive as per Katchalsky and colleagues [19]. As the processes are reversible it becomes possible, by means of mechanical work, to achieve chemical work as for example to develop concentration gradients of diverse nature. Practical applications could be desalination, the development of proton gradients, the production of the reduced component of a redox couple, etc.

Acknowledgment

The work was supported in part by the National Institutes of Health Grant No. HL24578 and the Department of the Navy, Office of Naval Research contract No. 0014-86-K-0402. The author also wishes to acknowledge the technical assistance of J. Jaggard.

References

[1] . W. Urry, Int. J. Quantum Chem. Quantum Biol. Symp. **14**, 261–280 (1987).
[2] D. W. Urry, M. M. Long, R. D. Harris, and K. U. Prasad, Biopolymers **25**, 1939–1953 (1986).
[3] D. W. Urry, R. D. Harris, M. M. Long, and K. U. Prasad, Int. J. Pept. Protein Res. **28**, 649–660 (1986).
[4] D. W. Urry, B. Haynes, H. Zhang, R. D. Harris, and K. U. Prasad, "Mechanochemical Coupling in Synthetic Polypeptides by Modulation of an Inverse Temperature Transition," Proc. Natl. Acad. Sci. U.S.A., **85**, 3407–3411 (1988).
[5] W. Kuhn, B. Hargitay, A. Katchalsky, and H. Eisenberg, Nature **165**, 514–516 (1950).
[6] A. Katchalsky, S. Lifson, I. Michaeli, and M. Zwick, "Size & Shape of Contractile Polymers: Conversion of Chemical into Mechanical Energy," A. Wasserman, Ed. (Pergamon, New York), pp. 1–40, 1960.
[7] W. Kuhn, A. Ramel, and D. H. Walters, "Size & Shape of Contractile Polymers: Conversion of Chemical Into Mechanical Energy," A. Wasserman, Ed. (Pergamon, New York), pp. 41–77.
[8] P. K. Nandi and D. R. Robinson, J. Am. Chem. Soc. **94**, 1308–1315 (1972).
[9] A. Hamabata and P. H. von Hippel, Biochemistry **12**, 1264–1271 (1973).
[10] H. S. Frank and M. W. Evans, J. Chem. Phys. **13**, 493–507 (1945).
[11] W. Kauzmann, Adv. Protein Chem. **14**, 1–63 (1959).
[12] C. Tanford, *The Hydrophobic Effect: Formation of Micelles and Biological Membranes* (Wiley, New York, 1973).
[13] D. W. Urry, D. K. Chang, H. Zhang, and K. U. Prasad, "pK Shift of Functional Group in Mechanochemical Coupling due to Hydrophobic Effect," Biochem. Biophys. Res. Commun., **153**, 832–839 (1988).
[14] T. Weis-Fogh and S. O. Andersen, Nature **227**, 718 (1970).
[15] D. W. Urry, "A New Mechanism of Mechanochemical Coupling: Stretch-Induced Increase in Carboxyl pK_a as a Diagnostic," in preparation.
[16] D. W. Urry, R. D. Harris, and K. U. Prasad, J. Am. Chem. Soc., **110**, 3303–3305 (1988).
[17] D. W. Urry, J. Protein Chem. **7**, 81–114 (1988).
[18] T. L. Hill, *Free Energy Transduction in Biology, The Steady State Kinetic and Thermodynamic Formalism* (Academic, New York, 1977).
[19] I. Z. Steinberg, A. Oplatka, and A. Katchalsky, Nature **210**, 568–571 (1966).

Received May 3, 1988.

Mechanochemical coupling in synthetic polypeptides by modulation of an inverse temperature transition

[elastin polypentapeptide/hydrophobic effect/elastomeric polypeptides/free energy (chemomechanical) transduction/solvent-induced apolar–polar repulsion free energy]

D. W. URRY, B. HAYNES, H. ZHANG, R. D. HARRIS, AND K. U. PRASAD

Proc. Natl. Acad. Sci. USA
Vol. 85, pp. 3407–3411, May 1988
Biophysics

Proc. Natl. Acad. Sci. USA
Vol. 85, pp. 3407–3411, May 1988
Biophysics

Mechanochemical coupling in synthetic polypeptides by modulation of an inverse temperature transition

[elastin polypentapeptide/hydrophobic effect/elastomeric polypeptides/free energy (chemomechanical) transduction/solvent-induced apolar–polar repulsion free energy]

D. W. URRY, B. HAYNES, H. ZHANG, R. D. HARRIS, AND K. U. PRASAD

Laboratory of Molecular Biophysics, The University of Alabama at Birmingham, P.O. Box 311, University Station, Birmingham, AL 35294

Communicated by Terrell L. Hill, January 4, 1988 (received for review October 19, 1987)

ABSTRACT **For the polypentapeptide of elastin, (L-Val-L-Pro-Gly-L-Val-Gly)$_n$, and appropriate analogs when suitably cross-linked, it has been previously demonstrated that development of elastomeric force at fixed length and length changes at fixed load occur as the result of an inverse temperature transition, with the temperature of the transition being inversely dependent on the hydrophobicity of the polypeptide. This suggests that at fixed temperature a chemical means of reversibly changing the hydrophobicity could be used for mechanochemical coupling. Evidence for this mechanism of mechanochemical coupling is given here with a 4%-Glu-polypentapeptide, in which the valine in position 4 is replaced in 1 out of 5 pentamers by a glutamic acid residue. Before cross-linking, the temperature for aggregation of 4%-Glu-polypentapeptide is remarkably sensitive to pH, shifting from 25°C at pH 2 to 70°C at pH 7.4 in phosphate-buffered saline (PBS). At 37°C, the cross-linked 4%-Glu-polypentapeptide matrix in PBS undergoes a pH-modulated contraction and relaxation with a change from pH 4.3 to 3.3 and back. The mean distance between carboxylates at pH 4.3 in the elastomeric matrix is greater than 40 Å, twice the mean distance between negatively charged species in PBS. Accordingly, charge–charge repulsion is expected to make little or no contribution to the coupling. Mechanochemical coupling is demonstrated at fixed load by monitoring pH dependence of length and at constant length by monitoring pH dependence of force. To our knowledge, this is the first demonstration of mechanochemical coupling in a synthetic polypeptide and the first system to provide a test of the recent proposal that chemical modulation of an inverse temperature transition can be a mechanism for mechanochemical coupling. It is suggested that phosphorylation and dephosphorylation may modulate structure and forces in proteins by locally shifting the temperatures of inverse temperature transitions.**

The polypeptide of interest is the polypentapeptide of elastin, (L-Val-L-Pro-Gly-L-Val-Gly)$_n$, discovered in porcine elastin (1, 2). In bovine elastin, the longest sequence between lysine residues, which can form the cross-links, is 72 residues; for a continuous and unsubstituted sequence of 57 residues, this is the polypentapeptide (3). The synthetic polypentapeptide is soluble in water in all proportions below 25°C, but when the temperature is raised above 25°C, aggregation occurs, followed by settling and phase separation. At 40°C, the more dense viscoelastic phase is 38% peptide and 62% water by weight (4). On γ-irradiation cross-linking at a dose of 20 Mrad (1 rad = 0.01 Gy), this viscoelastic phase, called a coacervate, forms an elastomer that exhibits dominantly entropic elastomeric force in the 40–60°C temperature range (5). Numerous physical characterizations* have demonstrated this transition to be an inverse temperature transition, in which the order in the polypeptide part of this two-component system increases as the temperature is raised through the transition. Those physical characterizations include (*i*) self-assembly studies, in which the polypeptide is found to assemble into several-micrometer-diameter fibers composed of fibrils that in turn are composed of approximately 50-Å-diameter filaments (8–10); (*ii*) circular dichroism and Raman spectroscopy, in which the polypeptide chains within the coacervate are seen to have a repeating β-turn conformation (11, 12); (*iii*) nuclear Overhauser effect studies, which demonstrate the specific hydrophobic side chain associations (ref. 13, D.W.U., D. K. Chang, R. Krishna, D. H. Huang, T. L. Trapane, and K.U.P., unpublished data); (*iv*) NMR studies, which show a decrease in backbone mobility as the temperature is raised through the transition under conditions of constant composition (14, 15); (*v*) dielectric relaxation studies, which show the development of an intense, localized, Debye-type relaxation near 10 MHz requiring the development of a regular dynamic backbone conformation (16); (*vi*) elastomer length studies, in which the elastomer shortens to less than 45% of its low-temperature length when the temperature is raised from 20°C to 40°C (17); and (*vii*) studies of slow thermal denaturation at 80°C in which the circular dichroism indicates the loss of order (4), composition studies show a dramatic expulsion of water to a new composition of 68% peptide and 32% water by weight (4), and, for the elastomer, there is a decrease in length and loss of elastic modulus (ref. 18 and references therein).

In thermoelasticity studies when the synthetic elastomer is stretched and held at fixed length and the temperature is raised through the transition range from 20°C to 40°C, there is a dramatic increase in elastomeric force (5). Above 40°C, however, in a plot of ln(elastomeric force/temperature) versus temperature the slope is nearly 0 (5); these data, along with composition studies that show a near constant coacervate volume and composition in the 40–60°C temperature range (4), provide one basis for indicating that the elastomeric force is dominantly entropic in origin. A most instructive demonstration that this transition, centered near 30°C, in which elastomeric force develops is an inverse temperature transition is given when the more hydrophobic polypentapeptide (L-Ile-L-Pro-Gly-L-Val-Gly)$_n$—i.e., the [Ile^1]polypentapeptide—is similarly cross-linked and studied (18). For this more hydrophobic elastomeric matrix, the temperature of the transition for development of elastomeric force in a thermo-

The publication costs of this article were defrayed in part by page charge payment. This article must therefore be hereby marked "*advertisement*" in accordance with 18 U.S.C. §1734 solely to indicate this fact.

Abbreviations: 4%-Glu-PPP, elastin polypentapeptide in which 4% of the residues are glutamic acid; X^{20}-, crosslinked at 20 Mrad γ-irradiation.

*With the exception of two reports from one other laboratory (6, 7), to our knowledge, the only synthesis and physical characterizations of the sequential polypeptides of elastin and their analogs are due to the work of, and collaborations involving, this laboratory. Because of this, an unseemly high proportion of the references in this article will necessarily be to our own publications.

elasticity study is 10°C rather than 30°C for the parent polypentapeptide. A less hydrophobic elastomeric matrix has also been made with the des-Val[4]-polypentapeptide—i.e., (L-Val-L-Pro-Gly-Gly)$_n$; in a thermoelasticity study this cross-linked matrix develops elastomeric force with the midpoint of the transition at 50°C (18). These studies of changes in hydrophobicity must be done with an understanding of the structure and mechanism of elasticity. For example, the [Ile[1]]polypentapeptide analog represents the insertion of a CH_2 moiety on the side chain of residue 1; if the CH_2 moiety is inserted instead at residue 5, as in [L-Ala[5]]polypentapeptide, there is a total loss of elastic properties (18).

The above findings, that appropriately changing the hydrophobicity of the polypeptide chain can change the temperature range at which elastomeric force develops in a thermoelasticity study, provide the basis for a mechanism of mechanochemical coupling; it should be possible to turn "on" and "off" elastomeric force at a fixed temperature by reversibly changing the hydrophobicity of the polypeptide chain by means of changing the chemical potential. This can be achieved by including in the polypeptide an occasional residue in which a change in chemical potential would change the hydrophobicity of the residue. In the present report, the polypentapeptide is the copolymer of L-Val-L-Pro-Gly-L-Val-Gly and L-Val-L-Pro-Gly-L-Glu-Gly at a mole ratio of 4:1. This gives a polypentapeptide matrix in which there are 4 Glu residues per 100 residues of polypentapeptide (abbreviated 4%-Glu-PPP). The change in chemical potential to be used is a change in pH. On ionization of the Glu side chains the polypentapeptide chain becomes less hydrophobic and, as reported here, the transition shifts to higher temperature and the elastomeric force turns off. To our knowledge, this report represents the first demonstration of mechanochemical coupling in a synthetic polypeptide and one in which the principle is to vary reversibly the hydrophobicity of a polypeptide to shift the temperature of an inverse temperature transition.

MATERIALS AND METHODS

Peptide Synthesis and Product Verification. For brevity, the details of peptide synthesis and product verification will be presented elsewhere. Here it is noted that the synthesis was by mixtures of two monomers, Boc-Gly-Glu(OMe)-Gly-Val-Pro-ONp and Boc-Gly-Val-Gly-Val-Pro-ONp (19, 20), which were mixed in a 1:4 ratio with polymerization initiated on removal of the Boc group by trifluoroacetic acid treatment (Boc, *t*-butoxycarbonyl; ONp, *p*-nitrophenoxy). The purity of the intermediates and the final products was checked by thin layer chromatography, elemental analysis, amino acid analysis, and C-13 NMR spectroscopy.

Temperature Profiles for Aggregation. Profiles for aggregation as a function of temperature were obtained by observing the turbidity of 40-mg/ml samples at 300 nm in a Cary 14 spectrophotometer with a 300-Hz vibrator to prevent settling. Also referred to as temperature profiles for coacervation, these data provide a means of monitoring the temperature of the inverse temperature transition, and the midpoints of the profiles are given in Fig. 1 as a function of pH for the polypeptide dissolved in phosphate-buffered saline (PBS; 0.15 N NaCl/0.01 M sodium phosphate); the titration curve shows a pK_a of 4.5. The curves for the parent polypentapeptide at pH 2.1 and 7.4 show no pH dependence.

Cross-Linking. The 4%-Glu-PPP, 400 mg/ml in distilled water, was formed in the bottom of a cryotube, and a pestle in which a channel had been turned was inserted, causing the viscoelastic material to flow into and to fill the circular channel. The sample was then γ-irradiated at a radiation absorbed dose of 20 Mrad. After cross-linking at 20 Mrad, the sample is designated by the prefix X^{20}-. This dose causes no significant changes in the carbon-13 and nitrogen-15 NMR spectra of isotopically enriched samples (14, 15), but it results in an insoluble matrix with an initial elastic modulus of 1×10^6 dynes/cm^2 (15).

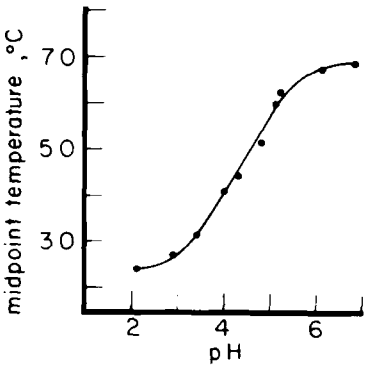

FIG. 1. pH dependence of the inverse temperature transition as determined from the midpoint of the temperature profiles for aggregation for 4%-Glu-PPP before cross-linking. The temperature of the inverse temperature transition shifts by a remarkable 45°C, from 25°C to 70°C, with an apparent pK_a of 4.5.

Stress/Strain Apparatus and Thermoelasticity Experiments. The custom-built stress/strain apparatus was as previously described (17, 19). Elastomers were equilibrated in PBS: 37°C for X^{20}-polypentapeptide at pH 7.4, 37°C for X^{20}-4%-Glu-PPP at pH 2.1, and 50°C for X^{20}-4%-Glu-PPP at pH 4.5. The samples were gripped; stress–strain data were taken; then samples were equilibrated below 15°C; the temperature was increased in 1°C increments, and the force was monitored to constancy.

Force Measurements at Constant Length. At 37°C, at constant length and at the completion of a pH 2.1 PBS thermoelasticity experiment involving X^{20}-4%-Glu-PPP, the changes in force due to changing the pH to 7.4 and then back to 2.1 were monitored with time.

Length Measurements at Constant Force. At 37°C, at constant force and at the end of a pH 2.1 thermoelasticity experiment to 35°C, the X^{20}-4%-Glu-PPP elastomer was placed under constant load of 1.5 g and the pH was varied between 3.3 and 4.3 with monitoring of the length change resulting from the pH change.

RESULTS

Thermoelasticity Studies. The temperature dependence of force development for elastomers held at a fixed extension are given in Fig. 2 for pH 2.1 and pH 4.5. The choice of pH 2.1 gives the state of essentially complete protonation—i.e., 4%-Glu(OH)-polypentapeptide. The choice of pH 4.5 derives from the data in Fig. 1—i.e., only two carboxylates per 100 residues are expected to shift the transition sufficiently such that the turn on of elastomeric force would begin above 37°C at pH 4.5. This is verified in Fig. 2. Elastic force development is seen to begin just above 40°C. As irreversible loss of elastomeric force occurs for X^{20}-polypentapeptide in distilled water above 60°C, this temperature was not exceeded (18). When the pH was lowered to 2.1 and the temperature was equilibrated below 20°C before the temperature increase was started, the development of elastomeric force was seen to begin at about 20°C. Thus the introduction of two charged groups (two carboxylates) per 100 residues causes the inverse temperature transition to shift by about 20°C to higher temperatures. Therefore, it should be possible to hold the temperature constant at 37°C and turn the elastomeric force on by lowering the pH to 2.1 and to turn it off by raising the pH to a value of 4.5 or above.

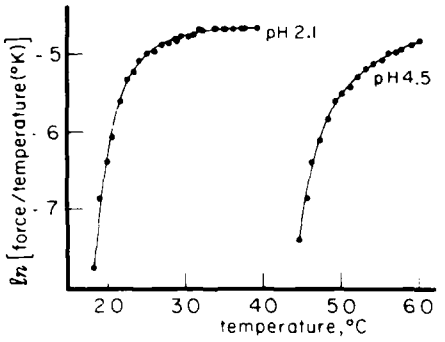

FIG. 2. Thermoelasticity studies on the γ-irradiation cross-linked 4%-Glu-PPP in PBS. For the left-hand curve, the sample had been equilibrated at 37°C and pH 2.1 and stretched to 60%, then the temperature was increased from below 20°C. For the right-hand curve, the sample was equilibrated at 50°C and extended to 50%; the development of elastomeric force is seen to begin about 45°C. The temperature was not raised above 60°C as irreversible loss of elastomeric force occurs above this temperature. This is the sample used in the length study at constant force of Fig. 3*A*. The data were plotted as ln[force/temperature (K)] (with force in g; 1 g force = 9.8 mN) versus temperature such that the slope of the pH 2.1 curve could be shown to be essentially 0 in the temperature range of the 37°C studies, indicating with composition data on the host polypentapeptide that the elastomeric force is dominantly entropic in origin. The primary purpose of these data is to demonstrate that at 37°C it should be possible to turn force on by going to pH 2.1 and turn it off by raising the pH to near 4.5 or greater.

Mechanochemical Coupling at Fixed Force. The sample was clamped in a pH 3.3 solution at a length of 5.3 mm and extended at 37°C to a force value of 1.5 g which gave a length of 6.3 mm. The pH was then changed to 4.3 and the length was adjusted to maintain a constant force as the elastomer extended to 8.7 mm. When the pH was changed to 3.3, the sample contracted toward the 6.3 mm length. As plotted in Fig. 3*A*, the sample repeatedly relaxes as the pH is changed to 4.3 and contracts as the pH is changed to 3.3. The relaxations involve an increase in length of 35–40%, and the final contraction involved the raising of 1.5 g through a distance of 2.6 mm. This choice of pH values represents an effort to optimize the amount of work performed for the change in chemical potential and the number of groups protonated (see Eq. **6** below). These experiments demonstrate in a synthetic polypeptide system that a change in chemical potential can bring about a contraction in which work is performed.

Mechanochemical Coupling at Fixed Length. With the temperature fixed at 37°C and a force reading of 6.8 g, when the pH was changed from 2.1 to 7.4, the elastomeric force turned off. This is shown in Fig. 3*B*. When the pH was lowered to 2.1, the force turned back on to a value of 4.8 g. The force was again turned off and again turned on to recover the same force value and so on. Clearly, mechanochemical coupling is demonstrated in a synthetic polypeptide as the result of a change in pH.

DISCUSSION

Characterizations of the Inverse Temperature Transition. Understanding of inverse temperature transitions goes back

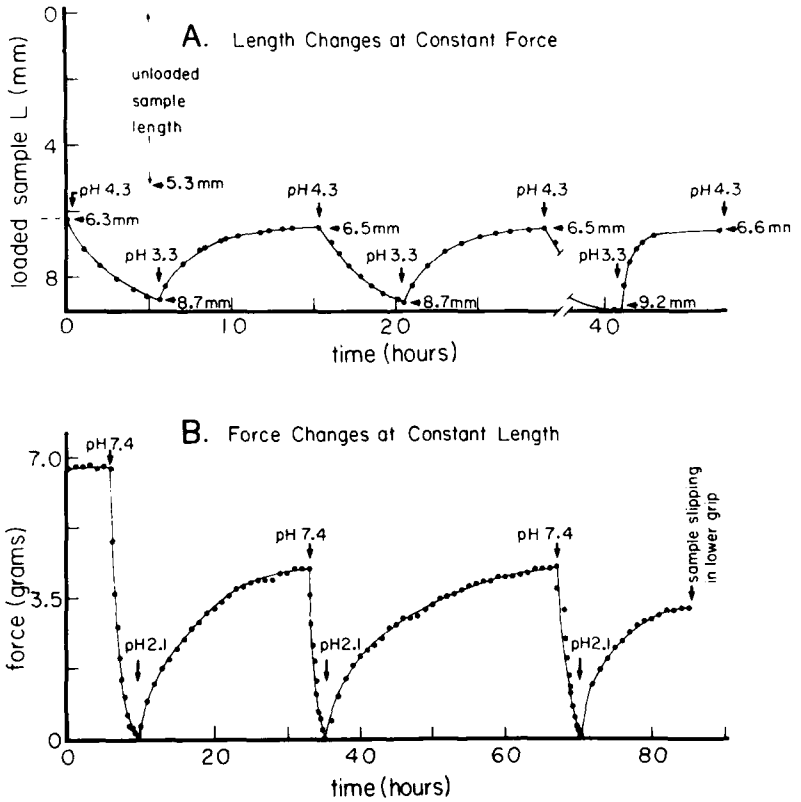

FIG. 3. Mechanochemical coupling exhibited by X^{20}-4%-Glu-PPP due to changes in pH at 37°C in PBS. (*A*) Length (*L*) changes at constant force. An elastomeric matrix 5.3 mm in length was loaded with 1.5 g and stretched to 6.3 mm at pH 3.3. When the pH was changed to 4.3, the sample elongated to 8.7 mm; returning the sample to pH 3.3 caused contraction to 6.5 mm with the lifting of the weight. This cycling was repeated. Finally, after waiting long enough, the limiting work is seen to be the shortening of the elastomer from 9.2 mm to 6.6 mm. There was a slow swelling as the sample was exposed for a prolonged period to the acid pH. (*B*) Force changes at constant length. An elastomeric matrix at pH 2.1 was stretched such that in a thermoelasticity study, the force of 6.8 g was reached at 37°C. When the pH was changed to 7.4, the force turned off; when the pH was returned to 2.1, the force turned on to 4.8 g; the force shifted between 4.8 g at pH 2.1 and 0 g at pH 7.4 until the sample began slipping in the lower grip, at which point the experiment was terminated.

to the work of Frank and Evans (21), which was then considered for proteins in the classic paper of Kauzmann (22) and was extensively developed with emphasis on membrane systems by Tanford (23) and in general by Ben-Naim (24). The basis of an inverse temperature transition may be referred to as the hydrophobic effect (23). As commonly stated, at temperatures below the transition the hydrophobic side chains are surrounded by clathrate-like water–i.e., by water that is more ordered than bulk water. As the temperature is raised through the transition, the clathrate-like water surrounding the hydrophobic side chains becomes less ordered bulk water as the hydrophobic side chains associate, increasing the order in the polypeptide part of the system. The transitions are endothermic with relatively small heat absorbed. For the polypentapeptide, the change in heat content is of the order of 1 cal/g (1 cal = 4.18 J) and, of course, there is a net increase in entropy for the complete system, polypentapeptide plus water. As detailed in the introduction, it is well established that the transition involved in the present studies is an inverse temperature transition.

Nature of Elastomeric Force at Temperatures Above the Inverse Temperature Transition. The data in Fig. 2 are plotted as ln[force/temperature (K)] versus temperature to demonstrate the entropic nature of the elastomeric force. The elastomeric force, f, may be written as

$$f = \left(\frac{\partial A}{\partial L}\right)_{V,T} = \left(\frac{\partial E}{\partial L}\right)_{V,T} - T\left(\frac{\partial S}{\partial L}\right)_{V,T}, \quad [1]$$

where A, E, S, V, T, and L are the work function, internal energy, entropy, volume, temperature in K, and length, respectively, and the subscripts indicate the conditions of constant volume and temperature (25). The two terms on the right hand side of Eq. **1** are the internal energy and entropy components of force, f_e and f_s, respectively. An evaluation of the f_e/f ratio allows an estimate of the magnitude of f_s with the expression (26)

$$\frac{f_e}{f} = -T\left(\frac{\partial \ln(f/T)}{\partial T}\right)_{V,L,n}, \quad [2]$$

when the experiment is carried out at constant volume, length, and composition, n. Composition studies on the polypentapeptide in water as a function of temperature have shown that above the temperature where the transition is complete and up to 60°C, above which temperature water is extruded, the volume and composition of the coacervate state are very nearly constant (4). Accordingly, Eq. **2** is applicable and a slope of 0 occurring in a plot of $\ln(f/T)$ versus T would indicate a 0 value for the f_e/f ratio—that is, the elastomeric force would be entirely entropic. In the pH 2.1 plot of Fig. 2, the near 0 slope in the 32–40°C temperature range calculates by Eq. **2** to have an f_e/f ratio of +0.104. In PBS at pH 7.4, the γ-irradiation-cross-linked polypentapeptide coacervate (X^{20}-polypentapeptide) at a 40% extension gave a calculated f_e/f ratio of −0.049 for the temperature range from 40°C to 55°C. Thus, these polypentapeptide elastomers appear to be dominantly entropic elastomers in the temperature interval in which the mechanochemical coupling studies were carried out.

Mechanochemical Coupling in Polyelectrolytes. The previous demonstration of mechanochemical coupling with a synthetic polymer was due to the fundamental work of Kuhn, Katchalsky, and co-workers, using polymethacrylic acid in water (27), where the mechanism was charge–charge repulsion and the charge density changes were very large. In considering mechanochemical coupling, Katchalsky *et al.* (28) began with the general expression

$$dE = TdS - PdV + fdl + \sum_i \mu_i dn_i, \quad [3]$$

where dE, dS, dV, dL, and dn_i are the change in internal energy, entropy, volume, length, and the number of moles of the ith chemical species introduced, respectively; and P and μ_i are the pressure and chemical potential of the ith introduced species, respectively. In an isothermic mechanochemical process, it was written (28)

$$dE = 0, \quad dS = 0, \quad dV = 0, \quad [4]$$

such that the change in the Helmholtz free energy (i.e., the work function, A) becomes

$$dA = fdL = -\sum_i \mu_i dn_i. \quad [5]$$

This provides a simple expression for analyzing mechanochemical coupling under isothermal conditions, but it is not appropriate for the mechanochemical coupling reported here, which is due to chemical modulation of an inverse temperature transition and involves a dominantly entropic elastomer such that dS cannot be taken as 0.

Charge Distribution in the X^{20}-4%-Glu-PPP Matrix. The concentration of polypentapeptide in water at 37°C is 400 mg/ml (4). With this concentration, with 4 carboxyls per 100 residues and with a mean residue weight of 83, there is a mean volume per carboxyl group of 8600 Å^3. In Fig. 2, the shift in transition temperature occurs with less than one-half of the carboxyls ionized, giving more than 17,200 Å^3 per charged side chain. This gives a mean distance between charges of greater than 26 Å in the contracted state. For the expanded state that is achieved by a pH of 4.3, where the volume is 4 times greater, the mean distance between charges would be greater than 40 Å. Such dilute concentrations of negative charge due to the polypeptide matrix, particularly in PBS, where the mean distance betwen negatively charged species is about 20 Å, are not expected to be capable of altering structure on the basis of charge–charge repulsion. Instead, as reviewed in the introduction, the mechanism is expected to be one in which a change in hydrophobicity of the polypeptide causes the shift in temperature of the inverse temperature transition. As the polypentapeptide becomes more hydrophilic, the temperature of the inverse temperature transition increases with remarkable sensitivity, as shown in Figs. 1 and 2.

Heats of Transition, Chemical Work, and Mechanical Work. A satisfactory analysis of the thermodynamics of this mechanism of mechanochemical coupling will have to await appropriate equations and more complete calorimetry data. Nonetheless, some qualitative considerations may be noted here. The heat of the inverse temperature transition (coacervation starting from a concentration of 40 mg/ml) for 4%-Glu-PPP in PBS at pH 3.5 is an endothermic 0.3 cal/g (C.-H. Luan and D.W.U., unpublished data). Since dissolution is limited by cross-linking in X^{20}-4%-Glu-PPP, the heat of transition would be somewhat less for the elastomer. This estimate of the heat of the transition is within a factor of 2 of the calculated chemical work that brought about the length changes observed in Fig. 3*A*, that is,

$$A = [\mu(\text{pH } 3.3) - \mu(\text{pH } 4.3)]\,[n_{O^-}(\text{pH } 3.3) - n_{O^-}(\text{pH } 4.3)] \approx 0.2 \text{ cal/g}, \quad [6]$$

where n_{O^-} is the number of moles of carboxylates at the indicated pH values. The mechanical work, $f\Delta L$, as approximated from Fig. 3*A*, is a much smaller quantity, about 0.002 cal/g. Apparently, the amount of mechanical work achieved on going from pH 4.3 to 3.3 is of the order of 1% of the chemical work, with the chemical work (chemical free energy) primarily providing for the endothermic transition.

Interestingly, the elastomer can repeatedly pick up and set down a weight 1000 times its dry weight.

Related Mechanochemical Systems. The 4%-Glu-[Ile^1]polypentapeptide, (L-Ile-L-Pro-Gly-ϕ-Gly)$_n$, where ϕ is Val or Glu at a ratio of 4:1, has been synthesized and partially characterized. This Ile^1 analog exhibits transitions that are shifted to lower temperature, which provides the opportunity of adding additional polar residues. For example, in place of the Glu residues could be introduced a Ser or Thr residue in proper relationship to an Arg or Lys residue in an effort to have a protein kinase site for phosphorylation. In such a case, phosphorylation could cause a relaxation, whereas dephosphorylation could cause a contraction. The proposal that the hydrophobicity be modulated by phosphorylation and dephosphorylation in order to turn off and on elastomeric force and therefore to cause relaxation and contraction or other structural transitions has been made recently (29, 30). This brings the work reported here to the issues of free energy transduction in biological systems so elegantly treated by Hill and colleagues (31–34), whether the molecular system be a soluble enzyme, a contractile filament, a cytosolic component of a membrane pump or channel, or a coupling component of oxidative phosphorylation.

We gratefully acknowledge Vickie King for her assistance in obtaining the data in Fig. 3*A*; Richard Knight, R. Gilchrist, and W. L. Alford of the Nuclear Science Center, Auburn University, for carrying out the γ-irradiation cross-linking; and E. M. Klingenberg and H. A. Scheraga for helpful discussions. This work was supported in part by National Institutes of Health Grant HL 29578 and the Department of Navy, Office of Naval Research Contract N00014-86-K-0402.

1. Sandberg, L. B., Soskel, N. T. & Leslie, J. G. (1981) *N. Engl. J. Med.* **304,** 566–579.
2. Sandberg, L. B., Leslie, J. G., Leach, C. T., Alvarez, V. L., Torres, A. R. & Smith, D. W. (1985) *Pathol. Biol.* **33,** 266–274.
3. Yeh, H., Ornstein-Goldstein, N., Indik, Z., Sheppard, P., Anderson, N., Rosenbloom, J. C., Cicila, G., Yoon, K. & Rosenbloom, J. (1987) *Collagen Relat. Res.* **7,** 235–247.
4. Urry, D. W., Trapane, T. L. & Prasad, K. U. (1985) *Biopolymers* **24,** 2345–2356.
5. Urry, D. W. (1984) *J. Protein Chem.* **3,** 403–436.
6. Bell, J. R., Boohan, R. C., Jones, J. H. & Moore, R. M. (1975) *Int. J. Pept. Protein Res.* **7,** 227–234.
7. Bell, J. R., Boohan, R. C., Jones, J. H. & Moore, R. M. (1974) *Int. J. Pept. Protein Res.* **6,** 155–156.
8. Urry, D. W., Okamoto, K., Harris, R. D., Hendrix, C. F. & Long, M. M. (1976) *Biochemistry* **15,** 4083–4089.
9. Urry, D. W. & Long, M. M. (1977) *Adv. Exp. Med. Biol.* **79,** 685–714.
10. Volpin, D., Urry, D. W., Pasquali-Ronchetti, I. & Gotte, L. (1976) *Micron* **7,** 193–198.
11. Urry, D. W., Long, M. M., Cox, B. A., Ohnishi, T., Mitchell, L. W. & Jacobs, M. (1974) *Biochim. Biophys. Acta* **371,** 597–602.
12. Thomas, G. J., Jr., Prescott, B. & Urry, D. W. (1987) *Biopolymers* **26,** 921–934.
13. Urry, D. W., Khaled, M. A., Rapaka, R. S. & Okamoto, K. (1977) *Biochem. Biophys. Res. Commun.* **79,** 700–706.
14. Urry, D. W., Trapane, T. L., Iqbal, M., Venkatachalam, C. M. & Prasad, K. U. (1985) *Biochemistry* **24,** 5182–5189.
15. Urry, D. W., Trapane, T. L., McMichens, R. B., Iqbal, M., Harris, R. D. & Prasad, K. U. (1986) *Biopolymers* **25,** S209–S228.
16. Henze, R. & Urry, D. W. (1985) *J. Am. Chem. Soc.* **107,** 2991–2993.
17. Urry, D. W., Haynes, B. & Harris, R. D. (1986) *Biochem. Biophys. Res. Commun.* **141,** 749–755.
18. Urry, D. W. (1988) *J. Protein Chem.* **7,** 1–34.
19. Urry, D. W. & Prasad, K. U. (1985) in *Biocompatibility of Tissue Analogues*, ed. Williams, D. F. (CRC, Boca Raton, FL), 89–116.
20. Prasad, K. U., Iqbal, M. A. & Urry, D. W. (1985) *Int. J. Pept. Protein Res.* **25,** 408–413.
21. Frank, H. S. & Evans, M. W. (1945) *J. Chem. Phys.* **13,** 493–507.
22. Kauzmann, W. (1959) *Adv. Protein Chem.* **14,** 1–63.
23. Tanford, C. (1973) *The Hydrophobic Effect* (Wiley, New York).
24. Ben-Naim, A. (1980) *Hydrophobic Interactions* (Plenum, New York).
25. Hill, T. L. (1968) *Thermodynamics for Chemists and Biologists* (Addison–Wesley, Reading, MA), pp. 25–37.
26. Flory, P. J., Ciferri, A. & Hoeve, C. A. J. (1960) *J. Polymer Sci.* **45,** 235–236.
27. Kuhn, W., Hargitay, B., Katchalsky, A. & Eisenberg, H. (1950) *Nature (London)* **165,** 514–516.
28. Katchalsky, A., Lifson, S., Michaeli, I. & Zwick, M. (1960) in *Size and Shape of Contractile Polymers: Conversion of Chemical and Mechanical Energy*, ed. Wassermann, A. (Pergamon, New York), pp. 1–40.
29. Urry, D. W. (1988) *J. Protein Chem.* **7,** 81–114.
30. Urry, D. W. (1987) *Int. J. Quantum Chem.: Quantum Biol. Symp.* **14,** 261–280.
31. Hill, T. L. (1983) *Proc. Natl. Acad. Sci. USA* **80,** 2922–2925.
32. Eisenberg, E. & Hill, T. L. (1985) *Science* **227,** 999–1006.
33. Hill, T. L. & Kirschner, M. W. (1982) *Proc. Natl. Acad. Sci. USA* **79,** 490–494.
34. Hill, T. L. & Inesi, G. (1982) *Proc. Natl. Acad. Sci. USA* **79,** 3978–3982.